FOCUS ARTICLE

WIREs COMPUTATIONAL MOLECULAR SCIENCE   WILEY

QUESTDB: A database of highly accurate excitation energies for the electronic structure community

Mickaël Véril[1] | **Anthony Scemama[1]** ⓘ | **Michel Caffarel[1]** | **Filippo Lipparini[2]** | **Martial Boggio-Pasqua[1]** | **Denis Jacquemin[3]** | **Pierre-François Loos[1]** ⓘ

[1]Laboratoire de Chimie et Physique Quantiques, Université de Toulouse, CNRS, UPS, Toulouse, France

[2]Dipartimento di Chimica e Chimica Industriale, University of Pisa, Pisa, Italy

[3]Université de Nantes, CNRS, CEISAM UMR 6230, Nantes, France

Correspondence
Denis Jacquemin, Université de Nantes, CNRS, CEISAM UMR 6230, F-44000 Nantes, France.
Email: denis.jacquemin@univ-nantes.fr
Pierre-François Loos, Laboratoire de Chimie et Physique Quantiques, Université de Toulouse, CNRS, UPS, France.
Email: loos@irsamc-ups-tlse.fr

Abstract

We describe our efforts of the past few years to create a large set of more than 500 highly accurate vertical excitation energies of various natures ($\pi \rightarrow \pi^*$, $n \rightarrow \pi^*$, double excitation, Rydberg, singlet, doublet, triplet, etc.) in small- and medium-sized molecules. These values have been obtained using an incremental strategy which consists in combining high-order coupled cluster and selected configuration interaction calculations using increasingly large diffuse basis sets in order to reach high accuracy. One of the key aspects of the so-called QUEST database of vertical excitations is that it does not rely on any experimental values, avoiding potential biases inherently linked to experiments and facilitating theoretical cross comparisons. Following this composite protocol, we have been able to produce theoretical best estimates (TBEs) with the aug-cc-pVTZ basis set for each of these transitions, as well as basis set corrected TBEs (i.e., near the complete basis set limit) for some of them. The TBEs/aug-cc-pVTZ have been employed to benchmark a large number of (lower-order) wave function methods such as CIS(D), ADC(2), CC2, STEOM-CCSD, CCSD, CCSDR(3), CCSDT-3, ADC(3), CC3, NEVPT2, and so on (including spin-scaled variants). In order to gather the huge amount of data produced during the QUEST project, we have created a website (https://lcpq.github.io/QUESTDB_website) where one can easily test and compare the accuracy of a given method with respect to various variables such as the molecule size or its family, the nature of the excited states, the type of basis set, and so on. We hope that the present review will provide a useful summary of our effort so far and foster new developments around excited-state methods.

This article is categorized under:

    Electronic Structure Theory > Ab Initio Electronic Structure Methods

KEYWORDS

benchmark, coupled cluster theory, database, excitation energies, excited states, full configuration interaction

1 | INTRODUCTION

Nowadays, there exist a very large number of electronic structure computational approaches, more or less expensive depending on their overall accuracy, able to quantitatively predict the absolute, and/or relative energies of electronic states in molecular systems.[1–4] One important aspect of some of these theoretical methods is their ability to access the energies of electronic excited states, that is, states that have higher total energies than the so-called ground (i.e., lowest-energy) state.[5–15] The faithful description of excited states is particularly challenging from a theoretical point of view but is key to a deeper understanding of photochemical and photophysical processes such as absorption, fluorescence, phosphorescence, chemiluminescence, and so on.[16–22] For a given level of theory, ground-state methods are usually more accurate than their excited-state analogs. The reasons behind this are (at least) threefold: (i) accurately modeling the electronic structure of excited states usually requires larger one-electron basis sets (including diffuse functions most of the times) than their ground-state counterpart, (ii) excited states can be governed by different amounts of dynamic/static correlations, present very different physical natures ($\pi \to \pi^*$, $n \to \pi^*$, charge transfer, double excitation, valence, Rydberg, singlet, doublet, triplet, etc.), yet be very close in energy from one another, and (iii) one usually has to rely on response theory formalisms,[23–30] which inherently introduce a ground-state "bias." Hence, designing excited-state methods able to tackle simultaneously and on an equal footing all these types of excited states at an affordable cost remains an open challenge in theoretical computational chemistry as evidenced by the large number of review articles on this particular subject.[5–15, 31]

When designing a new theoretical model, the first feature that one might want to test is its overall accuracy, that is, its ability to reproduce reference (or benchmark) values for a given system with a well-defined setup (same geometry, basis set, etc.). These values can be absolute and/or relative energies, geometrical parameters, physical or chemical spectroscopic properties extracted from experiments, high-level theoretical calculations, or any combination of these. To this end, the electronic structure community has designed along the years benchmark sets, that is, sets of molecules for which one can (very) accurately compute theoretical estimates and/or access solid experimental data for given properties. Regarding ground-state properties, two of the oldest and most employed sets are probably the Gaussian-1 and Gaussian-2 benchmark sets[32–34] developed by the group of Pople in the 1990s. For example, the Gaussian-2 set gathers atomization energies, ionization energies, electron affinities, proton affinities, bond dissociation energies, and reaction barriers. This set was subsequently extended and refined.[35, 36] Another very useful set for the design of methods able to catch dispersion effects[37] is the S22 benchmark set[38] (and its extended S66 version[39]) of Hobza and collaborators which provides benchmark interaction energies for weakly interacting (noncovalent) systems. One could also mentioned the GW100 set[40–42] (and its GW5000 extension[43]) of ionization energies which has helped enormously the community to compare the implementation of GW-type methods for molecular systems.[44–47] The extrapolated ab initio thermochemistry set designed to achieve high accuracy for enthalpies of formation of atoms and small molecules (without experimental data) is yet another successful example of benchmark set.[48–50] More recently, let us mention the benchmark datasets of the *Simons Collaboration on the Many-Electron Problem* providing, for example, highly accurate ground-state energies for hydrogen chains[51] as well as transition metal atoms and their ions and monoxides.[52] Let us also mention the set of Zhao and Truhlar for small transition metal complexes employed to compare the accuracy of density-functional methods[53] for $3d$ transition-metal chemistry,[54] the MGCDB84 molecular database of Mardirossian and Head-Gordon that they used to benchmark a total of 200 density functionals and design (using a combinatorial approach) the ωB97M-V functional,[55] and finally the popular GMTKN24,[56] GMTKN30,[57, 58] and GMTKN55[59] databases for general main group thermochemistry, kinetics, and noncovalent interactions developed by Goerigk, Grimme, and their coworkers.

The examples of benchmark sets presented above are all designed for ground-state properties, and there exist specific protocols tailored to accurately model excited-state energies and properties as well. Indeed, benchmark datasets of excited-state energies and/or properties are less numerous than their ground-state counterparts but their number has been growing at a consistent pace in the past few years. Below, we provide a short description for some of them. One of the most characteristic examples is the benchmark set of vertical excitation energies proposed by Thiel and coworkers.[60–63] The so-called Thiel (or Mülheim) set of excitation energies gathers a large number of excitation energies determined in 28 medium-sized organic CNOH molecules with a total of 223 valence excited states (152 singlet and 71 triplet states) for which theoretical best estimates (TBEs) were defined. In their first study, Thiel and collaborators performed CC2,[64, 65] CCSD,[25, 66–68] CC3,[26, 69] and CASPT2[5, 70–72] calculations (with the TZVP basis) on MP2/6-31G (d) geometries in order to provide (based on additional high-quality literature data) TBEs for these transitions. These TBEs were quickly refined with the larger aug-cc-pVTZ basis set.[62, 63] In the same spirit, it is also worth mentioning

Gordon's set of vertical transitions (based on experimental values)[73] used to benchmark the performance of time-dependent density-functional theory (TD-DFT),[74–77] as well as its extended version by Goerigk and coworkers who decided to replace the experimental reference values by CC3 excitation energies.[78–80] For comparisons with experimental values, there also exist various sets of measured 0-0 energies used in various benchmarks, notably by the Furche,[81, 82] Hättig,[83] and our[84–86] groups for gas-phase compounds and by Grimme[87, 88] and one of us[89, 90] for solvated dyes. Let us also mention the new benchmark set of charge-transfer excited states recently introduced by Szalay and coworkers (based on equation-of-motion coupled cluster [EOM-CC] methods)[91] as well as the Gagliardi-Truhlar set employed to compare the accuracy of multiconfiguration pair-density functional theory[13] against the well-established CASPT2 method.[92]

Following a similar philosophy and striving for chemical accuracy, we have recently reported in several studies highly accurate vertical excitations for small- and medium-sized molecules.[15, 93–96] The so-called QUEST dataset of vertical excitations which we will describe in detail in the present review article is composed by 5 subsets (see Figure 1): (i) a subset of excitations in small molecules containing from 1 to 3 non-hydrogen atoms known as QUEST#1, (ii) a subset of double excitations in molecules of small and medium sizes known as QUEST#2, (iii) a subset of excitation energies for medium-sized molecules containing from 4 to 6 non-hydrogen atoms known as QUEST#3, (iv) a subset composed by more "exotic" molecules and radicals labeled as QUEST#4, and (v) a subset known as QUEST#5, specifically designed for the present article, gathering excitation energies in larger molecules as well as additional smaller molecules. One of the key aspects of the QUEST dataset is that it does not rely on any experimental values, avoiding potential biases inherently linked to experiments and facilitating in the process theoretical comparisons. Moreover, our protocol has been designed to be as uniform as possible, which means that we have designed a very systematic procedure for all excited states in order to make cross-comparison as straightforward as possible. Importantly, it allowed us to benchmark, in a very systematic and balanced way, a series of popular excited-state wave function methods partially
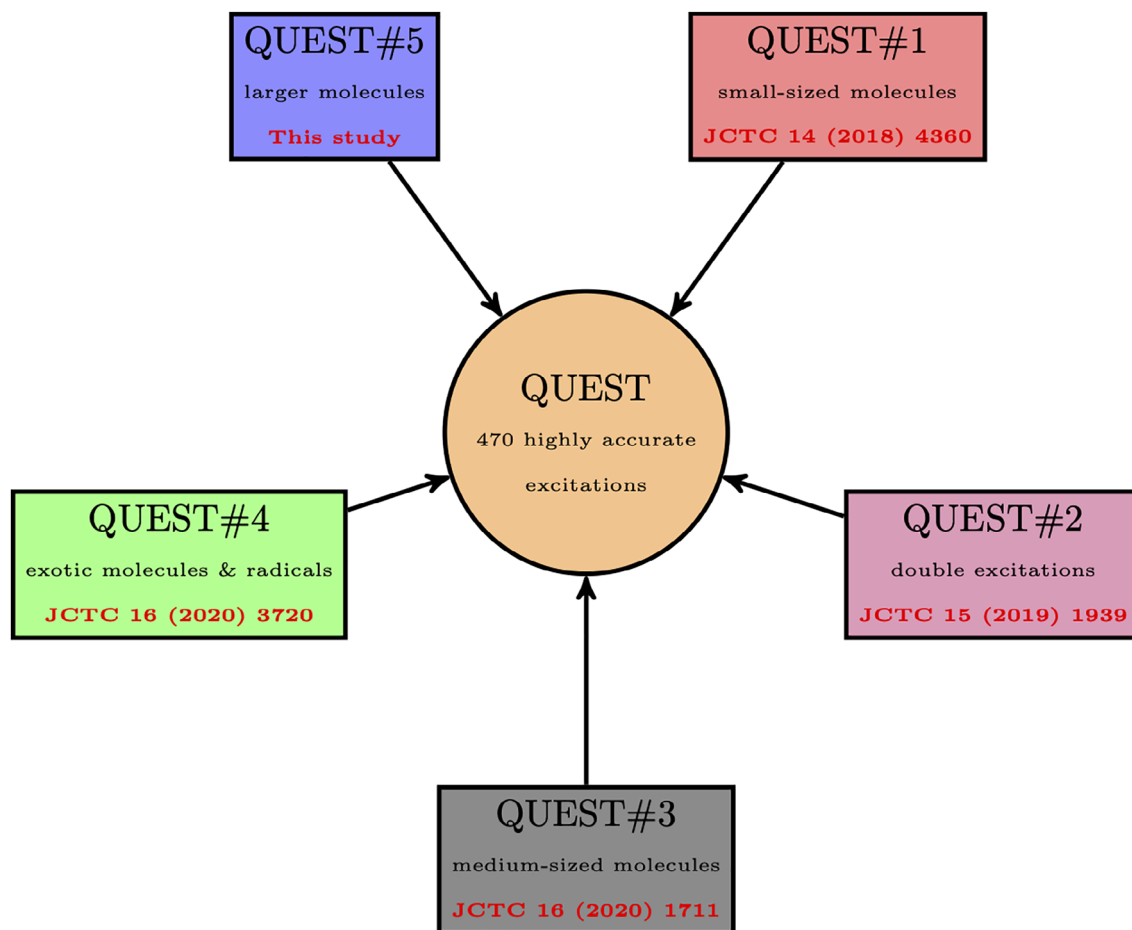
FIGURE 1 Composition of each of the five subsets making up the present QUEST dataset of highly accurate vertical excitation energies

or fully accounting for double and triple excitations as well as multiconfigurational methods (see below). In the same vein, as evoked above, we have also produced chemically accurate theoretical 0-0 energies[84–86] which can be more straightforwardly compared to experimental data.[81–83, 87–90, 97–99] We refer the interested reader to Ref. 86 for a review of the generic benchmark studies devoted to adiabatic and 0-0 energies performed in the past two decades.

The QUEST dataset has the particularity to be based to a large extent on selected configuration interaction (SCI) reference excitation energies as well as high-order linear-response (LR) CC methods such as LR-CCSDT and LR-CCSDTQ.[25, 27, 29, 100–106] Recently, SCI methods have been a force to reckon with for the computation of highly accurate energies in small- and medium-sized molecules as they yield near full configuration interaction (FCI) quality energies for only a very tiny fraction of the computational cost of a genuine FCI calculation.[15, 93–96, 107–128] Due to the fairly natural idea underlying these methods, the SCI family is composed of numerous members.[94, 116–118, 129–155] Their fundamental philosophy consists, roughly speaking, in retaining only the most relevant determinants of the FCI space following a given criterion to slow down the exponential increase of the size of the CI expansion. Originally developed in the late 1960s by Bender and Davidson[129] as well as Whitten and Hackmeyer,[130] new efficient SCI algorithms have resurfaced recently. Three examples are iCI,[151, 156–158] semistochastic heat-bath CI,[116, 118–120, 141, 142] and *configuration interaction using a perturbative selection made iteratively* (CIPSI).[131, 135, 137, 159] These flavors of SCI include a second-order perturbative (PT2) correction which is key to estimate the "distance" to the FCI solution (see below). The SCI calculations performed for the QUEST set of excitation energies rely on the CIPSI algorithm, which is, from a historical point of view, one of the oldest SCI algorithms. It was developed in 1973 by Huron et al.[131] (see also Refs. 160–164). Recently, the determinant-driven CIPSI algorithm has been efficiently implemented[159] in the open-source programming environment QUANTUM PACKAGE enabling to perform massively parallel computations.[127, 138, 145, 159] CIPSI is also frequently employed to provide accurate trial wave functions for quantum Monte Carlo calculations in molecules[135–137, 139, 140, 143, 144, 165–170] and more recently for periodic solids.[171] We refer the interested reader to Ref. 159 where one can find additional details regarding the implementation of the CIPSI algorithm.

The present article is organized as follows. In Section 2, we detail the specificities of our protocol by providing computational details regarding geometries, basis sets (reference and benchmarked), computational methods, and a new way of estimating rigorously the extrapolation error in SCI calculations which is tested by computing additional FCI values for five- and six-membered rings. We then describe in Section 3 the content of our five QUEST subsets providing for each of them the number of reference excitation energies, the nature and size of the molecules, the list of benchmarked methods, as well as other specificities. A special emphasis is placed on our latest (previously unpublished) add-on, QUEST#5, specifically designed for the present manuscript where we have considered, in particular but not only, larger molecules. Section 4 discusses the generation of the TBEs, whereas Section 5 proposes a comprehensive benchmark of various methods on the entire QUEST set which is composed by more than 400 excitations with, in addition, a specific analysis for each type of excited states. Section 6 describes the feature of the website that we have specifically designed to gather the entire data generated during these last few years. Thanks to this website, one can easily test and compare the accuracy of a given method with respect to various variables such as the molecule size or its family, the nature of the excited states, the size of the basis set, etc. Finally, we draw our conclusions in Section 7 where we discuss, in particular, future projects aiming at expanding and improving the usability and accuracy of the QUEST database.

2 | COMPUTATIONAL TOOLS

2.1 | Geometries

The ground-state structures of the molecules included in the QUEST dataset have been systematically optimized at the CC3/aug-cc-pVTZ level of theory, except for a very few cases. As shown in Refs. 30, 172, CC3 provides extremely accurate ground- and excited-state geometries. These optimizations have been performed using DALTON 2017[173] and CFOUR 2.1[174] applying default parameters. For the open-shell derivatives belonging to QUEST#4,[96] the geometries are optimized at the UCCSD(T)/aug-cc-pVTZ level using the GAUSSIAN16 program[175] and applying the "tight" convergence threshold. For the purpose of the present review article, we have gathered all the geometries in the Supporting information.

2.2 | Basis sets

For the entire set, we rely on the 6-31+G(d) Pople basis set,[176–182] the augmented family of Dunning basis sets aug-cc-pVXZ (where X = D, T, Q, and 5),[183–187] and sometimes its doubly- and triply-augmented variants, d-aug-cc-pVXZ and t-aug-cc-pVXZ respectively. Doubly- and triply-augmented basis sets are usually employed for Rydberg states where it is not uncommon to observe a strong basis set dependence due to the very diffuse nature of these excited states. These basis sets are available from the Basis Set Exchange website (https://www.basissetexchange.org).[188–190]

2.3 | Computational methods

2.3.1 | Reference computational methods

In order to compute reference vertical energies, we have designed different strategies depending on the actual nature of the transition and the size of the system. For small molecules (typically 1–3 non-hydrogen atoms), we mainly resort to SCI methods which can provide near-FCI excitation energies for compact basis sets. Obviously, the smaller the molecule, the larger the basis we can afford. For larger systems (i.e., 4–6 non-hydrogen atom), one cannot afford SCI calculations anymore except in a few special occasions, and we then rely on LR-CC theory (LR-CCSDT and LR-CCSDTQ typically[29, 101, 104–106]) to obtain accurate transition energies. In the following, we will omit the prefix LR for the sake of clarity, as equivalent values would be obtained with the EOM formalism.[66, 67]

The CC calculations are performed with several codes. For closed-shell molecules, CC3[26, 69] calculations are achieved with DALTON[173] and CFOUR.[174] CCSDT and CCSDTQ calculations are performed with CFOUR[174] and MRCC 2017,[191, 192] the latter code being also used for CCSDTQP. The reported oscillator strengths have been computed in the LR-CC3 formalism only. For open-shell molecules, the CCSDT, CCSDTQ, and CCSDTQP calculations performed with MRCC[191, 192] do consider an unrestricted Hartree–Fock wave function as reference but for a few exceptions. All excited-state calculations are performed, except when explicitly mentioned, in the frozen-core (FC) approximation using large cores for the third-row atoms.

All the SCI calculations are performed within the FC approximation using QUANTUM PACKAGE[159] where the CIPSI algorithm[131] is implemented. Details regarding this specific CIPSI implementation can be found in Refs. 159, 167. A state-averaged formalism is employed, that is, the ground and excited states are described with the same set of determinants and orbitals, but different CI coefficients. Our usual protocol[15, 93–96, 143, 144, 167] consists of performing a preliminary CIPSI calculation using Hartree–Fock orbitals in order to generate a CIPSI wave function with at least 10^7 determinants. Natural orbitals are then computed based on this wave function, and a new, larger CIPSI calculation is performed with this new set of orbitals. This has the advantage to produce a smoother and faster convergence of the SCI energy toward the FCI limit. The CIPSI energy E_{CIPSI} is defined as the sum of the variational energy E_{var} (computed via diagonalization of the CI matrix in the reference space) and a PT2 correction E_{PT2} which estimates the contribution of the determinants not included in the CI space.[138] By linearly extrapolating this second-order correction to zero, one can efficiently estimate the FCI limit for the total energies. These extrapolated total energies (simply labeled as E_{FCI} in the remainder of the paper) are then used to compute vertical excitation energies.

Depending on the set, we estimated the extrapolation error via different techniques. For example, in Ref. 95, we estimated the extrapolation error by the difference between the transition energies obtained with the largest SCI wave function and the FCI extrapolated value. This definitely cannot be viewed as a true error bar, but it provides an idea of the quality of the FCI extrapolation and estimate. Below, we provide a much cleaner way of estimating the extrapolation error in SCI methods, and we adopt this scheme for the five- and six-membered rings considered in the QUEST#3 subset. The particularity of the current implementation is that the selection step and the PT2 correction are computed *simultaneously* via a hybrid semistochastic algorithm.[138, 159] Moreover, a renormalized version of the PT2 correction (dubbed rPT2) has been recently implemented for a more efficient extrapolation to the FCI limit.[159] We refer the interested reader to Ref. 159 where one can find all the details regarding the implementation of the CIPSI algorithm. Note that all our SCI wave functions are eigenfunctions of the $\hat{S}^2$ spin operator which is, unlike ground-state calculations, paramount in the case of excited states.[193] In the case of ground-state calculations, this constraint can be relaxed without altering the final result (see, e.g., Ref. 127).

2.3.2 | Benchmarked computational methods

Using a large variety of codes, our benchmark effort consists in evaluating the accuracy of vertical transition energies obtained at lower levels of theory. For example, we rely on GAUSSIAN[175] and TURBOMOLE 7.3[194] for CIS(D)[195, 196]; Q-CHEM 5.2[197] for EOM-MP2 [CCSD(2)][198] and ADC(3)[31, 199, 200]; Q-CHEM[197] and TURBOMOLE[194] for ADC(2)[31, 201]; DALTON[173] and TURBOMOLE[194] for CC2[64, 65]; DALTON[173] and GAUSSIAN[175] for CCSD[25, 67, 68]; DALTON[173] for CCSDR(3)[202]; CFOUR[174] for CCSDT-3[203, 204]; and ORCA[205] for similarity-transformed EOM-CCSD (STEOM-CCSD).[206, 207] In addition, we evaluate the spin-opposite scaling (SOS) variants of ADC(2), SOS-ADC(2), as implemented in both Q-CHEM[208] and TURBOMOLE.[209] Note that these two codes have distinct SOS implementations, as explained in Ref. 208. We also test the SOS and spin-component scaled (SCS) versions of CC2, as implemented in TURBOMOLE.[194, 209] Discussion of various spin-scaling schemes can be found elsewhere.[88] For the STEOM-CCSD calculations, it was checked that the active character percentage was, at least, 98%. For radicals, we applied both the U (unrestricted) and RO (restricted open-shell) versions of CCSD and CC3 as implemented in the PSI4 code[210] to perform our benchmarks. Finally, the composite approach, ADC(2.5), which follows the spirit of Grimme's and Hobza's MP2.5 approach[211] by averaging the ADC(2) and ADC(3) excitation energies, is also tested in the following.[212]

For the double excitations composing the QUEST database, we have performed additional calculations using various multiconfigurational methods. In particular, state-averaged (SA) CASSCF and CASPT2[70, 72] have been performed with MOLPRO (RS2 contraction level).[213] Concerning the NEVPT2 calculations (which are also performed with MOLPRO), the partially contracted (PC) and strongly contracted (SC) variants have been tested.[214–216] From a strict theoretical point of view, we point out that PC-NEVPT2 is supposed to be more accurate than SC-NEVPT2 given that it has a larger number of perturbers and greater flexibility. PC-NEVPT2 calculations were also systematically performed for the QUEST#3. In the case of double excitations,[94] we have also performed calculations with multi-state (MS) CASPT2 (MS-MR formalism),[217] and its extended variant (XMS-CASPT2)[218] when there is a strong mixing between states with same spin and spatial symmetries. The CASPT2 calculations have been performed with level shift and IPEA parameters set to the standard values of 0.3 and 0.25 a.u., respectively. Large active spaces carefully chosen and tailored for the desired transitions have been selected. The definition of the active space considered for each system as well as the number of states in the state-averaged calculation is provided in their corresponding publication.

2.3.3 | Estimating the extrapolation error

In this section, we present our scheme to estimate the extrapolation error in SCI calculations. This new protocol is then applied to five- and six-membered ring molecules for which SCI calculations are particularly challenging even for small basis sets. Note that the present method does only apply to *state-averaged* SCI calculations where ground- and excited-state energies are produced during the same calculation with the same set of molecular orbitals, not to *state-specific* calculations where one computes solely the energy of a single state (like conventional ground-state calculations).

For the mth excited state (where $m = 0$ corresponds to the ground state), we usually estimate its FCI energy $E_{\text{FCI}}^{(m)}$ by performing a linear extrapolation of its variational energy $E_{\text{var}}^{(m)}$ as a function of its rPT2 correction $E_{\text{rPT2}}^{(m)}$ [116, 159] using

$$E_{\text{var}}^{(m)} \approx E_{\text{FCI}}^{(m)} - \alpha^{(m)} E_{\text{rPT2}}^{(m)}, \qquad (1)$$

where $E_{\text{var}}^{(m)}$ and $E_{\text{rPT2}}^{(m)}$ are calculated with CIPSI and $E_{\text{FCI}}^{(m)}$ is the FCI energy to be extrapolated. This relation is valid in the regime of a sufficiently large number of determinants where the second-order perturbational correction largely dominates. In theory, the coefficient $\alpha^{(m)}$ should be equal to one but, in practice, due to the residual higher-order terms, it deviates slightly from unity.

For the largest systems considered here, E_{rPT2} can be as large as 2 eV and, thus, the accuracy of the excitation energy estimates strongly depends on our ability to compensate the errors in the calculations. Here, we greatly enhance the compensation of errors by making use of our selection procedure ensuring that the rPT2 values of both states match as well as possible (a trick known as PT2 matching[168, 169]), that is, $E_{\text{rPT2}}^{(0)} \approx E_{\text{rPT2}}^{(m)}$, and by using a common set of state-averaged natural orbitals with equal weights for the ground and excited states.

Using Equation (1) the estimated error on the CIPSI energy is calculated as

$$E_{\text{CIPSI}}^{(m)} - E_{\text{FCI}}^{(m)} = \left(E_{\text{var}}^{(m)} + E_{\text{rPT2}}^{(m)} \right) - E_{\text{FCI}}^{(m)} = \left(1 - \alpha^{(m)} \right) E_{\text{rPT2}}^{(m)} \tag{2}$$

and thus the extrapolated excitation energy associated with the mth excited state is given by

$$\Delta E_{\text{FCI}}^{(m)} = \left[E_{\text{var}}^{(m)} + E_{\text{rPT2}}^{(m)} + \left(\alpha^{(m)} - 1 \right) E_{\text{rPT2}}^{(m)} \right] - \left[E_{\text{var}}^{(0)} + E_{\text{rPT2}}^{(0)} + \left(\alpha^{(0)} - 1 \right) E_{\text{rPT2}}^{(0)} \right]. \tag{3}$$

The slopes $\alpha^{(m)}$ and $\alpha^{(0)}$ deviating only slightly from the unity, the error in $\Delta E_{\text{FCI}}^{(m)}$ can be expressed at leading order as $\left(\alpha^{(m)} - \alpha^{(0)} \right) \bar{E}_{\text{rPT2}} + \mathcal{O}\left[\bar{E}_{\text{rPT2}}^2 \right]$, where $\bar{E}_{\text{rPT2}} = \left(E_{\text{rPT2}}^{(m)} + E_{\text{rPT2}}^{(0)} \right)/2$ is the averaged second-order correction.

In the ideal case where one is able to fully correlate the CIPSI calculations associated with the ground and excited states, the fluctuations of $\Delta E_{\text{CIPSI}}^{(m)}(n)$ as a function of the iteration number n would completely vanish and the exact excitation energy would be obtained from the first CIPSI iterations. Quite remarkably, in practice, numerical experience shows that the fluctuations with respect to the extrapolated value $\Delta E_{\text{FCI}}^{(m)}$ are small, zero-centered, and display a Gaussian-like distribution. In addition, as evidenced in Figure 2, these fluctuations are found to be (very weakly) dependent on the iteration number n (as far as not too close n values are considered). Hence, this weak dependency does not significantly alter our results and will not be considered here.

We thus introduce the following random variable

$$X^{(m)} = \frac{\Delta E_{\text{CIPSI}}^{(m)}(n) - \Delta E_{\text{FCI}}^{(m)}}{\sigma(n)}, \tag{4}$$

where

$$\Delta E_{\text{CIPSI}}^{(m)}(n) = \left[E_{\text{var}}^{(m)}(n) + E_{\text{rPT2}}^{(m)}(n) \right] - \left[E_{\text{var}}^{(0)}(n) + E_{\text{rPT2}}^{(0)}(n) \right] \tag{5}$$

and $\sigma(n)$ is a quantity proportional to the average fluctuations of $\Delta E_{\text{CIPSI}}^{(m)}$. A natural choice for $\sigma^2(n)$, playing here the role of a variance, is

$$\sigma^2(n) \propto \left[E_{\text{rPT2}}^{(m)}(n) \right]^2 + \left[E_{\text{rPT2}}^{(0)}(n) \right]^2, \tag{6}$$

which vanishes in the large-n limit (as it should).

The histogram of $X^{(m)}$ resulting from the singlet and triplet excitation energies obtained at various iteration number n for the 13 five- and six-membered ring molecules is shown in Figure 2. To avoid transient effects, only excitation energies at sufficiently large n are retained in the dataset. The statistical criterion used to decide from which precise value of n the data should be kept is presented below. In the present example, the total number of values employed to construct

FIGURE 2 Histogram of the random variable $X^{(m)}$ (see Equation (4) in the main text for its definition). About 200 values of singlet and triplet excitation energies taken at various iteration number n for the 13 five- and six-membered ring molecules have been considered to build the present histogram. The number M of iterations kept at each calculation is chosen according to the statistical test presented in the text
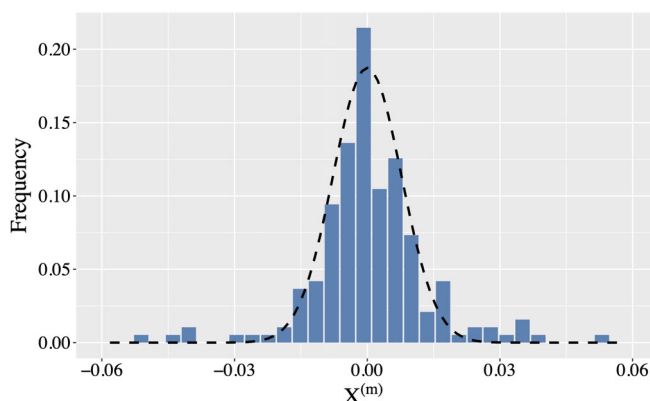
the histogram of Figure 2 is about 200. The dashed line represents the best (in a least-squares sense) Gaussian fit reproducing the data. As clearly seen from Figure 2, the distribution can be fairly well described by a Gaussian probability distribution

$$P\left[X^{(m)}\right] \propto \exp\left[-\frac{X^{(m)2}}{2\sigma^{*2}}\right],\tag{7}$$

where σ^{*2} is some "universal" variance depending only on the way the correlated selection of both states is done, not on the molecule considered in our set.

For each CIPSI calculation, an estimate of $\Delta E_{\text{FCI}}^{(m)}$ is thus

$$\Delta E_{\text{FCI}}^{(m)} = \frac{\sum_{n=1}^{M} \frac{\Delta E_{\text{CIPSI}}^{(m)}(n)}{\sigma(n)}}{\sum_{n=1}^{M} \frac{1}{\sigma(n)}},\tag{8}$$

where M is the number of iterations that has been retained to compute the statistical quantities. Regarding the estimate of the error on $\Delta E_{\text{FCI}}^{(m)}$ some caution is required since, although the distribution is globally Gaussian-like (see Figure 2), there exists some significant deviation from it and we must take this feature into account.

More precisely, we search for a confidence interval $\mathscr{I}$ such that the true value of the excitation energy $\Delta E_{\text{FCI}}^{(m)}$ lies within one standard deviation of $\Delta E_{\text{CIPSI}}^{(m)}$, that is, $P\left(\Delta E_{\text{FCI}}^{(m)} \in \left[\Delta E_{\text{CIPSI}}^{(m)} \pm \sigma\right] \Big| \mathscr{G}\right) = p = 0.6827$. In a Bayesian framework, the probability that $\Delta E_{\text{FCI}}^{(m)}$ is in an interval $\mathscr{I}$ is

$$P\left(\Delta E_{\text{FCI}}^{(m)} \in \text{I}\right) = P\left(\Delta E_{\text{FCI}}^{(m)} \in I | \mathscr{G}\right) \times P(\mathscr{G}),\tag{9}$$

where $P(\mathscr{G})$ is the probability that the random variables considered in the latest CIPSI iterations are normally distributed. A common test in statistics of the normality of a distribution is the Jarque-Bera test J and we have

$$P(\mathscr{G}) = 1 - \chi_{\text{CDF}}^2(J, 2),\tag{10}$$

where $\chi_{\text{CDF}}^2(x, k)$ is the cumulative distribution function (CDF) of the χ^2-distribution with k degrees of freedom. As the number of samples M is usually small, we use Student's t-distribution to estimate the statistical error. The inverse of the CDF of the t-distribution, t_{CDF}^{-1}, allows us to find how to scale the interval by a parameter

$$\beta = t_{\text{CDF}}^{-1}\left[\frac{1}{2}\left(1 + \frac{0.6827}{P(\mathscr{G})}\right), M\right]\tag{11}$$

such that $P\left(\Delta E_{\text{FCI}}^{(m)} \in \left[\Delta E_{\text{CIPSI}}^{(m)} \pm \beta\sigma\right]\right) = p$. Only the last $M > 2$ computed transition energies are considered. M is chosen such that $P(\mathscr{G}) > 0.8$ and such that the error bar is minimal. If all the values of $P(\mathscr{G})$ are below 0.8, M is chosen such that $P(\mathscr{G})$ is maximal. A Python code associated with this procedure is provided in the Supporting information.

The singlet and triplet FCI/6-31+G(d) excitation energies and their corresponding error bars estimated with the method presented above based on Gaussian random variables are reported in Table 1. For the sake of comparison, we also report the CC3 and CCSDT vertical energies from Ref. 95 computed in the same basis. We note that there is for the vast majority of considered states a very good agreement between the CC3 and CCSDT values, indicating that the CC values can be trusted. The estimated values of the excitation energies obtained via a three-point linear extrapolation considering the three largest CIPSI wave functions are also gathered in Table 1. In this case, the error bar is estimated via the extrapolation distance, that is, the difference in excitation energies obtained with the three-point linear extrapolation and the largest CIPSI wave function. This strategy has been considered in some of our previous works.[95, 96, 127]

The deviation from the CCSDT excitation energies for the same set of excitations is depicted in Figure 3, where the red dots correspond to the excitation energies and error bars estimated via the present method, and the blue dots correspond to the excitation energies obtained via a three-point linear fit and error bars estimated via the extrapolation
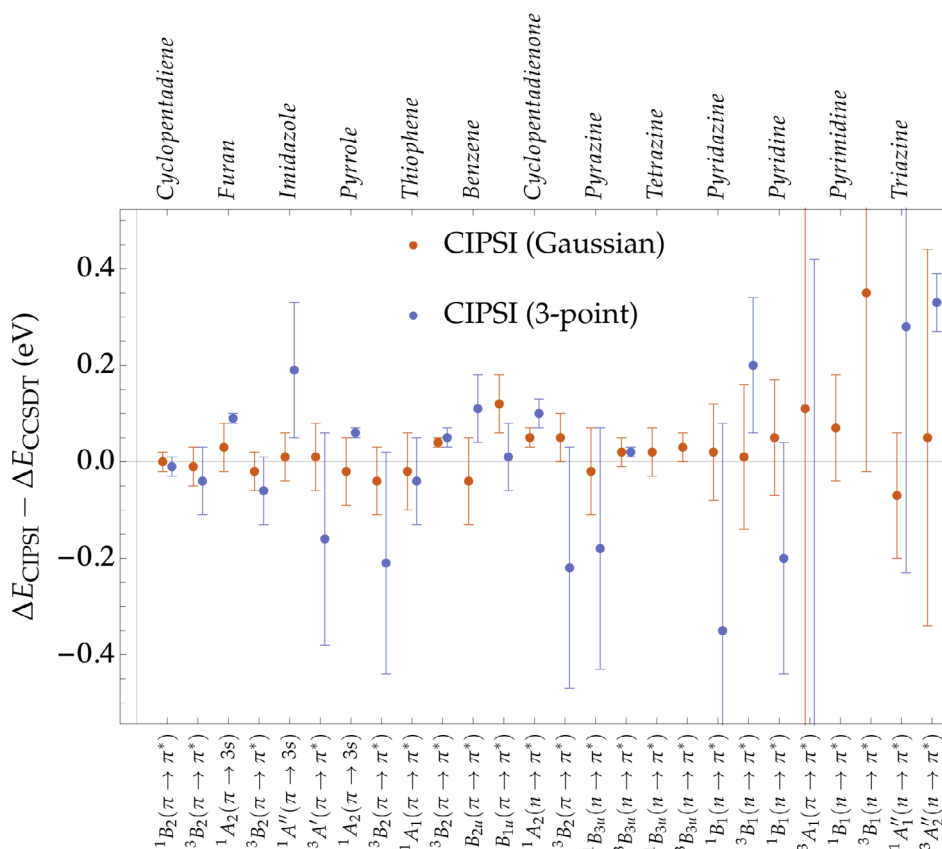
TABLE 1 Singlet and triplet excitation energies (in eV) obtained at the CC3, CCSDT, and CIPSI levels of theory with the 6-31+G(d) basis set for various five- and six-membered rings

Molecule	Transition	CC3	CCSDT	CIPSI (Gaussian)[a]	CIPSI (3-point)[b]
Five-membered rings					
Cyclopentadiene	$^1B_2(\pi \rightarrow \pi^*)$	5.79	5.80	5.80 (2)	5.79 (2)
	$^3B_2(\pi \rightarrow \pi^*)$	3.33	3.33	3.32 (4)	3.29 (7)
Furan	$^1A_2(\pi \rightarrow 3s)$	6.26	6.28	6.31 (5)	6.37 (1)
	$^3B_2(\pi \rightarrow \pi^*)$	4.28	4.28	4.26 (4)	4.22 (7)
Imidazole	$^1A''(\pi \rightarrow 3s)$	5.77	5.77	5.78 (5)	5.96 (14)
	$^3A'(\pi \rightarrow \pi^*)$	4.83	4.81	4.82 (7)	4.65 (22)
Pyrrole	$^1A_2(\pi \rightarrow 3s)$	5.25	5.25	5.23 (7)	5.31 (1)
	$^3B_2(\pi \rightarrow \pi^*)$	4.59	4.58	4.54 (7)	4.37 (23)
Thiophene	$^1A_1(\pi \rightarrow \pi^*)$	5.79	5.77	5.75 (8)	5.73 (9)
	$^3B_2(\pi \rightarrow \pi^*)$	3.95	3.94	3.98 (1)	3.99 (2)
Six-membered rings					
Benzene	$^1B_{2u}(\pi \rightarrow \pi^*)$	5.13	5.10	5.06 (9)	5.21 (7)
	$^3B_{1u}(\pi \rightarrow \pi^*)$	4.18	4.16	4.28 (6)	4.17 (7)
Cyclopentadienone	$^1A_2(n \rightarrow \pi^*)$	3.03	3.03	3.08 (2)	3.13 (3)
	$^3B_2(\pi \rightarrow \pi^*)$	2.30	2.32	2.37 (5)	2.10 (25)
Pyrazine	$^1B_{3u}(n \rightarrow \pi^*)$	4.28	4.28	4.26 (9)	4.10 (25)
	$^3B_{3u}(n \rightarrow \pi^*)$	3.68	3.68	3.70 (3)	3.70 (1)
Tetrazine	$^1B_{3u}(n \rightarrow \pi^*)$	2.53	2.54	2.56 (5)	5.07 (16)
	$^3B_{3u}(n \rightarrow \pi^*)$	1.87	1.88	1.91 (3)	4.04 (49)
Pyridazine	$^1B_1(n \rightarrow \pi^*)$	3.95	3.95	3.97 (10)	3.60 (43)
	$^3B_1(n \rightarrow \pi^*)$	3.27	3.26	3.27 (15)	3.46 (14)
Pyridine	$^1B_1(n \rightarrow \pi^*)$	5.12	5.10	5.15 (12)	4.90 (24)
	$^3A_1(\pi \rightarrow \pi^*)$	4.33	4.31	4.42 (85)	3.68 (105)
Pyrimidine	$^1B_1(n \rightarrow \pi^*)$	4.58	4.57	4.64 (11)	2.54 (5)
	$^3B_1(n \rightarrow \pi^*)$	4.20	4.20	4.55 (37)	2.18 (27)
Triazine	$^1A_1''(n \rightarrow \pi^*)$	4.85	4.84	4.77 (13)	5.12 (51)
	$^3A_2''(n \rightarrow \pi^*)$	4.40	4.40	4.45 (39)	4.73 (6)

[a]Excitation energies and error bars (in eV) estimated via the novel statistical method based on Gaussian random variables (see Section 2.3.3). The error bars reported in parenthesis correspond to one standard deviation.
[b]Excitation energies obtained via a three-point linear fit using the three largest CIPSI variational wave functions, and error bars (in eV) estimated via the extrapolation distance, that is, the difference in excitation energies obtained with the three-point linear extrapolation and the largest CIPSI wave function.

distance. These results contain a good balance between well-behaved and ill-behaved cases. For example, cyclopentadiene and furan correspond to well-behaved scenarios where the two flavors of extrapolations yield nearly identical estimates and the error bars associated with these two methods nicely overlap. In these cases, one can observe that our method based on Gaussian random variables provides almost systematically smaller error bars. Even in less idealistic situations (like in imidazole, pyrrole, and thiophene), the results are very satisfactory and stable. The six-membered rings represent much more challenging cases for SCI methods, and even for these systems the newly developed method provides realistic error bars, and allows to easily detect problematic events (like pyridine for instance). The present scheme has also been tested on smaller systems when one can tightly converge the CIPSI calculations. In such cases, the agreement is nearly perfect in every scenario that we have encountered. A selection of these results can be found in the Supporting information.

FIGURE 3 Deviation from the CCSDT excitation energies for the lowest singlet and triplet excitation energies (in eV) of five- and six-membered rings obtained at the CIPSI/6-31+G(d) level of theory. Red dots: excitation energies and error bars estimated via the present method (see Section 2.3.3). Blue dots: excitation energies obtained via a three-point linear fit using the three largest CIPSI wave functions, and error bars estimated via the extrapolation distance, that is, the difference in excitation energies obtained with the three-point linear extrapolation and the largest CIPSI wave function

3 | THE QUEST DATABASE

3.1 | Overview

The QUEST database gathers more than 500 highly accurate excitation energies of various natures (valence, Rydberg, $n \rightarrow \pi^*$, $\pi \rightarrow \pi^*$, singlet, doublet, triplet, and double excitations) for molecules ranging from diatomics to molecules as large as naphthalene (see Figure 4). This set is also chemically diverse, with organic and inorganic systems, open- and closed-shell compounds, acyclic and cyclic systems, pure hydrocarbons and various heteroatomic structures, and so on. Each of the five subsets making up the QUEST dataset is detailed below. Throughout the present review, we report several statistical indicators: the mean signed error (MSE), mean absolute error (MAE), root-mean square error, and standard deviation of the errors, as well as the maximum positive [Max(+)] and maximum negative [Max(−)] errors.

3.2 | QUEST#1

The QUEST#1 benchmark set[93] consists of 110 vertical excitation energies (as well as oscillator strengths) from 18 molecules with sizes ranging from one to three non-hydrogen atoms (water, hydrogen sulfide, ammonia, hydrogen chloride, dinitrogen, carbon monoxide, acetylene, ethylene, formaldehyde, methanimine, thioformaldehyde, acetaldehyde, cyclopropene, diazomethane, formamide, ketene, nitrosomethane, and the smallest streptocyanine). For this set, we provided two sets of TBEs: (i) one obtained within the FC approximation and the aug-cc-pVTZ basis set, and (ii) another one including further corrections for basis set incompleteness and "all electron" effects. For the former set,

1 (non-H) atom molecules

Ammonia | Be | BeH (rad) | BH₂ (rad) | CH (rad) | CH₃ (rad) | Hydrogen chloride | Hydrogen sulfide | NH₂ (rad) | OH (rad) | PH₂ (rad) | Water

2 (non-H) atom molecules

Acetylene | BeF (rad) | Carbon dimer | C=O | Carbon monoxide | CO⁺ (rad) | CN (rad) | Dinitrogen | Ethylene | Formaldehyde | HCCl | HCF

HCO | HCP | HOC | HPO | HPS | HSiF | H₂BO (rad) | H₂PO (rad) | H₂PS (rad) | Methanimine | Nitroxyl

NO (rad) | Silylidene | Thioformaldehyde | Vinyl (rad)

3 (non-H) atom molecules

Acetaldehyde | Allyl (rad) | Carbon trimer | CCl₂ | CClF | CF₂ | CON (rad) | CNO (rad) | Cyclopropene | Diazirine

Diazomethane | Formamide | Formyl fluoride | Ketene | NCO (rad) | Nitrosomethane | SiCl₂ | Streptocyanine-1

4 (non-H) atom molecules

Acetone | Acrolein | Butadiene | Carbonyl fluoride | Cyanoacetylene | Cyanoformaldehyde | Cyanogen | Cyclopropenone

Cyclopropenethione | Diacetylene | F₂BO (rad) | F₂BS (rad) | Glyoxal | Isobutene | Methylenecyclopropene

Nitromethyl (rad) | Propynal | Thioacetone | Thioacrolein | Thiopropynal

5 (non-H) atom molecules

Cyclopentadiene | Difluorodiazirine | Furan | Imidazole | Pyrrole | Streptocyanine-3 | Thiophene

6-10 (non-H) atom molecules

Benzene | Cyclopentadienone | Cyclopentadienethione | Hexatriene | Pyrazine | Pyridazine | Pyridine | Pyrimidine | Tetrazine

Triazine | Maleimide | Streptocyanine-5 | Benzoquinone | Octatetraene | Azanaphthalene | Naphthalene

FIGURE 4 Molecules from each of the five subsets making up the present QUEST dataset of highly accurate vertical excitation energies: QUEST#1 (red), QUEST#2 (magenta and/or underlined), QUEST#3 (black), QUEST#4 (green), and QUEST#5 (blue)

we systematically employed FCI/aug-cc-pVTZ values to define our TBEs, except for a few cases. For the latter set, both the "all electron" correlation and the basis set corrections were systematically obtained at the CC3 level of theory and with the d-aug-cc-pV5Z basis for the nine smallest molecules, and slightly more compact basis sets for the larger

compounds. Our TBE/aug-cc-pVTZ reference excitation energies were employed to benchmark a series of popular excited-state wave function methods partially or fully accounting for double and triple excitations, namely CIS(D), CC2, CCSD, STEOM-CCSD, CCSDR(3), CCSDT-3, CC3, ADC(2), and ADC(3). Our main conclusions were that (i) ADC(2) and CC2 show strong similarities in terms of accuracy, (ii) STEOM-CCSD is, on average, as accurate as CCSD, the latter overestimating transition energies, (iii) CC3 is extremely accurate (with a mean absolute error of only ∼0.03 eV) and that although slightly less accurate than CC3, CCSDT-3 could be used as a reliable reference for benchmark studies, and (iv) ADC(3) was found to be significantly less accurate than CC3 by overcorrecting ADC(2) excitation energies.

3.3 | QUEST#2

The QUEST#2 benchmark set[94] reports reference energies for double excitations. This set gathers 20 vertical transitions from 14 small- and medium-sized molecules (acrolein, benzene, beryllium atom, butadiene, carbon dimer and trimer, ethylene, formaldehyde, glyoxal, hexatriene, nitrosomethane, nitroxyl, pyrazine, and tetrazine). The TBEs of the QUEST#2 set are obtained with SCI and/or multiconfigurational (CASSCF, CASPT2, (X)MS-CASPT2, and NEVPT2) calculations depending on the size of the molecules and the level of theory that we could afford. An important addition to this second study was also the inclusion of various flavors of multiconfigurational methods (CASSCF, CASPT2, and NEVPT2) in addition to high-order CC methods including, at least, perturbative triples (CC3, CCSDT, CCSDTQ, etc.). Our results demonstrated that the error of CC methods is intimately linked to the amount of double-excitation character in the vertical transition. For "pure" double excitations (i.e., for transitions which do not mix with single excitations), the error in CC3 and CCSDT can easily reach 1 and 0.5 eV, respectively, while it goes down to a few tenths of an eV for more common transitions involving a significant amount of single excitations (such as the well-known A_g transition in butadiene or the E_{2g} excitation in benzene). The quality of the excitation energies obtained with CASPT2 and NEVPT2 was harder to predict as the overall accuracy of these methods is highly dependent on both the system and the selected active space. Nevertheless, these two methods were found to be more accurate for transitions with a very small percentage of single excitations (error usually below 0.1 eV) than for excitations dominated by single excitations where the error is closer to 0.1–0.2 eV.

3.4 | QUEST#3

The QUEST#3 benchmark set[95] is, by far, our largest set, and consists of highly accurate vertical transition energies and oscillator strengths obtained for 27 molecules encompassing 4, 5, and 6 non-hydrogen atoms (acetone, acrolein, benzene, butadiene, cyanoacetylene, cyanoformaldehyde, cyanogen, cyclopentadiene, cyclopropenone, cyclopropenethione, diacetylene, furan, glyoxal, imidazole, isobutene, methylenecyclopropene, propynal, pyrazine, pyridazine, pyridine, pyrimidine, pyrrole, tetrazine, thioacetone, thiophene, thiopropynal, and triazine) for a total of 238 vertical transition energies and 90 oscillator strengths with a reasonably good balance between singlet, triplet, valence, and Rydberg excited states. For these 238 transitions, we have estimated that 224 are chemically accurate for the aug-cc-pVTZ basis and for the considered geometry. To define the TBEs of the QUEST#3 set, we employed CC methods up to the highest technically possible order (CC3, CCSDT, and CCSDTQ), and, when affordable SCI calculations with very large reference spaces (up to hundred million determinants in certain cases), as well as one of the most reliable multiconfigurational methods, NEVPT2, for double excitations. Most of our TBEs are based on CCSDTQ (4 non-hydrogen atoms) or CCSDT (5 and 6 non-hydrogen atoms) excitation energies. For all the transitions of the QUEST#3 set, we reported at least CCSDT/aug-cc-pVTZ (sometimes with basis set extrapolation) and CC3/aug-cc-pVQZ transition energies as well as CC3/aug-cc-pVTZ oscillator strengths for each dipole-allowed transition. Pursuing our previous benchmarking efforts, we confirmed that CC3 almost systematically delivers transition energies in agreement with higher-level theoretical models (±0.04 eV) except for transitions presenting a dominant double-excitation character where multiconfigurational methods like NEVPT2 have logically the edge. This settles down, at least for now, the debate by demonstrating the superiority of CC3 (in terms of accuracy) compared to methods like CCSDT-3 or ADC(3). For the latter model, this was further demonstrated in a recent study by two of the present authors.[212]

3.5 | QUEST#4

The QUEST#4 benchmark set[96] consists of two subsets of excitations and oscillator strengths. An "exotic" subset of 30 excited states for closed-shell molecules containing F, Cl, P, and Si atoms (carbonyl fluoride, CCl_2, CClF, CF_2, difluorodiazirine, formyl fluoride, HCCl, HCF, HCP, HPO, HPS, HSiF, $SiCl_2$, and silylidene) and a "radical" subset of 51 doublet-doublet transitions in 24 small radicals (allyl, BeF, BeH, BH_2, CH, CH_3, CN, CNO, CON, CO^+, F_2BO, F_2BS, H_2BO, HCO, HOC, H_2PO, H_2PS, NCO, NH_2, nitromethyl, NO, OH, PH_2, and vinyl) characterized by open-shell electronic configurations and an unpaired electron. This represents a total of 81 high-quality TBEs, the vast majority being obtained at the FCI level with at least the aug-cc-pVTZ basis set. We additionally performed high-order CC calculations to ascertain these estimates. For the exotic set, these TBEs have been used to assess the performances of 15 "lower-order" wave function approaches, including several CC and ADC variants. Consistent with our previous works, we found that CC3 is very accurate, whereas the trends for the other methods are similar to that obtained on more standard CNOSH organic compounds. In contrast, for the radical set, even the refined ROCC3 method yields a comparatively large MAE of 0.05 eV. Likewise, the excitation energies obtained with CCSD are much less satisfying for open-shell derivatives (MAE of 0.20 eV with UCCSD and 0.15 eV with ROCCSD) than for closed-shell systems of similar size (MAE of 0.07 eV).

3.6 | QUEST#5

The QUEST#5 subset is composed of additional accurate excitation energies that we have produced for the present article. This new set gathers 13 new systems composed by small molecules as well as larger molecules (see blue molecules in Figure 4): aza-naphthalene, benzoquinone, cyclopentadienone, cyclopentadienethione, diazirine, hexatriene, maleimide, naphthalene, nitroxyl, octatetraene, streptocyanine-C3, streptocyanine-C5, and thioacrolein. For these new transitions, we report again quality vertical transition energies, the vast majority being of CCSDT quality, and we consider that, out of these 80 new transitions, 55 of them can be labeled as "safe," that is, considered as chemically accurate or within 0.05 eV of the FCI limit for the given geometry and basis set. We refer the interested reader to the Supporting information for a detailed discussion of each molecule for which comparisons are made with literature data.

4 | THEORETICAL BEST ESTIMATES

We discuss in this section the generation of the TBEs obtained with the aug-cc-pVTZ basis. For the closed-shell compounds, the exhaustive list of TBEs can be found in Table 2 alongside various specifications: the molecule's name, the excitation, its nature (valence, Rydberg, or charge transfer), its oscillator strength (when symmetry- and spin-allowed), and its percentage of single excitations $\%T_1$ (computed at the LR-CC3 level). All these quantities are computed with the same aug-cc-pVTZ basis. Importantly, we also report the composite approach considered to compute the TBEs (see column "Method"). Following an ONIOM-like strategy,[219, 220] the TBEs are computed as "A/SB + [B/TB − B/SB]," where A/SB is the excitation energy computed with a method A in a smaller basis (SB), and B/SB and B/TB are excitation energies computed with a method B in the small basis and target basis TB, respectively. Table 3 reports the TBEs for the open-shell molecules belonging to the QUEST#4 subset.

Talking about numbers, the QUEST database is composed of 551 excitation energies, including 302 singlet, 197 triplet, 51 doublet, 412 valence, and 176 Rydberg excited states. Among the valence transitions in closed-shell compounds, 135 transitions correspond to $n \rightarrow \pi^*$ excitations, 200 to $\pi \rightarrow \pi^*$ excitations, and 23 are doubly-excited states. In terms of molecular sizes, 146 excitations are obtained in molecules having in-between 1 and 3 non-hydrogen atoms, 97 excitations from 4 non-hydrogen atom compounds, 177 from molecules composed by 5 and 6 non-hydrogen atoms, and, finally, 68 excitations are obtained from systems with 7 to 10 non-hydrogen atoms. In addition, QUEST is composed by 24 open-shell molecules with a single unpaired electron. Among these excited states, 485 of them are considered as "safe," that is, chemically accurate for the considered basis set and geometry. Besides this energetic criterion, we consider as "safe" transitions that are either: (i) computed with FCI or CCSDTQ, or (ii) in which the difference between CC3 and CCSDT excitation energies is small (i.e., around 0.03–0.04 eV) with a large $\%T_1$ value.

TABLE 2 Theoretical best estimates TBEs (in eV), oscillator strengths f, percentage of single excitations $\%T_1$ involved in the transition (computed at the CC3 level) for the full set of closed-shell compounds of the QUEST database

#	Molecule	Excitation	Nature	$\%T_1$	f	TBE	Method	Safe?
1	Acetaldehyde	$^1A''(n \to \pi^*)$	V	91	0.000	4.31	FCI/AVTZ	Y
2		$^3A''(n \to \pi^*)$	V	97		3.97	FCI/AVDZ + [CCSDT/AVTZ − CCSDT/AVDZ]	Y
3	Acetone	$^1A_2(n \to \pi^*)$	V	91		4.47	CCSDTQ/6-31+G(d) + [CCSDT/AVTZ − CCSDT/6-31+G(d)]	Y
4		$^1B_2(n \to 3s)$	R	90	0.000	6.46	CCSDTQ/6-31+G(d) + [CCSDT/AVTZ − CCSDT/6-31+G(d)]	Y
5		$^1A_2(n \to 3p)$	R	90		7.47	CCSDTQ/6-31+G(d) + [CCSDT/AVTZ − CCSDT/6-31+G(d)]	Y
6		$^1A_1(n \to 3p)$	R	90	0.004	7.51	CCSDTQ/6-31+G(d) + [CCSDT/AVTZ − CCSDT/6-31+G(d)]	Y
7		$^1B_2(n \to 3p)$	R	91	0.029	7.62	CCSDTQ/6-31+G(d) + [CCSDT/AVTZ − CCSDT/6-31+G(d)]	Y
8		$^3A_2(n \to \pi^*)$	V	97		4.13	CCSDT/AVDZ + [CC3/AVTZ − CC3/AVDZ]	Y
9		$^3A_1(\pi \to \pi^*)$	V	98		6.25	CCSDT/AVDZ + [CC3/AVTZ − CC3/AVDZ]	Y
10	Acetylene	$^1\Sigma_u^-(\pi \to \pi^*)$	V	96		7.10	FCI/AVTZ	Y
11		$^1\Delta_u(\pi \to \pi^*)$	V	93		7.44	FCI/AVTZ	Y
12		$^3\Sigma_u^+(\pi \to \pi^*)$	V	99		5.53	FCI/AVTZ	Y
13		$^3\Delta_u(\pi \to \pi^*)$	V	99		6.40	FCI/AVTZ	Y
14		$^3\Sigma_u^-(\pi \to \pi^*)$	V	98		7.08	FCI/AVTZ	Y
15		$^1A_u[F](\pi \to \pi^*)$	V	95		3.64	FCI/AVTZ	Y
16		$^1A_2[F](\pi \to \pi^*)$	V	95		3.85	FCI/AVTZ	Y
17	Acrolein	$^1A''(n \to \pi^*)$	V	87	0.000	3.78	FCI/6-31+G(d) + [CCSDT/AVTZ − CCSDT/6-31+G(d)]	Y
18		$^1A'(\pi \to \pi^*)$	V	91	0.344	6.69	CCSDT/AVTZ	Y
19		$^1A''(n \to \pi^*)$	V	79	0.000	6.72	CCSDT/AVDZ + [CC3/AVTZ − CC3/AVDZ]	N
20		$^1A'(n \to 3s)$	R	89	0.109	7.08	CCSDT/AVDZ + [CC3/AVTZ − CC3/AVDZ]	Y
21		$^1A'(\text{double})$	V	75	(n.d.)	7.87	FCI/6-31+G(d) + [CC3/AVTZ − CC3/6-31+G(d)]	Y
22		$^3A''(n \to \pi^*)$	V	97		3.51	FCI/6-31+G(d) + [CC3/AVTZ − CC3/6-31+G(d)]	Y
23		$^3A'(\pi \to \pi^*)$	V	98		3.94	CCSDT/AVDZ + [CC3/AVTZ − CC3/AVDZ]	Y
24		$^3A'(\pi \to \pi^*)$	V	98		6.18	CCSDT/AVDZ + [CC3/AVTZ − CC3/AVDZ]	Y
25		$^3A''(n \to \pi^*)$	V	92		6.54	CCSDT/6-31+G(d) + [CC3/AVTZ − CC3/6-31+G(d)]	N
26	Ammonia	$^1A_2(n \to 3s)$	R	93	0.086	6.59	FCI/AVTZ	Y
27		$^1E(n \to 3p)$	R	93	0.006	8.16	FCI/AVTZ	Y
28		$^1A_1(n \to 3p)$	R	94	0.003	9.33	FCI/AVTZ	Y
29		$^1A_2(n \to 3s)$	R	93	0.008	9.96	FCI/AVTZ	Y
30		$^3A_2(n \to 3s)$	R	98		6.31	FCI/AVTZ	Y

TABLE 2 (Continued)

#	Molecule	Excitation	Nature	%T_1	f	TBE	Method	Safe?
31	Aza-naphthalene	$^1B_{3g}(n \to \pi^*)$	V	88		3.14	CCSDT/6-31+G(d) + [CC3/AVTZ − CC3/6-31+G(d)]	Y
32		$^1B_{2u}(\pi \to \pi^*)$	V	86	0.190	4.28	CCSDT/6-31+G(d) + [CC3/AVTZ − CC3/6-31+G(d)]	Y
33		$^1B_{1u}(n \to \pi^*)$	V	88	(n.d.)	4.34	CCSDT/6-31+G(d) + [CC3/AVTZ − CC3/6-31+G(d)]	Y
34		$^1B_{2g}(n \to \pi^*)$	V	87		4.55	CCSDT/6-31+G(d) + [CC3/AVTZ − CC3/6-31+G(d)]	Y
35		$^1B_{2g}(n \to \pi^*)$	V	84		4.89	CCSDT/6-31+G(d) + [CC3/AVTZ − CC3/6-31+G(d)]	Y
36		$^1B_{1u}(n \to \pi^*)$	V	82	(n.d.)	5.24	CCSDT/6-31+G(d) + [CC3/AVTZ − CC3/6-31+G(d)]	N
37		$^1A_u(n \to \pi^*)$	V	83		5.34	CCSDT/6-31+G(d) + [CC3/AVTZ − CC3/6-31+G(d)]	Y
38		$^1B_{3u}(\pi \to \pi^*)$	V	88	0.028	5.68	CCSDT/6-31+G(d) + [CC3/AVTZ − CC3/6-31+G(d)]	N
39		$^1A_g(\pi \to \pi^*)$	V	85		5.80	CCSDT/6-31+G(d) + [CC3/AVTZ − CC3/6-31+G(d)]	Y
40		$^1A_u(n \to \pi^*)$	V	84		5.92	CCSDT/6-31+G(d) + [CC3/AVTZ − CC3/6-31+G(d)]	Y
41		$^1A_g(n \to 3s)$	R	90		6.50	CCSDT/6-31+G(d) + [CC3/AVTZ − CC3/6-31+G(d)]	Y
42		$^3B_{3g}(n \to \pi^*)$	V	96		2.82	CC3/AVTZ	N
43		$^3B_{2u}(\pi \to \pi^*)$	V	97		3.67	CC3/AVTZ	N
44		$^3B_{3u}(\pi \to \pi^*)$	V	97		3.75	CC3/AVTZ	N
45		$^3B_{1u}(n \to \pi^*)$	V	97		3.77	CC3/AVTZ	N
46		$^3B_{2g}(n \to \pi^*)$	V	96		4.34	CC3/AVTZ	N
47		$^3B_{2g}(n \to \pi^*)$	V	95		4.61	CC3/AVTZ	N
48		$^3B_{3u}(\pi \to \pi^*)$	V	96		4.75	CC3/AVTZ	N
49		$^3A_u(n \to \pi^*)$	V	96		4.87	CC3/AVTZ	N
50	Beryllium	^1D(double)	R	32		7.15	FCI/AVTZ	Y
51	Benzene	$^1B_{2u}(\pi \to \pi^*)$	V	86		5.06	CCSDT/AVTZ	Y
52		$^1B_{1u}(\pi \to \pi^*)$	V	92		6.45	CCSDT/AVTZ	Y
53		$^1E_{1g}(\pi \to 3s)$	R	92		6.52	CCSDT/AVTZ	Y
54		$^1A_{2u}(\pi \to 3p)$	R	93	0.066	7.08	CCSDT/AVTZ	Y
55		$^1E_{2u}(\pi \to 3p)$	R	92		7.15	CCSDT/AVTZ	Y
56		$^1E_{2g}(\pi \to \pi^*)$	V	73		8.28	FCI/6-31+G(d) + [CC3/AVTZ − CC3/6-31+G(d)]	Y
57		$^1A_{1g}$(double)	V	n.d.		10.55	XMS-CASPT2/AVTZ	N
58		$^3B_{1u}(\pi \to \pi^*)$	V	98		4.16	CCSDT/AVDZ + [CC3/AVTZ − CC3/AVDZ]	Y
59		$^3E_{1u}(\pi \to \pi^*)$	V	97		4.85	CCSDT/AVDZ + [CC3/AVTZ − CC3/AVDZ]	Y
60		$^3B_{2u}(\pi \to \pi^*)$	V	98		5.81	CCSDT/AVDZ + [CC3/AVTZ − CC3/AVDZ]	Y
61	Benzoquinone	$^1B_{1g}(n \to \pi^*)$	V	85		2.82	CCSDT/AVDZ + [CC3/AVTZ − CC3/AVDZ]	Y

(Continues)

TABLE 2 (Continued)

#	Molecule	Excitation	Nature	%T_1	f	TBE	Method	Safe?
62		$^1A_u(n \to \pi^*)$	V	84		2.96	CCSDT/AVDZ + [CC3/AVTZ − CC3/AVDZ]	Y
63		^1A_g(double)	V	0		4.57	NEVPT2/AVTZ	N
64		$^1B_{3g}(\pi \to \pi^*)$	V	88		4.58	CCSDT/AVDZ + [CC3/AVTZ − CC3/AVDZ]	N
65		$^1B_{1u}(\pi \to \pi^*)$	V	88	0.471	5.62	CCSDT/AVDZ + [CC3/AVTZ − CC3/AVDZ]	N
66		$^1B_{3u}(n \to \pi^*)$	V	79	0.001	5.79	CCSDT/AVDZ + [CC3/AVTZ − CC3/AVDZ]	N
67		$^1B_{2g}(n \to \pi^*)$	V	76		5.95	CCSDT/AVDZ + [CC3/AVTZ − CC3/AVDZ]	Y
68		$^1A_u(n \to \pi^*)$	V	74		6.35	CCSDT/AVDZ + [CC3/AVTZ − CC3/AVDZ]	N
69		$^1B_{1g}(n \to \pi^*)$	V	83		6.38	CCSDT/AVDZ + [CC3/AVTZ − CC3/AVDZ]	N
70		$^1B_{2g}(n \to \pi^*)$	V	86		7.22	CCSDT/AVDZ + [CC3/AVTZ − CC3/AVDZ]	Y
71		$^3B_{1g}(n \to \pi^*)$	V	96		2.58	CCSDT/6-31+G(d) + [CC3/AVTZ − CC3/6-31+G(d)]	Y
72		$^3A_u(n \to \pi^*)$	V	95		2.72	CCSDT/6-31+G(d) + [CC3/AVTZ − CC3/6-31+G(d)]	Y
73		$^3B_{1u}(\pi \to \pi^*)$	V	97		3.12	CCSDT/6-31+G(d) + [CC3/AVTZ − CC3/6-31+G(d)]	Y
74		$^3B_{3g}(\pi \to \pi^*)$	V	97		3.46	CCSDT/6-31+G(d) + [CC3/AVTZ − CC3/6-31+G(d)]	Y
75	Butadiene	$^1B_u(\pi \to \pi^*)$	V	93	0.664	6.22	CCSDTQ/6-31+G(d) + [CCSDT/AVTZ − CCSDT/6-31+G(d)]	Y
76		$^1B_g(\pi \to 3s)$	R	94		6.33	CCSDTQ/6-31+G(d) + [CCSDT/AVTZ − CCSDT/6-31+G(d)]	Y
77		$^1A_g(\pi \to \pi^*)$	V	75		6.50	FCI/AVDZ + [CCSDT/AVTZ − CCSDT/AVDZ]	Y
78		$^1A_u(\pi \to 3p)$	R	94	0.001	6.64	CCSDTQ/6-31+G(d) + [CCSDT/AVTZ − CCSDT/6-31+G(d)]	Y
79		$^1A_u(\pi \to 3p)$	R	94	0.049	6.80	CCSDTQ/6-31+G(d) + [CCSDT/AVTZ − CCSDT/6-31+G(d)]	Y
80		$^1B_u(\pi \to 3p)$	R	93	0.055	7.68	CCSDTQ/6-31+G(d) + [CC3/AVTZ − CC3/6-31+G(d)]	Y
81		$^3B_u(\pi \to \pi^*)$	V	98		3.36	CCSDT/AVDZ + [CC3/AVTZ − CC3/AVDZ]	Y
82		$^3A_g(\pi \to \pi^*)$	V	98		5.20	CCSDT/AVDZ + [CC3/AVTZ − CC3/AVDZ]	Y
83		$^3B_g(\pi \to 3s)$	R	97		6.29	CCSDT/AVDZ + [CC3/AVTZ − CC3/AVDZ]	Y
84	Carbon dimer	$^1\Delta_g$(double)	R	0		2.09	FCI/AVTZ	Y
85		$^1\Sigma_g^+$ (double)	R	0		2.42	FCI/AVTZ	Y
86	Carbon monoxide	$^1\Pi(n \to \pi^*)$	V	93	0.168	8.49	FCI/AVTZ	Y
87		$^1\Sigma^-(\pi \to \pi^*)$	V	93		9.92	FCI/AVTZ	Y

TABLE 2 (Continued)

#	Molecule	Excitation	Nature	%T_1	f	TBE	Method	Safe?
88		$^1\Delta(\pi \to \pi^*)$	V	91		10.06	FCI/AVTZ	Y
89		$^1\Sigma^+$(n. d.)	R	91	0.003	10.95	FCI/AVTZ	Y
90		$^1\Sigma^+$(n. d.)	R	92	0.200	11.52	FCI/AVTZ	Y
91		$^1\Pi$(n. d.)	R	92	0.106	11.72	FCI/AVTZ	Y
92		$^3\Pi(n \to \pi^*)$	V	98		6.28	FCI/AVTZ	Y
93		$^3\Sigma^+(\pi \to \pi^*)$	V	98		8.45	FCI/AVTZ	Y
94		$^3\Delta(\pi \to \pi^*)$	V	98		9.27	FCI/AVTZ	Y
95		$^3\Sigma^-(\pi \to \pi^*)$	V	97		9.80	FCI/AVTZ	Y
96		$^3\Sigma^+$(n. d.)	R	98		10.47	FCI/AVTZ	Y
97	Carbon dimer	$^1\Delta_g$(double)	R	1		5.22	FCI/AVTZ	Y
98		$^1\Sigma_g^+$ (double)	R	1		5.91	FCI/AVTZ	Y
99	Carbonylfluoride	$^1A_2(n \to \pi^*)$	V	91		7.31	FCI/6-31+G(d) + [CCSDT/AVTZ − CCSDT/6-31+G(d)]	Y
100		$^3A_2(n \to \pi^*)$	V	97		7.06	FCI/AVDZ + [CCSDT/AVTZ − CCSDT/AVDZ]	Y
101	CCl2	$^1B_1(\sigma \to \pi^*)$	V	93	0.002	2.59	FCI/AVDZ + [CCSDT/AVTZ − CCSDT/AVDZ]	Y
102		$^1A_2$(n. d.)	V	88		4.40	FCI/AVDZ + [CCSDT/AVTZ − CCSDT/AVDZ]	Y
103		$^3B_1(\sigma \to \pi^*)$	V	98		1.22	FCI/AVDZ + [CCSDT/AVTZ − CCSDT/AVDZ]	Y
104		$^3A_2$(n. d.)	V	96		4.31	FCI/AVDZ + [CCSDT/AVTZ − CCSDT/AVDZ]	Y
105	CClF	$^1A''(\sigma \to \pi^*)$	V	93	0.007	3.57	FCI/AVDZ + [CCSDT/AVTZ − CCSDT/AVDZ]	Y
106	CF2	$^1B_1(\sigma \to \pi^*)$	V	94	0.034	5.09	FCI/AVTZ	Y
107		$^3B_1(\sigma \to \pi^*)$	V	99		2.77	FCI/AVTZ	Y
108	Cyanoacetylene	$^1\Sigma^-(\pi \to \pi^*)$	V	94		5.80	CCSDTQ/AVDZ + [CCSDT/AVTZ − CCSDT/AVDZ]	Y
109		$^1\Delta(\pi \to \pi^*)$	V	94		6.07	CCSDTQ/AVDZ + [CCSDT/AVTZ − CCSDT/AVDZ]	Y
110		$^3\Sigma^+(\pi \to \pi^*)$	V	98		4.44	CCSDT/AVTZ	Y
111		$^3\Delta(\pi \to \pi^*)$	V	98		5.21	CCSDT/AVTZ	Y
112		$^1A''[F](\pi \to \pi^*)$	V	93	0.004	3.54	CCSDTQ/AVDZ + [CCSDT/AVTZ − CCSDT/AVDZ]	Y
113	Cyanoformaldehyde	$^1A''(n \to \pi^*)$	V	89	0.001	3.81	CCSDT/AVTZ	Y
114		$^1A''(\pi \to \pi^*)$	V	91	0.000	6.46	CCSDT/AVTZ	Y
115		$^3A''(n \to \pi^*)$	V	97		3.44	CCSDT/AVDZ + [CC3/AVTZ − CC3/AVDZ]	Y
116		$^3A'(\pi \to \pi^*)$	V	98		5.01	CCSDT/AVDZ + [CC3/AVTZ − CC3/AVDZ]	Y
117	Cyanogen	$^1\Sigma_u^-(\pi \to \pi^*)$	V	94		6.39	CCSDTQ/AVDZ + [CCSDT/AVTZ − CCSDT/AVDZ]	Y
118		$^1\Delta_u(\pi \to \pi^*)$	V	93		6.66	CCSDTQ/AVDZ + [CCSDT/AVTZ − CCSDT/AVDZ]	Y

(Continues)

T A B L E 2 (Continued)

#	Molecule	Excitation	Nature	%T_1	f	TBE	Method	Safe?
119		$^3\Sigma_u^+ (\pi \rightarrow \pi^*)$	V	98		4.91	CCSDTQ/6-31+G(d) + [CCSDT/AVTZ − CCSDT/6-31+G(d)]	Y
120		$^1\Sigma_u^- [F](\pi \rightarrow \pi^*)$	V	93		5.05	CCSDTQ/AVDZ + [CCSDT/AVTZ − CCSDT/AVDZ]	Y
121	Cyclopentadiene	$^1B_2(\pi \rightarrow \pi^*)$	V	93	0.084	5.54	FCI/6-31+G(d) + [CCSDT/AVTZ − CCSDT/6-31+G(d)]	Y
122		$^1A_2(\pi \rightarrow 3s)$	R	94		5.78	CCSDT/AVTZ	Y
123		$^1B_1(\pi \rightarrow 3p)$	R	94	0.037	6.41	CCSDT/AVTZ	Y
124		$^1A_2(\pi \rightarrow 3p)$	R	93		6.46	CCSDT/AVTZ	Y
125		$^1B_2(\pi \rightarrow 3p)$	R	94	0.046	6.56	CCSDT/AVTZ	Y
126		$^1A_1(\pi \rightarrow \pi^*)$	V	78	0.010	6.52	CCSDT/AVTZ	N
127		$^3B_2(\pi \rightarrow \pi^*)$	V	98		3.31	CCSDT/AVDZ + [CC3/AVTZ − CC3/AVDZ]	Y
128		$^3A_1(\pi \rightarrow \pi^*)$	V	98		5.11	CCSDT/AVDZ + [CC3/AVTZ − CC3/AVDZ]	Y
129		$^3A_2(\pi \rightarrow 3s)$	R	97		5.73	CCSDT/AVDZ + [CC3/AVTZ − CC3/AVDZ]	Y
130		$^3B_1(\pi \rightarrow 3p)$	R	97		6.36	CCSDT/AVDZ + [CC3/AVTZ − CC3/AVDZ]	Y
131	Cyclopentadienone	$^1A_2(n \rightarrow \pi^*)$	V	88		2.94	CCSDT/AVDZ + [CC3/AVTZ − CC3/AVDZ]	Y
132		$^1B_2(\pi \rightarrow \pi^*)$	V	91	0.004	3.58	CCSDT/AVDZ + [CC3/AVTZ − CC3/AVDZ]	Y
133		$^1B_1$(double)	V	3	0.000	5.02	NEVPT2/AVTZ	N
134		$^1A_1$(double)	V	49	0.131	6.00	NEVPT2/AVTZ	N
135		$^1A_1(\pi \rightarrow \pi^*)$	V	73	0.090	6.09	CCSDT/AVDZ + [CC3/AVTZ − CC3/AVDZ]	N
136		$^3B_2(\pi \rightarrow \pi^*)$	V	98		2.29	CCSDT/AVDZ + [CC3/AVTZ − CC3/AVDZ]	Y
137		$^3A_2(n \rightarrow \pi^*)$	V	96		2.65	CCSDT/AVDZ + [CC3/AVTZ − CC3/AVDZ]	Y
138		$^3A_1(\pi \rightarrow \pi^*)$	V	98		4.19	CCSDT/AVDZ + [CC3/AVTZ − CC3/AVDZ]	Y
139		$^3B_1$(double)	V	10		4.91	NEVPT2/AVTZ	N
140	Cyclopentadienethione	$^1A_2(n \rightarrow \pi^*)$	V	87		1.70	CCSDT/AVDZ + [CC3/AVTZ − CC3/AVDZ]	Y
141		$^1B_2(\pi \rightarrow \pi^*)$	V	85	0.000	2.63	CCSDT/AVDZ + [CC3/AVTZ − CC3/AVDZ]	Y
142		$^1B_1$(double)	V	1	0.000	3.16	NEVPT2/AVTZ	N
143		$^1A_1(\pi \rightarrow \pi^*)$	V	89	0.378	4.96	CCSDT/AVDZ + [CC3/AVTZ − CC3/AVDZ]	Y
144		$^1A_1$(double)	V	51	0.003	5.43	NEVPT2/AVTZ	N
145		$^3A_2(n \rightarrow \pi^*)$	V	97		1.47	CCSDT/AVDZ + [CC3/AVTZ − CC3/AVDZ]	Y
146		$^3B_2(\pi \rightarrow \pi^*)$	V	97		1.88	CCSDT/AVDZ + [CC3/AVTZ − CC3/AVDZ]	Y

TABLE 2 (Continued)

#	Molecule	Excitation	Nature	%T_1	f	TBE	Method	Safe?
147		$^3A_1(\pi \rightarrow \pi^*)$	V	98		2.51	CCSDT/AVDZ + [CC3/AVTZ − CC3/AVDZ]	Y
148		$^3B_1$(double)	V	4		3.13	NEVPT2/AVTZ	N
149	Cyclopropene	$^1B_1(\sigma \rightarrow \pi^*)$	V	92	0.001	6.68	CCSDT/AVTZ	Y
150		$^1B_2(\pi \rightarrow \pi^*)$	V	95	0.071	6.79	FCI/AVDZ + [CCSDT/AVTZ − CCSDT/AVDZ]	Y
151		$^3B_2(\pi \rightarrow \pi^*)$	V	98		4.38	FCI/AVTZ	Y
152		$^3B_1(\sigma \rightarrow \pi^*)$	V	98		6.45	FCI/AVTZ	Y
153	Cyclopropenone	$^1B_1(n \rightarrow \pi^*)$	V	87	0.000	4.26	CCSDTQ/6-31+G(d) + [CCSDT/AVTZ − CCSDT/6-31+G(d)]	Y
154		$^1A_2(n \rightarrow \pi^*)$	V	91		5.55	CCSDTQ/6-31+G(d) + [CCSDT/AVTZ − CCSDT/6-31+G(d)]	Y
155		$^1B_2(n \rightarrow 3s)$	R	90	0.003	6.34	CCSDTQ/6-31+G(d) + [CCSDT/AVTZ − CCSDT/6-31+G(d)]	Y
156		$^1B_2(\pi \rightarrow \pi^*)$	V	86	0.047	6.54	CCSDTQ/6-31+G(d) + [CCSDT/AVTZ − CCSDT/6-31+G(d)]	Y
157		$^1B_2(n \rightarrow 3p)$	R	91	0.018	6.98	CCSDTQ/6-31+G(d) + [CCSDT/AVTZ − CCSDT/6-31+G(d)]	Y
158		$^1A_1(n \rightarrow 3p)$	R	91	0.003	7.02	CCSDTQ/6-31+G(d) + [CCSDT/AVTZ − CCSDT/6-31+G(d)]	Y
159		$^1A_1(\pi \rightarrow \pi^*)$	V	90	0.320	8.28	CCSDTQ/6-31+G(d) + [CCSDT/AVTZ − CCSDT/6-31+G(d)]	Y
160		$^3B_1(n \rightarrow \pi^*)$	V	96		3.93	CCSDT/AVTZ	Y
161		$^3B_2(\pi \rightarrow \pi^*)$	V	97		4.88	CCSDT/AVTZ	Y
162		$^3A_2(n \rightarrow \pi^*)$	V	97		5.35	CCSDT/AVTZ	Y
163		$^3A_1(\pi \rightarrow \pi^*)$	V	98		6.79	CCSDT/AVTZ	Y
164	Cyclopropenethione	$^1A_2(n \rightarrow \pi^*)$	V	89		3.41	CCSDTQ/6-31+G(d) + [CCSDT/AVTZ − CCSDT/6-31+G(d)]	Y
165		$^1B_1(n \rightarrow \pi^*)$	V	84	0.000	3.45	CCSDTQ/6-31+G(d) + [CCSDT/AVTZ − CCSDT/6-31+G(d)]	Y
166		$^1B_2(\pi \rightarrow \pi^*)$	V	83	0.007	4.60	CCSDTQ/6-31+G(d) + [CCSDT/AVTZ − CCSDT/6-31+G(d)]	Y
167		$^1B_2(n \rightarrow 3s)$	R	91	0.048	5.34	CCSDTQ/6-31+G(d) + [CCSDT/AVTZ − CCSDT/6-31+G(d)]	Y
168		$^1A_1(\pi \rightarrow \pi^*)$	V	89	0.228	5.46	CCSDTQ/6-31+G(d) + [CCSDT/AVTZ − CCSDT/6-31+G(d)]	Y
169		$^1B_2(n \rightarrow 3p)$	R	91	0.084	5.92	CCSDTQ/6-31+G(d) + [CCSDT/AVTZ − CCSDT/6-31+G(d)]	Y
170		$^3A_2(n \rightarrow \pi^*)$	V	97		3.28	CCSDT/AVDZ + [CC3/AVTZ − CC3/AVDZ]	Y
171		$^3B_1(n \rightarrow \pi^*)$	V	94		3.32	CCSDT/AVTZ	Y
172		$^3B_2(\pi \rightarrow \pi^*)$	V	96		4.01	CCSDT/AVDZ + [CC3/AVTZ − CC3/AVDZ]	Y
173		$^3A_1(\pi \rightarrow \pi^*)$	V	98		4.01	CCSDT/AVDZ + [CC3/AVTZ − CC3/AVDZ]	Y
174	Diacetylene	$^1\Sigma_u^-(\pi \rightarrow \pi^*)$	V	94		5.33	CCSDTQ/AVDZ + [CCSDT/AVTZ − CCSDT/AVDZ]	Y

(Continues)

TABLE 2 (Continued)

#	Molecule	Excitation	Nature	%T_1	f	TBE	Method	Safe?
175		$^1\Delta_u(\pi \to \pi^*)$	V	94		5.61	CCSDTQ/AVDZ + [CCSDT/AVTZ − CCSDT/AVDZ]	Y
176		$^3\Sigma_u^+ (\pi \to \pi^*)$	V	98		4.10	CCSDTQ/6-31+G(d) + [CC3/AVTZ − CC3/6-31+G(d)]	Y
177		$^3\Delta_u(\pi \to \pi^*)$	V	98		4.78	CCSDTQ/AVDZ + [CCSDT/AVTZ − CCSDT/AVDZ]	Y
178	Diazirine	$^1B_1(n \to \pi^*)$	V	92	0.002	4.09	CCSDTQ/AVDZ + [CCSDT/AVTZ − CCSDT/AVDZ]	Y
179		$^1B_2(\sigma \to \pi^*)$	V	90		7.27	CCSDTQ/AVDZ + [CCSDT/AVTZ − CCSDT/AVDZ]	Y
180		$^1A_2(n \to 3s)$	R	93	0.000	7.44	CCSDTQ/AVDZ + [CCSDT/AVTZ − CCSDT/AVDZ]	Y
181		$^1A_1(n \to 3p)$	R	93	0.132	8.03	CCSDTQ/AVDZ + [CCSDT/AVTZ − CCSDT/AVDZ]	Y
182		$^3B_1(n \to \pi^*)$	V	98		3.49	CCSDTQ/6-31+G(d) + [CCSDT/AVTZ − CCSDT/6-31+G(d)]	Y
183		$^3B_2(\pi \to \pi^*)$	V	98		5.06	CCSDTQ/6-31+G(d) + [CCSDT/AVTZ − CCSDT/6-31+G(d)]	Y
184		$^3A_2(n \to \pi^*)$	V	98		6.12	CCSDTQ/6-31+G(d) + [CCSDT/AVTZ − CCSDT/6-31+G(d)]	Y
185		$^3A_1(n \to 3p)$	R	98		6.81	CCSDTQ/6-31+G(d) + [CCSDT/AVTZ − CCSDT/6-31+G(d)]	Y
186	Diazomethane	$^1A_2(\pi \to \pi^*)$	V	90		3.14	FCI/AVTZ	Y
187		$^1B_1(\pi \to 3s)$	R	93	0.016	5.54	FCI/AVTZ	Y
188		$^1A_1(\pi \to \pi^*)$	V	91	0.234	5.90	FCI/AVTZ	Y
189		$^3A_2(\pi \to \pi^*)$	V	97		2.79	FCI/AVDZ + [CCSDT/AVTZ − CCSDT/AVDZ]	Y
190		$^3A_1(\pi \to \pi^*)$	V	98		4.05	FCI/AVTZ	Y
191		$^3B_1(\pi \to 3s)$	R	98		5.35	FCI/AVTZ	Y
192		$^3A_1(\pi \to 3p)$	R	98		6.82	FCI/AVTZ	Y
193		$^1A''[F](\pi \to \pi^*)$	V	87	0.000	0.71	FCI/AVTZ	Y
194	Difluorodiazirine	$^1B_1(n \to \pi^*)$	V	93	0.002	3.74	CCSDT/AVTZ	Y
195		$^1A_2(\pi \to \pi^*)$	V	91		7.00	CCSDT/AVTZ	Y
196		$^1B_2(\pi \to \pi^*)$	V	93	0.026	8.52	CCSDT/AVTZ	Y
197		$^3B_1(n \to \pi^*)$	V	98		3.03	CCSDT/AVDZ + [CC3/AVTZ − CC3/AVDZ]	Y
198		$^3B_2(\pi \to \pi^*)$	V	98		5.44	CCSDT/AVDZ + [CC3/AVTZ − CC3/AVDZ]	Y
199		$^3A_2(\pi \to \pi^*)$	V	98		5.80	CCSDT/AVDZ + [CC3/AVTZ − CC3/AVDZ]	Y
200	Dinitrogen	$^1\Pi_g(n \to \pi^*)$	V	92		9.34	FCI/AVTZ	Y
201		$^1\Sigma_u^- (\pi \to \pi^*)$	V	97		9.88	FCI/AVTZ	Y
202		$^1\Delta_u(\pi \to \pi^*)$	V	95	0.000	10.29	FCI/AVTZ	Y
203		$^1\Sigma_g^+$ (n.d.)	R	92		12.98	FCI/AVTZ	Y
204		$^1\Pi_u$(n. d.)	R	82	0.458	13.03	FCI/AVTZ	Y
205		$^1\Sigma_u^+$ (n.d.)	R	92	0.296	13.09	FCI/AVTZ	Y

TABLE 2 (Continued)

#	Molecule	Excitation	Nature	%T_1	f	TBE	Method	Safe?
206		$^1\Pi_u$(n. d.)	R	87	0.000	13.46	FCI/AVTZ	Y
207		$^3\Sigma_u^+$ ($\pi \to \pi^*$)	V	99		7.70	FCI/AVTZ	Y
208		$^3\Pi_g$($n \to \pi^*$)	V	98		8.01	FCI/AVTZ	Y
209		$^3\Delta_u$($\pi \to \pi^*$)	V	99		8.87	FCI/AVTZ	Y
210		$^3\Sigma_u^-$ ($\pi \to \pi^*$)	V	98		9.66	FCI/AVTZ	Y
211	Ethylene	$^1B_{3u}p3s$	R	95	0.078	7.39	FCI/AVTZ	Y
212		$^1B_{1u}$($\pi \to \pi^*$)	V	95	0.346	7.93	FCI/AVTZ	Y
213		$^1B_{1g}$($\pi \to 3p$)	R	95		8.08	FCI/AVTZ	Y
214		^1A_g(double)	V	20		12.92	FCI/AVTZ	Y
215		$^3B_{1u}$($\pi \to \pi^*$)	V	99		4.54	FCI/AVTZ	Y
216		$^3B_{3u}p3s$	R	98		7.23	FCI/AVDZ + [CCSDT/AVTZ − CCSDT/AVDZ]	Y
217		$^3B_{1g}$($\pi \to 3p$)	R	98		7.98	FCI/AVDZ + [CCSDT/AVTZ − CCSDT/AVDZ]	Y
218	Formaldehyde	$^1A_2$($n \to \pi^*$)	V	91		3.98	FCI/AVTZ	Y
219		$^1B_2$($n \to 3s$)	R	91	0.021	7.23	FCI/AVTZ	Y
220		$^1B_2$($n \to 3p$)	R	92	0.037	8.13	FCI/AVTZ	Y
221		$^1A_1$($n \to 3p$)	R	91	0.052	8.23	FCI/AVTZ	Y
222		$^1A_2$($n \to 3p$)	R	91		8.67	FCI/AVTZ	Y
223		$^1B_1$(n. d.)	V	90	0.001	9.22	FCI/AVTZ	Y
224		$^1A_1$($\pi \to \pi^*$)	V	90	0.135	9.43	FCI/AVTZ	Y
225		$^1A_1$(double)	V	5	(n.d.)	10.35	FCI/AVTZ	Y
226		$^3A_2$($n \to \pi^*$)	V	98		3.58	FCI/AVTZ	Y
227		$^3A_1$($\pi \to \pi^*$)	V	99		6.06	FCI/AVTZ	Y
228		$^3B_2$($n \to 3s$)	R	97		7.06	FCI/AVTZ	Y
229		$^3B_2$($n \to 3p$)	R	97		7.94	FCI/AVTZ	Y
230		$^3A_1$($n \to 3p$)	R	97		8.10	FCI/AVTZ	Y
231		$^3B_1$(n. d.)	R	97		8.42	FCI/AVTZ	Y
232		$^1A''[F]$($n \to \pi^*$)	V	87	0.000	2.80	FCI/AVTZ	Y
233	Formamide	$^1A''$($n \to \pi^*$)	V	90	0.000	5.65	FCI/AVDZ + [CCSDT/AVTZ − CCSDT/AVDZ]	Y
234		$^1A'$($n \to 3s$)	R	88	0.001	6.77	FCI/AVDZ + [CCSDT/AVTZ − CCSDT/AVDZ]	N
235		$^1A'$($n \to 3p$)	R	89	0.111	7.38	CCSDT/AVTZ	N
236		$^1A'$($\pi \to \pi^*$)	V	89	0.251	7.63	FCI/AVTZ	N
237		$^3A''$($n \to \pi^*$)	V	97		5.38	FCI/AVDZ + [CC3/AVTZ − CCS3/AVDZ]	Y
238		$^3A'$($\pi \to \pi^*$)	V	98		5.81	FCI/AVDZ + [CC3/AVTZ − CCS3/AVDZ]	Y
239	Formylfluoride	$^1A''$($n \to \pi^*$)	V	91		5.96	FCI/AVDZ + [CCSDT/AVTZ − CCSDT/AVDZ]	Y
240		$^3A''$($n \to \pi^*$)	V	98	0.001	5.63	FCI/AVDZ + [CCSDT/AVTZ − CCSDT/AVDZ]	Y
241	Furan	$^1A_2$($\pi \to 3s$)	R	93		6.09	CCSDT/AVTZ	Y

(Continues)

TABLE 2 (Continued)

#	Molecule	Excitation	Nature	%T_1	f	TBE	Method	Safe?
242		$^1B_2(\pi \to \pi^*)$	V	93	0.163	6.37	CCSDT/AVTZ	Y
243		$^1A_1(\pi \to \pi^*)$	V	92	0.000	6.56	CCSDT/AVTZ	Y
244		$^1B_1(\pi \to 3p)$	R	93	0.038	6.64	CCSDT/AVTZ	Y
245		$^1A_2(\pi \to 3p)$	R	93		6.81	CCSDT/AVTZ	Y
246		$^1B_2(\pi \to 3p)$	R	93	0.007	7.24	CCSDT/AVDZ + [CC3/AVTZ − CC3/AVDZ]	Y
247		$^3B_2(\pi \to \pi^*)$	V	98		4.20	CCSDT/AVDZ + [CC3/AVTZ − CC3/AVDZ]	Y
248		$^3A_1(\pi \to \pi^*)$	V	98		5.46	CCSDT/AVDZ + [CC3/AVTZ − CC3/AVDZ]	Y
249		$^3A_2(\pi \to 3s)$	R	97		6.02	CCSDT/AVDZ + [CC3/AVTZ − CC3/AVDZ]	Y
250		$^3B_1(\pi \to 3p)$	R	97		6.59	CCSDT/AVDZ + [CC3/AVTZ − CC3/AVDZ]	Y
251	Glyoxal	$^1A_u(n \to \pi^*)$	V	91	0.000	2.88	CCSDTQ/6-31+G(d) + [CCSDT/AVTZ − CCSDT/6-31+G(d)]	Y
252		$^1B_g(n \to \pi^*)$	V	88		4.24	CCSDTQ/6-31+G(d) + [CCSDT/AVTZ − CCSDT/6-31+G(d)]	Y
253		^1A_g(double)	V	0	0.000	5.61	FCI/AVDZ + [CCSDT/AVTZ − CCSDT/AVDZ]	Y
254		$^1B_g(n \to \pi^*)$	V	83		6.57	CCSDTQ/6-31+G(d) + [CCSDT/AVTZ − CCSDT/6-31+G(d)]	Y
255		$^1B_u(n \to 3p)$	R	91	0.095	7.71	CCSDTQ/6-31+G(d) + [CCSDT/AVTZ − CCSDT/6-31+G(d)]	Y
256		$^3A_u(n \to \pi^*)$	V	97		2.49	CCSDT/AVTZ	Y
257		$^3B_g(n \to \pi^*)$	V	97		3.89	CCSDT/AVTZ	Y
258		$^3B_u(\pi \to \pi^*)$	V	98		5.15	CCSDT/AVTZ	Y
259		$^3A_g(\pi \to \pi^*)$	V	98		6.30	CCSDT/AVTZ	Y
260	HCCl	$^1A''(\sigma \to \pi^*)$	V	94	0.003	1.98	FCI/AVTZ	Y
261	HCF	$^1A''(\sigma \to \pi^*)$	V	95	0.006	2.49	FCI/AVTZ	Y
262	HCP	$^1\Sigma^-(\pi \to \pi^*)$	V	94		4.84	FCI/AVTZ	Y
263		$^1\Delta(\pi \to \pi^*)$	V	94		5.15	FCI/AVTZ	Y
264		$^3\Sigma^+(\pi \to \pi^*)$	V	98		3.47	FCI/AVTZ	Y
265		$^3\Delta(\pi \to \pi^*)$	V	98		4.22	FCI/AVTZ	Y
266	Hexatriene	$^1B_u(\pi \to \pi^*)$	V	92	1.115	5.37	CCSDT/AVDZ + [CC3/AVTZ − CC3/AVDZ]	Y
267		$^1A_g(\pi \to \pi^*)$	V	65		5.62	CCSDT/AVDZ + [CC3/AVTZ − CC3/AVDZ]	N
268		$^1A_u(\pi \to 3s)$	R	93	0.009	5.79	CCSDT/AVDZ + [CC3/AVTZ − CC3/AVDZ]	Y
269		$^1B_g(\pi \to 3p)$	R	93		5.94	CCSDT/AVDZ + [CC3/AVTZ − CC3/AVDZ]	Y
270		$^3B_u(\pi \to \pi^*)$	V	97		2.73	CCSDT/6-31+G(d) + [CC3/AVTZ − CC3/6-31+G(d)]	Y
271		$^3A_g(\pi \to \pi^*)$	V	98		4.36	CCSDT/6-31+G(d) + [CC3/AVTZ − CC3/6-31+G(d)]	Y

T A B L E 2 (Continued)

#	Molecule	Excitation	Nature	%T_1	f	TBE	Method	Safe?
272	HPO	$^1A''(n \rightarrow \pi^*)$	V	90	0.003	2.47	FCI/AVTZ	Y
273	HPS	$^1A''(n \rightarrow \pi^*)$	V	90	0.001	1.59	FCI/AVTZ	Y
274	HSiF	$^1A''(\sigma \rightarrow \pi^*)$	V	93	0.024	3.05	FCI/AVTZ	Y
275	Hydrogen chloride	$^1\Pi$	CT	94	0.056	7.84	FCI/AVTZ	Y
276	Hydrogen sulfide	$^1A_2(n \rightarrow 3p)$	R	94		6.18	FCI/AVTZ	Y
277		$^1B_1(n \rightarrow 3p)$	R	94	0.063	6.24	FCI/AVTZ	Y
278		$^3A_2(n \rightarrow 3p)$	R	98		5.81	FCI/AVTZ	Y
279		$^3B_1(n \rightarrow 3p)$	R	98		5.88	FCI/AVTZ	Y
280	Imidazole	$^1A''(\pi \rightarrow 3s)$	R	93	0.001	5.71	CCSDT/AVDZ + [CC3/AVTZ − CC3/AVDZ]	Y
281		$^1A'(\pi \rightarrow \pi^*)$	V	89	0.124	6.41	CCSDT/AVDZ + [CC3/AVTZ − CC3/AVDZ]	Y
282		$^1A''(n \rightarrow \pi^*)$	V	93	0.028	6.50	CCSDT/AVDZ + [CC3/AVTZ − CC3/AVDZ]	Y
283		$^1A'(\pi \rightarrow 3p)$	R	88	0.035	6.83	CCSDT/AVDZ + [CC3/AVTZ − CC3/AVDZ]	N
284		$^3A'(\pi \rightarrow \pi^*)$	V	98		4.73	CCSDT/6-31+G(d) + [CC3/AVTZ − CC3/6-31+G(d)]	Y
285		$^3A''(\pi \rightarrow 3s)$	R	97		5.66	CCSDT/AVDZ + [CC3/AVTZ − CC3/AVDZ]	Y
286		$^3A'(\pi \rightarrow \pi^*)$	V	97		5.74	CCSDT/6-31+G(d) + [CC3/AVTZ − CC3/6-31+G(d)]	Y
287		$^3A''(n \rightarrow \pi^*)$	V	97		6.31	CCSDT/AVDZ + [CC3/AVTZ − CC3/AVDZ]	Y
288	Isobutene	$^1B_1(\pi \rightarrow 3s)$	R	94	0.006	6.46	CCSDT/AVTZ	Y
289		$^1A_1(\pi \rightarrow 3p)$	R	94	0.228	7.01	CCSDT/AVTZ	Y
290		$^3A_1(\pi \rightarrow \pi^*)$	V	98		4.53	CCSDT/AVDZ + [CC3/AVTZ − CC3/AVDZ]	Y
291	Ketene	$^1A_2(\pi \rightarrow \pi^*)$	V	91		3.85	FCI/AVDZ + [CCSDT/AVTZ − CCSDT/AVDZ]	Y
292		$^1B_1(n \rightarrow 3s)$	R	93	0.035	6.01	FCI/AVTZ	Y
293		$^1A_1(\pi \rightarrow \pi^*)$	V	92	0.154	7.25	CCSDTQ/AVDZ + [CCSDT/AVTZ − CCSDT/AVDZ]	Y
294		$^1A_2(\pi \rightarrow 3p)$	R	94		7.18	FCI/AVTZ	Y
295		$^3A_2(n \rightarrow \pi^*)$	V	91		3.77	FCI/AVTZ	Y
296		$^3A_1(\pi \rightarrow \pi^*)$	V	98		5.61	FCI/AVTZ	Y
297		$^3B_1(n \rightarrow 3p)$	R	98		5.79	FCI/AVTZ	Y
298		$^3A_2(\pi \rightarrow 3p)$	R	94		7.12	FCI/AVTZ	Y
299		$^1A''[F](\pi \rightarrow \pi^*)$	V	87	0.000	1.00	FCI/AVTZ	Y
300	Maleimide	$^1B_1(n \rightarrow \pi^*)$	V	87	0.000	3.80	CCSDT/AVDZ + [CC3/AVTZ − CC3/AVDZ]	Y
301		$^1A_2(n \rightarrow \pi^*)$	V	85		4.52	CCSDT/AVDZ + [CC3/AVTZ − CC3/AVDZ]	Y
302		$^1B_2(\pi \rightarrow \pi^*)$	V	88	0.025	4.89	CCSDT/AVDZ + [CC3/AVTZ − CC3/AVDZ]	Y

(Continues)

TABLE 2 (Continued)

#	Molecule	Excitation	Nature	%T_1	f	TBE	Method	Safe?
303		$^1B_2(\pi \to \pi^*)$	V	89	0.373	6.21	CCSDT/AVDZ + [CC3/AVTZ − CC3/AVDZ]	Y
304		$^1B_2(n \to 3s)$	R	89	0.034	7.20	CCSDT/AVDZ + [CC3/AVTZ − CC3/AVDZ]	Y
305		$^3B_1(n \to \pi^*)$	V	96		3.57	CCSDT/6-31+G(d) + [CC3/AVTZ − CC3/6-31+G(d)]	Y
306		$^3B_2(\pi \to \pi^*)$	V	98		3.74	CCSDT/6-31+G(d) + [CC3/AVTZ − CC3/6-31+G(d)]	Y
307		$^3B_2(\pi \to \pi^*)$	V	96		4.24	CCSDT/6-31+G(d) + [CC3/AVTZ − CC3/6-31+G(d)]	Y
308		$^3A_2(n \to \pi^*)$	V	96		4.32	CCSDT/6-31+G(d) + [CC3/AVTZ − CC3/6-31+G(d)]	Y
309	Methanimine	$^1A''(n \to \pi^*)$	V	90	0.003	5.23	FCI/AVTZ	Y
310		$^3A''(n \to \pi^*)$	V	98		4.65	FCI/AVTZ	Y
311	Methylenecyclopropene	$^1B_2(\pi \to \pi^*)$	V	85	0.011	4.28	CCSDTQ/6-31+G(d) + [CCSDT/AVTZ − CCSDT/6-31+G(d)]	Y
312		$^1B_1(\pi \to 3s)$	R	93	0.005	5.44	CCSDTQ/6-31+G(d) + [CCSDT/AVTZ − CCSDT/6-31+G(d)]	Y
313		$^1A_2(\pi \to 3p)$	R	93		5.96	CCSDTQ/6-31+G(d) + [CCSDT/AVTZ − CCSDT/6-31+G(d)]	Y
314		$^1A_1(\pi \to \pi^*)$	V	92	0.224	6.12	CCSDTQ/6-31+G(d) + [CCSDT/AVTZ − CCSDT/6-31+G(d)]	N
315		$^3B_2(\pi \to \pi^*)$	V	97		3.49	CCSDT/AVTZ	Y
316		$^3A_1(\pi \to \pi^*)$	V	98		4.74	CCSDT/AVDZ + [CC3/AVTZ − CC3/AVDZ]	Y
317	Naphthalene	$^1B_{3u}(\pi \to \pi^*)$	V	85	0.000	4.27	CCSDT/6-31+G(d) + [CC3/AVTZ − CC3/6-31+G(d)]	Y
318		$^1B_{2u}(\pi \to \pi^*)$	V	90	0.067	4.90	CCSDT/6-31+G(d) + [CC3/AVTZ − CC3/6-31+G(d)]	Y
319		$^1A_u(\pi \to 3s)$	R	92		5.65	CCSDT/6-31+G(d) + [CC3/AVTZ − CC3/6-31+G(d)]	Y
320		$^1B_{1g}(\pi \to \pi^*)$	V	84		5.84	CCSDT/6-31+G(d) + [CC3/AVTZ − CC3/6-31+G(d)]	Y
321		$^1A_g(\pi \to \pi^*)$	V	83		5.89	CCSDT/6-31+G(d) + [CC3/AVTZ − CC3/6-31+G(d)]	N
322		$^1B_{3g}(\pi \to 3p)$	R	92		6.07	CCSDT/6-31+G(d) + [CC3/AVTZ − CC3/6-31+G(d)]	Y
323		$^1B_{2g}(\pi \to 3p)$	R	92		6.09	CCSDT/6-31+G(d) + [CC3/AVTZ − CC3/6-31+G(d)]	Y
324		$^1B_{3u}(\pi \to \pi^*)$	V	90	(n.d.)	6.19	CCSDT/6-31+G(d) + [CC3/AVTZ − CC3/6-31+G(d)]	N
325		$^1B_{1u}(\pi \to 3s)$	R	91	(n.d.)	6.33	CCSDT/6-31+G(d) + [CC3/AVTZ − CC3/6-31+G(d)]	Y
326		$^1B_{2u}(\pi \to \pi^*)$	V	90	(n.d.)	6.42	CCSDT/6-31+G(d) + [CC3/AVTZ − CC3/6-31+G(d)]	Y
327		$^1B_{1g}(\pi \to \pi^*)$	V	87		6.48	CCSDT/6-31+G(d) + [CC3/AVTZ − CC3/6-31+G(d)]	Y

TABLE 2 (Continued)

#	Molecule	Excitation	Nature	%T_1	f	TBE	Method	Safe?
328		$^1A_g(\pi \to \pi^*)$	V	71		6.87	CCSDT/6-31+G(d) + [CC3/AVTZ − CC3/6-31+G(d)]	Y
329		$^3B_{2u}(\pi \to \pi^*)$	V	97		3.17	CC3/AVTZ	N
330		$^3B_{3u}(\pi \to \pi^*)$	V	96		4.16	CC3/AVTZ	N
331		$^3B_{1g}(\pi \to \pi^*)$	V	97		4.48	CC3/AVTZ	N
332		$^3B_{2u}(\pi \to \pi^*)$	V	96		4.64	CC3/AVTZ	N
333		$^3B_{3u}(\pi \to \pi^*)$	V	97		4.95	CC3/AVTZ	N
334		$^3A_g(\pi \to \pi^*)$	V	97		5.49	CC3/AVTZ	N
335		$^3B_{1g}(\pi \to \pi^*)$	V	95		6.17	CC3/AVTZ	N
336		$^3A_g(\pi \to \pi^*)$	V	95		6.39	CC3/AVTZ	N
337	Nitrosomethane	$^1A''(n \to \pi^*)$	V	93	0.000	1.96	FCI/AVDZ + [CCSDT/AVTZ − CCSDT/AVDZ]	Y
338		$^1A'(\text{double})$	V	2	0.000	4.76	FCI/AVTZ	Y
339		$^1A'(\text{n. d.})$	R	90	0.006	6.29	CCSDTQ/AVDZ + [CCSDT/AVTZ − CCSDT/AVDZ]	Y
340		$^3A''(n \to \pi^*)$	V	98		1.16	FCI/AVTZ	Y
341		$^3A'(\pi \to \pi^*)$	V	98		5.60	FCI/AVTZ	Y
342		$^1A''[F](n \to \pi^*)$	V	92	0.000	1.67	FCI/AVDZ + [CCSDT/AVTZ − CCSDT/AVDZ]	Y
343	Nitroxyl (HNO)	$^1A''(n \to \pi^*)$	V	93	0.000	1.74	FCI/AVTZ	Y
344		$^1A'(\text{double})$	V	0	0.000	4.33	FCI/AVTZ	Y
345		$^1A'(\text{n. d.})$	R	92	0.038	6.27	CCSDTQ/AVDZ + [CCSDT/AVTZ − CCSDT/AVDZ]	Y
346		$^3A''(n \to \pi^*)$	V	99		0.88	FCI/AVTZ	Y
347		$^3A'(\pi \to \pi^*)$	V	98		5.61	FCI/AVTZ	Y
348	Octatetraene	$^1B_u(\pi \to \pi^*)$	V	91	1.557	4.78	CCSDT/6-31+G(d) + [CC3/AVTZ − CC3/6-31+G(d)]	Y
349		$^1A_g(\pi \to \pi^*)$	V	63		4.90	CCSDT/6-31+G(d) + [CC3/AVTZ − CC3/6-31+G(d)]	N
350		$^3B_u(\pi \to \pi^*)$	V	97		2.36	CC3/AVTZ	N
351		$^3A_g(\pi \to \pi^*)$	V	98		3.73	CC3/AVTZ	N
352	Propynal	$^1A''(n \to \pi^*)$	V	89	0.000	3.80	CCSDT/AVTZ	Y
353		$^1A''(\pi \to \pi^*)$	V	92	0.000	5.54	CCSDT/AVTZ	Y
354		$^3A''(n \to \pi^*)$	V	97		3.47	CCSDT/AVDZ + [CC3/AVTZ − CC3/AVDZ]	Y
355		$^3A'(\pi \to \pi^*)$	V	98		4.47	CCSDT/AVDZ + [CC3/AVTZ − CC3/AVDZ]	Y
356	Pyrazine	$^1B_{3u}(n \to \pi^*)$	V	90	0.006	4.15	CCSDT/AVTZ	Y
357		$^1A_u(n \to \pi^*)$	V	88		4.98	CCSDT/AVTZ	Y
358		$^1B_{2u}(\pi \to \pi^*)$	V	86	0.078	5.02	CCSDT/AVTZ	Y
359		$^1B_{2g}(n \to \pi^*)$	V	85		5.71	CCSDT/AVTZ	Y
360		$^1A_g(n \to 3s)$	R	91		6.65	CCSDT/AVTZ	Y
361		$^1B_{1g}(n \to \pi^*)$	V	84		6.74	CCSDT/AVTZ	Y
362		$^1B_{1u}(\pi \to \pi^*)$	V	92	0.063	6.88	CCSDT/AVTZ	Y
363		$^1B_{1g}(\pi \to 3s)$	R	93		7.21	CCSDT/AVTZ	Y

(Continues)

TABLE 2 (Continued)

#	Molecule	Excitation	Nature	%T_1	f	TBE	Method	Safe?
364		$^1B_{2u}(n \rightarrow 3p)$	R	90	0.037	7.24	CCSDT/AVDZ + [CC3/AVTZ − CC3/AVDZ]	Y
365		$^1B_{1u}(n \rightarrow 3p)$	R	91	0.128	7.44	CCSDT/AVDZ + [CC3/AVTZ − CC3/AVDZ]	Y
366		$^1B_{1u}(\pi \rightarrow \pi^*)$	V	90	0.285	7.98	CCSDT/AVDZ + [CC3/AVTZ − CC3/AVDZ]	N
367		$^1A_g(\text{double})$	V	12		8.04	NEVPT2/AVTZ	N
368		$^1A_g(\pi \rightarrow \pi^*)$	V	71		8.69	CC3/AVTZ	N
369		$^3B_{3u}(n \rightarrow \pi^*)$	V	97		3.59	CCSDT/AVDZ + [CC3/AVTZ − CC3/AVDZ]	Y
370		$^3B_{1u}(\pi \rightarrow \pi^*)$	V	98		4.35	CCSDT/AVDZ + [CC3/AVTZ − CC3/AVDZ]	Y
371		$^3B_{2u}(\pi \rightarrow \pi^*)$	V	97		4.39	CCSDT/AVDZ + [CC3/AVTZ − CC3/AVDZ]	Y
372		$^3A_u(n \rightarrow \pi^*)$	V	96		4.93	CCSDT/AVDZ + [CC3/AVTZ − CC3/AVDZ]	Y
373		$^3B_{2g}(n \rightarrow \pi^*)$	V	97		5.08	CCSDT/AVDZ + [CC3/AVTZ − CC3/AVDZ]	Y
374		$^3B_{1u}(\pi \rightarrow \pi^*)$	V	97		5.28	CCSDT/AVDZ + [CC3/AVTZ − CC3/AVDZ]	Y
375	Pyridazine	$^1B_1(n \rightarrow \pi^*)$	V	89	0.005	3.83	CCSDT/AVDZ + [CC3/AVTZ − CC3/AVDZ]	Y
376		$^1A_2(n \rightarrow \pi^*)$	V	86		4.37	CCSDT/AVDZ + [CC3/AVTZ − CC3/AVDZ]	Y
377		$^1A_1(\pi \rightarrow \pi^*)$	V	85	0.016	5.26	CCSDT/AVDZ + [CC3/AVTZ − CC3/AVDZ]	Y
378		$^1A_2(n \rightarrow \pi^*)$	V	86		5.72	CCSDT/AVDZ + [CC3/AVTZ − CC3/AVDZ]	Y
379		$^1B_2(n \rightarrow 3s)$	R	88	0.001	6.17	CCSDT/AVDZ + [CC3/AVTZ − CC3/AVDZ]	Y
380		$^1B_1(n \rightarrow \pi^*)$	V	87	0.004	6.37	CCSDT/AVDZ + [CC3/AVTZ − CC3/AVDZ]	Y
381		$^1B_2(\pi \rightarrow \pi^*)$	V	90	0.010	6.75	CCSDT/AVDZ + [CC3/AVTZ − CC3/AVDZ]	Y
382		$^3B_1(n \rightarrow \pi^*)$	V	97		3.19	CCSDT/AVDZ + [CC3/AVTZ − CC3/AVDZ]	Y
383		$^3A_2(n \rightarrow \pi^*)$	V	96		4.11	CCSDT/AVDZ + [CC3/AVTZ − CC3/AVDZ]	Y
384		$^3B_2(\pi \rightarrow \pi^*)$	V	98		4.34	CCSDT/AVDZ + [CC3/AVTZ − CC3/AVDZ]	N
385		$^3A_1(\pi \rightarrow \pi^*)$	V	97		4.82	CCSDT/AVDZ + [CC3/AVTZ − CC3/AVDZ]	Y
386	Pyridine	$^1B_1(n \rightarrow \pi^*)$	V	88	0.004	4.95	CCSDT/AVDZ + [CC3/AVTZ − CC3/AVDZ]	Y
387		$^1B_2(\pi \rightarrow \pi^*)$	V	86	0.028	5.14	CCSDT/AVDZ + [CC3/AVTZ − CC3/AVDZ]	Y
388		$^1A_2(n \rightarrow \pi^*)$	V	87		5.40	CCSDT/AVDZ + [CC3/AVTZ − CC3/AVDZ]	Y

TABLE 2 (Continued)

#	Molecule	Excitation	Nature	%T_1	f	TBE	Method	Safe?
389		$^1A_1(\pi \rightarrow \pi^*)$	V	92	0.010	6.62	CCSDT/AVDZ + [CC3/AVTZ − CC3/AVDZ]	Y
390		$^1A_1(n \rightarrow 3s)$	R	89	0.011	6.76	CCSDT/AVDZ + [CC3/AVTZ − CC3/AVDZ]	Y
391		$^1A_2(\pi \rightarrow 3s)$	R	93		6.82	CCSDT/AVDZ + [CC3/AVTZ − CC3/AVDZ]	Y
392		$^1B_1(\pi \rightarrow 3p)$	R	93	0.045	7.38	CCSDT/AVDZ + [CC3/AVTZ − CC3/AVDZ]	Y
393		$^1A_1(\pi \rightarrow \pi^*)$	V	90	0.291	7.39	CCSDT/AVDZ + [CC3/AVTZ − CC3/AVDZ]	Y
394		$^1B_2(\pi \rightarrow \pi^*)$	V	90	0.319	7.40	CCSDT/AVDZ + [CC3/AVTZ − CC3/AVDZ]	N
395		$^3A_1(\pi \rightarrow \pi^*)$	V	98		4.30	CCSDT/AVDZ + [CC3/AVTZ − CC3/AVDZ]	Y
396		$^3B_1(n \rightarrow \pi^*)$	V	97		4.46	CCSDT/AVDZ + [CC3/AVTZ − CC3/AVDZ]	Y
397		$^3B_2(\pi \rightarrow \pi^*)$	V	97		4.79	CCSDT/AVDZ + [CC3/AVTZ − CC3/AVDZ]	Y
398		$^3A_1(\pi \rightarrow \pi^*)$	V	97		5.04	CCSDT/AVDZ + [CC3/AVTZ − CC3/AVDZ]	Y
399		$^3A_2(n \rightarrow \pi^*)$	V	95		5.36	CCSDT/AVDZ + [CC3/AVTZ − CC3/AVDZ]	Y
400		$^3B_2(\pi \rightarrow \pi^*)$	V	97		6.24	CCSDT/AVDZ + [CC3/AVTZ − CC3/AVDZ]	Y
401	Pyrimidine	$^1B_1(n \rightarrow \pi^*)$	V	88	0.005	4.44	CCSDT/AVDZ + [CC3/AVTZ − CC3/AVDZ]	Y
402		$^1A_2(n \rightarrow \pi^*)$	V	88		4.85	CCSDT/AVDZ + [CC3/AVTZ − CC3/AVDZ]	Y
403		$^1B_2(\pi \rightarrow \pi^*)$	V	86	0.028	5.38	CCSDT/AVDZ + [CC3/AVTZ − CC3/AVDZ]	Y
404		$^1A_2(n \rightarrow \pi^*)$	V	86		5.92	CCSDT/AVDZ + [CC3/AVTZ − CC3/AVDZ]	Y
405		$^1B_1(n \rightarrow \pi^*)$	V	86	0.005	6.26	CCSDT/AVDZ + [CC3/AVTZ − CC3/AVDZ]	Y
406		$^1B_2(n \rightarrow 3s)$	R	90	0.005	6.70	CCSDT/AVDZ + [CC3/AVTZ − CC3/AVDZ]	Y
407		$^1A_1(\pi \rightarrow \pi^*)$	V	91	0.036	6.88	CCSDT/AVDZ + [CC3/AVTZ − CC3/AVDZ]	Y
408		$^3B_1(n \rightarrow \pi^*)$	V	96		4.09	CCSDT/AVDZ + [CC3/AVTZ − CC3/AVDZ]	Y
409		$^3A_1(\pi \rightarrow \pi^*)$	V	98		4.51	CCSDT/AVDZ + [CC3/AVTZ − CC3/AVDZ]	N
410		$^3A_2(n \rightarrow \pi^*)$	V	96		4.66	CCSDT/AVDZ + [CC3/AVTZ − CC3/AVDZ]	Y
411		$^3B_2(\pi \rightarrow \pi^*)$	V	97		4.96	CCSDT/AVDZ + [CC3/AVTZ − CC3/AVDZ]	Y
412	Pyrrole	$^1A_2(\pi \rightarrow 3s)$	R	92		5.24	CCSDT/AVTZ	Y
413		$^1B_1(\pi \rightarrow 3p)$	R	92	0.015	6.00	CCSDT/AVTZ	Y

(Continues)

TABLE 2 (Continued)

#	Molecule	Excitation	Nature	%T_1	f	TBE	Method	Safe?
414		$^1A_2(\pi \to 3p)$	R	93		6.00	CCSDT/AVDZ + [CC3/AVTZ − CC3/AVDZ]	Y
415		$^1B_2(\pi \to \pi^*)$	V	92	0.164	6.26	CCSDT/AVTZ	Y
416		$^1A_1(\pi \to \pi^*)$	V	86	0.001	6.30	CCSDT/AVTZ	Y
417		$^1B_2(\pi \to 3p)$	R	92	0.003	6.83	CCSDT/AVDZ + [CC3/AVTZ − CC3/AVDZ]	Y
418		$^3B_2(\pi \to \pi^*)$	V	98		4.51	CCSDT/AVDZ + [CC3/AVTZ − CC3/AVDZ]	Y
419		$^3A_2(\pi \to 3s)$	R	97		5.21	CCSDT/AVDZ + [CC3/AVTZ − CC3/AVDZ]	Y
420		$^3A_1(\pi \to \pi^*)$	V	97		5.45	CCSDT/AVDZ + [CC3/AVTZ − CC3/AVDZ]	Y
421		$^3B_1(\pi \to 3p)$	R	97		5.91	CCSDT/AVDZ + [CC3/AVTZ − CC3/AVDZ]	Y
422	SiCl$_2$	$^1B_1(\sigma \to \pi^*)$	V	92	0.031	3.91	FCI/AVDZ + [CCSDT/AVTZ − CCSDT/AVDZ]	Y
423		$^3B_1(\sigma \to \pi^*)$	V	98		2.48	CCSDTQ/6-31+G(d) + [CCSDT/AVTZ − CCSDT/6-31+G(d)]	Y
424	Silylidene	$^1A_2(\text{n. d.})$	R	92		2.11	FCI/AVTZ	Y
425		$^1B_2(\text{n. d.})$	R	88	0.033	3.78	FCI/AVTZ	Y
426	Streptocyanine-1	$^1B_2(\pi \to \pi^*)$	V	88	0.347	7.13	FCI/AVDZ + [CCSDT/AVTZ − CCSDT/AVDZ]	Y
427		$^3B_2(\pi \to \pi^*)$	V	98		5.52	FCI/AVTZ	Y
428	Streptocyanine-3	$^1B_2(\pi \to \pi^*)$	V	87	0.755	4.82	FCI/6-31+G(d) + [CC3/AVTZ − CC3/6-31+G(d)]	Y
429		$^3B_2(\pi \to \pi^*)$	V	98		3.44	FCI/6-31+G(d) + [CC3/AVTZ − CC3/6-31+G(d)]	Y
430	Streptocyanine-5	$^1B_2(\pi \to \pi^*)$	V	85	1.182	3.64	CCSDT/AVDZ + [CC3/AVTZ − CC3/AVDZ]	Y
431		$^3B_2(\pi \to \pi^*)$	V	97		2.47	CCSDT/6-31+G(d) + [CC3/AVTZ − CC3/6-31+G(d)]	Y
432	Tetrazine	$^1B_{3u}(n \to \pi^*)$	V	89	0.006	2.47	CCSDT/AVTZ	Y
433		$^1A_u(n \to \pi^*)$	V	87		3.69	CCSDT/AVTZ	Y
434		$^1A_g(\text{double})$	V	0		4.61	NEVPT2/AVTZ	N
435		$^1B_{1g}(n \to \pi^*)$	V	83		4.93	CCSDT/AVTZ	Y
436		$^1B_{2u}(\pi \to \pi^*)$	V	85	0.055	5.21	CCSDT/AVTZ	Y
437		$^1B_{2g}(n \to \pi^*)$	V	81		5.45	CCSDT/AVTZ	Y
438		$^1A_u(n \to \pi^*)$	V	87		5.53	CCSDT/AVTZ	Y
439		$^1B_{3g}(\text{double})$	V	0		6.15	NEVPT2/AVTZ	N
440		$^1B_{2g}(n \to \pi^*)$	V	80		6.12	CCSDT/AVDZ + [CC3/AVTZ − CC3/AVDZ]	Y
441		$^1B_{1g}(n \to \pi^*)$	V	85		6.91	CCSDT/AVDZ + [CC3/AVTZ − CC3/AVDZ]	Y
442		$^3B_{3u}(n \to \pi^*)$	V	97		1.85	CCSDT/AVDZ + [CC3/AVTZ − CC3/AVDZ]	Y
443		$^3A_u(n \to \pi^*)$	V	96		3.45	CCSDT/AVDZ + [CC3/AVTZ − CC3/AVDZ]	Y

TABLE 2 (Continued)

#	Molecule	Excitation	Nature	%T_1	f	TBE	Method	Safe?
444		$^3B_{1g}(n \rightarrow \pi^*)$	V	97		4.20	CCSDT/AVDZ + [CC3/AVTZ − CC3/AVDZ]	Y
445		$^1B_{1u}(\pi \rightarrow \pi^*)$	V	98		4.49	CCSDT/AVDZ + [CC3/AVTZ − CC3/AVDZ]	N
446		$^3B_{2u}(\pi \rightarrow \pi^*)$	V	97		4.52	CCSDT/AVDZ + [CC3/AVTZ − CC3/AVDZ]	Y
447		$^3B_{2g}(n \rightarrow \pi^*)$	V	96		5.04	CCSDT/AVDZ + [CC3/AVTZ − CC3/AVDZ]	Y
448		$^3A_u(n \rightarrow \pi^*)$	V	96		5.11	CCSDT/AVDZ + [CC3/AVTZ − CC3/AVDZ]	Y
449		$^3B_{3g}$(double)	V	5		5.51	NEVPT2/AVTZ	N
450		$^3B_{1u}(\pi \rightarrow \pi^*)$	V	96		5.42	CCSDT/AVDZ + [CC3/AVTZ − CC3/AVDZ]	Y
451	Thioacetone	$^1A_2(n \rightarrow \pi^*)$	V	88		2.53	CCSDTQ/6-31+G(d) + [CCSDT/AVTZ − CCSDT/6-31+G(d)]	Y
452		$^1B_2(n \rightarrow 3s)$	R	91	0.052	5.56	CCSDTQ/6-31+G(d) + [CCSDT/AVTZ − CCSDT/6-31+G(d)]	Y
453		$^1A_1(\pi \rightarrow \pi^*)$	V	90	0.242	5.88	CCSDTQ/6-31+G(d) + [CCSDT/AVTZ − CCSDT/6-31+G(d)]	Y
454		$^1B_2(n \rightarrow 3p)$	R	92	0.028	6.51	CCSDTQ/6-31+G(d) + [CC3/AVTZ − CC3/6-31+G(d)]	Y
455		$^1A_1(n \rightarrow 3p)$	R	91	0.023	6.61	CCSDTQ/6-31+G(d) + [CCSDT/AVTZ − CCSDT/6-31+G(d)]	Y
456		$^3A_2(n \rightarrow \pi^*)$	V	97		2.33	CCSDT/AVDZ + [CC3/AVTZ − CC3/AVDZ]	Y
457		$^3A_1(\pi \rightarrow \pi^*)$	V	98		3.45	CCSDT/AVDZ + [CC3/AVTZ − CC3/AVDZ]	Y
458	Thioacrolein	$^1A''(n \rightarrow \pi^*)$	V	86	0.000	2.11	CCSDT/AVTZ	Y
459		$^3A''(n \rightarrow \pi^*)$	V	96		1.91	CCSDT/AVDZ + [CC3/AVTZ − CC3/AVDZ]	Y
460	Thioformaldehyde	$^1A_2(n \rightarrow \pi^*)$	V	89		2.22	FCI/AVTZ	Y
461		$^1B_2(n \rightarrow 3s)$	R	92	0.012	5.96	FCI/AVTZ	Y
462		$^1A_1(\pi \rightarrow \pi^*)$	V	90	0.178	6.38	CCSDTQ/AVDZ + [CCSDT/AVTZ − CCSDT/AVDZ]	Y
463		$^3A_2(n \rightarrow \pi^*)$	V	97		1.94	FCI/AVTZ	Y
464		$^3A_1(\pi \rightarrow \pi^*)$	V	98		3.43	FCI/AVTZ	Y
465		$^3B_2(n \rightarrow 3s)$	R	97		5.72	FCI/AVDZ + [CCSDT/AVTZ − CCSDT/AVDZ]	Y
466		$^1A_2[F](n \rightarrow \pi^*)$	V	87		1.95	FCI/AVTZ	Y
467	Thiophene	$^1A_1(\pi \rightarrow \pi^*)$	V	87	0.070	5.64	CCSDT/AVTZ	Y
468		$^1B_2(\pi \rightarrow \pi^*)$	V	91	0.079	5.98	CCSDT/AVTZ	Y
469		$^1A_2(\pi \rightarrow 3s)$	R	92		6.14	CCSDT/AVTZ	Y
470		$^3B_1(\pi \rightarrow 3p)$	R	90	0.010	6.14	CCSDT/AVTZ	Y
471		$^1A_2(\pi \rightarrow 3p)$	R	91		6.21	CCSDT/AVTZ	Y
472		$^1B_1(\pi \rightarrow 3s)$	R	92	0.000	6.49	CCSDT/AVTZ	Y
473		$^1B_2(\pi \rightarrow 3p)$	R	92	0.082	7.29	CCSDT/AVTZ	Y
474		$^1A_1(\pi \rightarrow \pi^*)$	V	86	0.314	7.31	CCSDT/6-31+G(d) + [CC3/AVTZ − CC3/6-31+G(d)]	N

(Continues)

TABLE 2 (Continued)

#	Molecule	Excitation	Nature	%T_1	f	TBE	Method	Safe?
475		$^3B_2(\pi \to \pi^*)$	V	98		3.97	FCI/6-31+G(d) + [CC3/AVTZ − CC3/ 6-31+G(d)]	Y
476		$^3A_1(\pi \to \pi^*)$	V	97		4.76	CCSDT/AVDZ + [CC3/AVTZ − CC3/ AVDZ]	Y
478		$^3B_1(\pi \to 3p)$	R	96		5.93	CCSDT/AVDZ + [CC3/AVTZ − CC3/ AVDZ]	Y
478		$^3A_2(\pi \to 3s)$	R	97		6.08	CCSDT/AVDZ + [CC3/AVTZ − CC3/ AVDZ]	Y
479	Thiopropynal	$^1A''(n \to \pi^*)$	V	87	0.000	2.03	CCSDT/AVTZ	Y
480		$^3A''(n \to \pi^*)$	V	97		1.80	CCSDT/AVDZ + [CC3/AVTZ − CC3/ AVDZ]	Y
481	Triazine	$^1A_{1''}(n \to \pi^*)$	V	88		4.72	CCSDT/AVTZ	Y
482		$^1A_{2''}(n \to \pi^*)$	V	88	0.014	4.75	CCSDT/AVTZ	Y
483		$^1E''(n \to \pi^*)$	V	88		4.78	CCSDT/AVTZ	Y
484		$^1A_{2'}(\pi \to \pi^*)$	V	85		5.75	CCSDT/AVTZ	Y
485		$^1A_{1'}(\pi \to \pi^*)$	V	90		7.24	CCSDT/AVTZ	Y
486		$^1E'(n \to 3s)$	R	90	0.016	7.32	CCSDT/AVTZ	Y
487		$^1E''(n \to \pi^*)$	V	82		7.78	CCSDT/AVTZ	Y
488		$^1E'(\pi \to \pi^*)$	V	90	0.451	7.94	CCSDT/AVTZ	Y
489		$^3A_{2''}(n \to \pi^*)$	V	96		4.33	CCSDT/AVDZ + [CC3/AVTZ − CC3/ AVDZ]	Y
490		$^3E''(n \to \pi^*)$	V	96		4.51	CCSDT/AVDZ + [CC3/AVTZ − CC3/ AVDZ]	Y
491		$^3A_{1''}(n \to \pi^*)$	V	96		4.73	CCSDT/AVDZ + [CC3/AVTZ − CC3/ AVDZ]	Y
492		$^3A_{1'}(\pi \to \pi^*)$	V	98		4.85	CCSDT/AVDZ + [CC3/AVTZ − CC3/ AVDZ]	Y
493		$^3E'(\pi \to \pi^*)$	V	96		5.59	CCSDT/6-31+G(d) + [CC3/AVTZ − CC3/6-31+G(d)]	Y
494		$^3A_{2'}(\pi \to \pi^*)$	V	97		6.62	CCSDT/AVDZ + [CC3/AVTZ − CC3/ AVDZ]	Y
495	Water	$^1B_1(n \to 3s)$	R	93	0.054	7.62	FCI/AVTZ	Y
496		$^1A_2(n \to 3p)$	R	93		9.41	FCI/AVTZ	Y
497		$^1A_1(n \to 3s)$	R	93	0.100	9.99	FCI/AVTZ	Y
498		$^3B_1(n \to 3s)$	R	98		7.25	FCI/AVTZ	Y
499		$^3A_2(n \to 3p)$	R	98		9.24	FCI/AVTZ	Y
500		$^3A_1(n \to 3s)$	R	98		9.54	FCI/AVTZ	Y

Note: "Method" provides the protocol employed to compute the TBEs. The nature of the excitation is also provided: V, R, and CT stands for valence, Rydberg, and charge transfer, respectively. [F] indicates a fluorescence transition, that is, a vertical transition energy computed from an excited-state geometry. AVXZ stands for aug-cc-pVXZ.

5 | BENCHMARKS

In this section, we report a comprehensive benchmark of various lower-order methods on the entire set of closed-shell compounds belonging to the QUEST database. Statistical quantities are reported in Table 4 (the entire set of data can be found in the Supporting information). In addition, we also provide a specific analysis for each type of excited states. Hence, the statistical values are reported for various types of excited states and molecular sizes for the MSE and MAE.

TABLE 3 Theoretical best estimates TBEs (in eV) for the doublet–doublet transitions of the open-shell molecules belonging to QUEST#4

#	Molecule	Transition	TBE/aug-cc-pVTZ	Method
1	Allyl	$^2B_1$	3.39	FCI/6-31+G(d) + [CCSDT/aug-cc-pVTZ − CCSDT/6-31+G(d)]
2		$^2A_1$	4.99	FCI/6-31+G(d) + [CCSDT/aug-cc-pVTZ − CCSDT/6-31+G(d)]
3	BeF	$^2\Pi$	4.14	FCI/aug-cc-pVTZ
4		$^2\Sigma^+$	6.21	FCI/aug-cc-pVTZ
5	BeH	$^2\Pi$	2.49	FCI/aug-cc-pVTZ
6		$^2\Pi$	6.46	FCI/aug-cc-pVTZ
7	BH_2	$^2B_1$	1.18	FCI/aug-cc-pVTZ
8	CH	$^2\Delta$	2.91	FCI/aug-cc-pVTZ
9		$^2\Sigma^-$	3.29	FCI/aug-cc-pVTZ
10		$^2\Sigma^+$	3.98	FCI/aug-cc-pVTZ
11	CH_3	$^2A_{1'}$	5.85	FCI/aug-cc-pVTZ
12		$^2E'$	6.96	FCI/aug-cc-pVTZ
13		$^2E'$	7.18	FCI/aug-cc-pVTZ
14		$^2A_{2''}$	7.65	FCI/aug-cc-pVTZ
15	CN	$^2\Pi$	1.34	FCI/aug-cc-pVTZ
16		$^2\Sigma^+$	3.22	FCI/aug-cc-pVTZ
17	CNO	$^2\Sigma^+$	1.61	FCI/aug-cc-pVTZ
18		$^2\Pi$	5.49	FCI/6-31+G(d) + [CCSDT/aug-cc-pVTZ − CCSDT/6-31+G(d)]
19	CON	$^2\Pi$	3.53	FCI/aug-cc-pVDZ + [CCSDT/aug-cc-pVTZ − CCSDT/aug-cc-pVDZ]
20		$^2\Sigma^+$	3.86	CCSDTQ/6-31+G(d) + [CCSDT/aug-cc-pVTZ − CCSDT/6-31+G(d)]
21	CO^+	$^2\Pi$	3.28	FCI/aug-cc-pVTZ
22		$^2\Sigma^+$	5.81	FCI/aug-cc-pVTZ
23	F_2BO	$^2B_1$	0.73	FCI/aug-cc-pVDZ + [CCSDT/aug-cc-pVTZ − CCSDT/aug-cc-pVDZ]
24		$^2A_1$	2.80	FCI/aug-cc-pVDZ + [CCSDT/aug-cc-pVTZ − CCSDT/aug-cc-pVDZ]
25	F_2BS	$^2B_1$	0.51	FCI/aug-cc-pVDZ + [CCSDT/aug-cc-pVTZ − CCSDT/aug-cc-pVDZ]
26		$^2A_1$	2.99	FCI/aug-cc-pVDZ + [CCSDT/aug-cc-pVTZ − CCSDT/aug-cc-pVDZ]
27	H_2BO	$^2B_1$	2.15	FCI/aug-cc-pVTZ
28		$^2A_1$	3.49	FCI/aug-cc-pVTZ
29	HCO	$^2A''$	2.09	FCI/aug-cc-pVTZ
30		$^2A'$	5.45	FCI/aug-cc-pVDZ + [CCSDT/aug-cc-pVTZ − CCSDT/aug-cc-pVDZ]
31	HOC	$^2A''$	0.92	FCI/aug-cc-pVTZ
32	H_2PO	$^2A''$	2.80	FCI/aug-cc-pVTZ
33		$^2A'$	4.21	FCI/aug-cc-pVDZ + [CCSDT/aug-cc-pVTZ − CCSDT/aug-cc-pVDZ]
34	H_2PS	$^2A''$	1.16	FCI/aug-cc-pVTZ
35		$^2A'$	2.72	FCI/aug-cc-pVTZ
36	NCO	$^2\Sigma^+$	2.89	FCI/aug-cc-pVDZ + [CCSDT/aug-cc-pVTZ − CCSDT/aug-cc-pVDZ]
37		$^2\Pi$	4.73	FCI/aug-cc-pVDZ + [CCSDT/aug-cc-pVTZ − CCSDT/aug-cc-pVDZ]
38	NH_2	$^2A_1$	2.12	FCI/aug-cc-pVTZ
39	Nitromethyl	$^2B_2$	2.05	CCSDT/aug-cc-pVTZ
40		$^2A_2$	2.38	CCSDT/aug-cc-pVTZ
41		$^2A_1$	2.56	CCSDT/aug-cc-pVTZ
42		$^2B_1$	5.35	CCSDT/aug-cc-pVTZ

(Continues)

TABLE 3 (Continued)

#	Molecule	Transition	TBE/aug-cc-pVTZ	Method
43	NO	$^2\Sigma^+$	6.13	FCI/aug-cc-pVTZ
44		$^2\Sigma^+$	7.29	CCSDTQ/aug-cc-pVTZ
45	OH	$^2\Sigma^+$	4.10	FCI/aug-cc-pVTZ
46		$^2\Sigma^-$	8.02	FCI/aug-cc-pVTZ
47	PH$_2$	$^2A_1$	2.77	FCI/aug-cc-pVTZ
48	Vinyl	$^2A''$	3.26	FCI/aug-cc-pVTZ
49		$^2A''$	4.69	FCI/aug-cc-pVTZ
50		$^2A'$	5.60	FCI/aug-cc-pVTZ
51		$^2A'$	6.20	FCI/6-31+G(d) + [CCSDT/aug-cc-pVTZ − CCSDT/6-31+G(d)]

Note: These TBEs are obtained with the aug-cc-pVTZ basis set, and "Method" indicates the protocol employed to compute them.

The distribution of the errors in vertical excitation energies (with respect to the TBE/aug-cc-pVTZ reference values) is represented in Figure 5 for all the "safe" excitations having a dominant single excitation character (i.e., the double excitations are discarded). Similar graphs are reported in the Supporting information for specific sets of transitions and molecules. For the vast majority of the cases, the comparison between methods presented here is performed for Franck-Condon geometries only. Therefore, it is important to stress that the present method ranking might change significantly when moving away from the Franck-Condon region as most excited-state methods do not provide a uniform description of potential energy surfaces.

The most striking feature from the statistical indicators gathered in Table 4 is the overall accuracy of CC3 with MAEs and MSEs systematically below the chemical accuracy threshold (errors <0.043 eV or 1 kcal/mol), irrespective of the nature of the transition and the size of the molecule. CCSDR(3) are CCCSDT-3 can also be regarded as excellent performers with overall MAEs below 0.05 eV, though one would notice a slight degradation of their performances for the $n \rightarrow \pi^*$ excitations and the largest molecules of the database. The other third-order method, ADC(3), which enjoys a lower computational cost, is significantly less accurate and does not really improve upon its second-order analog, even for the largest systems considered here, an observation in line with a previous analysis by some of the authors.[212] Nonetheless, ADC(3)'s accuracy improves in larger compounds, with a MAE of 0.24 eV (0.16 eV) for the subsets of the most compact (extended) compounds considered herein. The ADC(2.5) composite method introduced in Ref. 212, which corresponds to grossly average the ADC(2) and ADC(3) values, yields an appreciable accuracy improvement, as shown in Figure 4. Indeed, we note that the MAE of 0.07 eV obtained for "large" compounds is comparable to the one obtained with CCSDR(3) and CCSDT-3 for these molecules. All these third-order methods are rather equally efficient for valence and Rydberg transitions.

Concerning the second-order methods (which have the indisputable advantage to be applicable to larger molecules than the ones considered here), we have the following ranking in terms of MAEs: EOM-MP2 ≈ CIS(D) < CC2 ≈ ADC (2) < CCSD ≈ STEOM-CCSD, which fits our previous conclusions on the specific subsets.[93–96, 212] A very similar ranking is obtained when one looks at the MSEs. It is noteworthy that the performances of EOM-MP2 and CCSD are getting notably worse when the system size increases, while CIS(D) and STEOM-CCSD have a very stable behavior with respect to system size. Indeed, the EOM-MP2 MAE attains 0.42 eV for molecules containing between 7 and 10 non-hydrogen atoms, whereas the CCSD tendency to overshoot the transition energies yield a MSE of 0.22 eV for the same set (a rather large error).

For CCSD, this conclusion fits benchmark studies published by other groups.[60, 207, 221–224] For example, Kánnár and Szalay obtained a MAE of 0.18 eV on Thiel's set for the states exhibiting a dominant single excitation character. The CCSD degradation with system size might partially explain the similar (though less pronounced) trend obtained for CCSDR(3). Regarding the apparently better performances of STEOM-CCSD as compared to CCSD, we recall that several challenging states have been naturally removed from the STEOM-CCSD statistics because the active character percentage was lower than 98% (see above).

In contrast to EOM-MP2 and CCSD, the overall accuracy of CC2 and ADC(2) does significantly improve for larger molecules, the performances of the two methods being, as expected, similar.[200] Let us note that these two methods show similar accuracies for singlet and triplet transitions, but are significantly less accurate for Rydberg transitions, as

TABLE 4 Mean signed error (MSE), mean absolute error (MAE), root-mean-square error (RMSE), standard deviation of the errors (SDE), as well as the maximum positive error [Max(+)] and negative error [Max(−)] with respect to the TBE/aug-cc-pVTZ for the entire QUEST database

		CIS(D)	CC2	EOM-MP2	STEOM-CCSD	CCSD	CCSDR(3)	CCSDT-3	CC3	SOS-ADC(2)[a]	SOS-CC2[a]	SCS-CC2[a]	SOS-ADC(2)[b]	ADC(2)	ADC(3)	ADC(2.5)
Count		429	431	427	360	431	259	251	431	430	430	430	430	426	423	423
Max(+)		1.06	0.63	0.80	0.59	0.80	0.43	0.26	0.19	0.87	0.84	0.76	0.73	0.64	0.60	0.24
Max(−)		−0.69	−0.71	−0.38	−0.56	−0.25	−0.07	−0.07	−0.09	−0.29	−0.24	−0.92	−0.46	−0.76	−0.79	−0.34
MSE		0.13	0.02	0.18	−0.01	0.10	0.04	0.04	0.00	0.18	0.21	0.15	0.02	−0.01	−0.12	−0.06
	Singlet	0.10	−0.02	0.22	0.03	0.14	0.04	0.04	0.00	0.18	0.20	0.13	0.00	−0.04	−0.08	−0.06
	Triplet	0.19	0.08	0.14	−0.07	0.03			0.00	0.19	0.22	0.17	0.04	0.04	−0.18	−0.07
	valence	0.20	0.10	0.20	−0.06	0.10	0.06	0.05	0.00	0.19	0.24	0.20	0.02	0.04	−0.16	−0.06
	Rydberg	−0.04	−0.17	0.15	0.09	0.08	0.01	0.03	−0.01	0.16	0.12	0.01	0.02	−0.13	−0.02	−0.07
	$n \rightarrow \pi^*$	0.16	0.02	0.24	−0.03	0.17	0.07	0.07	0.00	0.26	0.32	0.22	0.05	−0.05	−0.01	−0.03
	$\pi \rightarrow \pi^*$	0.25	0.17	0.20	−0.07	0.06	0.05	0.04	0.00	0.15	0.19	0.19	0.00	0.12	−0.27	−0.07
	1–3 non-H	0.10	0.03	0.03	−0.02	0.04	0.01	0.01	0.00	0.13	0.16	0.11	−0.01	−0.01	−0.17	−0.09
	4 non-H	0.13	0.04	0.12	0.00	0.09	0.03	0.04	0.00	0.19	0.26	0.19	0.03	−0.04	−0.10	−0.07
	5–6 non-H	0.17	0.02	0.30	−0.01	0.11	0.05	0.05	0.00	0.21	0.20	0.14	0.03	0.03	−0.10	−0.04
	7–10 non-H	0.15	−0.03	0.42	−0.05	0.22	0.10	0.08	−0.01	0.26	0.29	0.19	0.05	−0.06	−0.02	−0.04
SDE		0.24	0.20	0.21	0.13	0.12	0.05	0.04	0.02	0.17	0.16	0.16	0.15	0.20	0.22	0.08
RMSE		0.29	0.22	0.28	0.15	0.16	0.07	0.06	0.03	0.25	0.26	0.22	0.17	0.21	0.26	0.10
MAE		0.22	0.16	0.22	0.11	0.12	0.05	0.04	0.02	0.20	0.22	0.18	0.13	0.15	0.21	0.08
	Singlet	0.22	0.16	0.25	0.10	0.14	0.05	0.04	0.02	0.21	0.22	0.17	0.14	0.16	0.20	0.09
	Triplet	0.23	0.15	0.18	0.12	0.08			0.01	0.20	0.23	0.19	0.11	0.15	0.22	0.08
	Valence	0.22	0.14	0.24	0.12	0.13	0.06	0.05	0.02	0.21	0.25	0.20	0.12	0.13	0.22	0.08
	Rydberg	0.22	0.21	0.19	0.10	0.08	0.03	0.03	0.02	0.20	0.15	0.13	0.14	0.21	0.18	0.09
	$n \rightarrow \pi^*$	0.18	0.08	0.28	0.08	0.17	0.07	0.07	0.01	0.26	0.32	0.22	0.11	0.10	0.14	0.07
	$\pi \rightarrow \pi^*$	0.27	0.19	0.21	0.14	0.11	0.06	0.04	0.02	0.18	0.21	0.20	0.12	0.16	0.28	0.09
	1–3 non-H	0.23	0.19	0.13	0.10	0.07	0.03	0.03	0.02	0.18	0.20	0.19	0.14	0.19	0.24	0.10
	4 non-H	0.22	0.19	0.15	0.11	0.11	0.03	0.04	0.02	0.19	0.26	0.22	0.13	0.18	0.23	0.08
	5–6 non-H	0.21	0.12	0.30	0.12	0.13	0.06	0.05	0.01	0.22	0.21	0.15	0.11	0.11	0.19	0.07
	7–10 non-H	0.24	0.11	0.42	0.12	0.23	0.10	0.08	0.02	0.27	0.29	0.19	0.12	0.14	0.16	0.07

Note: Only the "safe" TBEs are considered (see Table 2). For the MSE and MAE, the statistical values are reported for various types of excited states and molecular sizes. All quantities are given in eV. "Count" refers to the number of transitions considered for each method.
[a]Excitation energies computed with TURBOMOLE.
[b]Excitation energies computed with Q-CHEM.
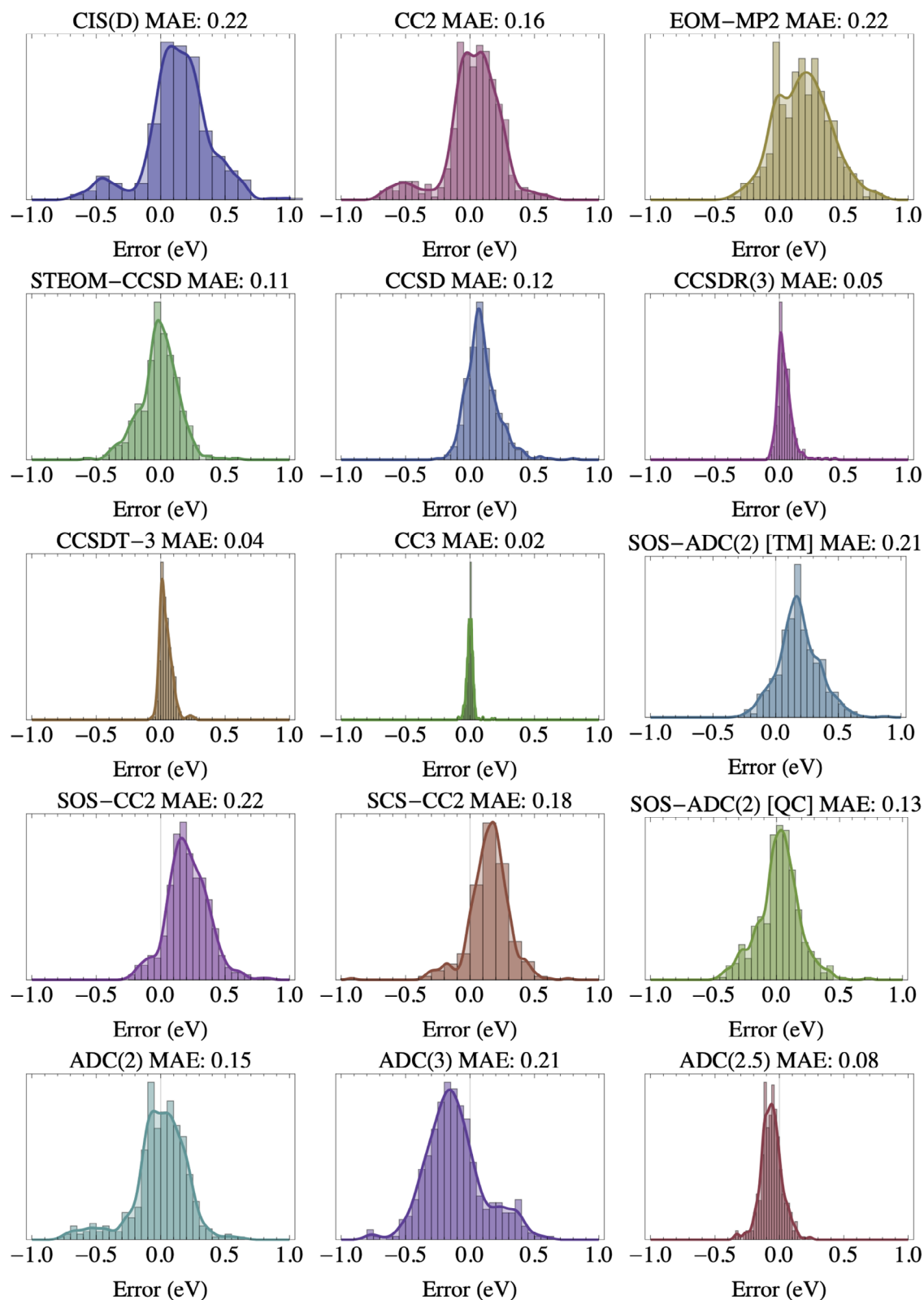
FIGURE 5 Distribution of the error (in eV) in excitation energies (with respect to the TBE/aug-cc-pVTZ values) for various methods for the entire QUEST database considering only closed-shell compounds. Only the "safe" TBEs are considered (see Table 2). See Table 4 for the values of the corresponding statistical quantities. QC and TM indicate that Q-CHEM and TURBOMOLE scaling factors are considered, respectively. The SOS-CC2 and SCS-CC2 approaches are obtained with the latter code

already pointed out previously.[224] Therefore, both CC2 and ADC(2) offer an appealing cost-to-accuracy ratio for large compounds, which explains their popularity in realistic chemical scenarios.[30, 82, 83, 88, 90, 99] For the scaled methods (SOS-ADC(2), SOS-CC2, and SCS-CC2), the TURBOMOLE scaling factors do not seem to improve things upon the unscaled versions, while the Q-CHEM scaling factors for ADC(2) provide a small, yet significant improvement for this set of molecules. Of course, one of the remaining open questions regarding all these methods is their accuracy for even larger systems.

6 | THE QUESTDB WEBSITE

Quite a large number of calculations were required for each of the QUEST articles.[93–96, 212] Up to now, all the curated data were shared as supplementary information presented as a file in portable document format. This way of sharing data does not require too much effort for the authors, but it is obviously not optimal from the user's point of view. We have now addressed this problem by creating a database which contains all the vertical and fluorescence transition energies as well the corresponding molecular geometries. These data can be manipulated via a web application which allows to plot the statistical indicators (generated with the Plotly library) computed on selected subsets of molecules, methods, and basis sets. The application also gives the possibility to the user to import external data files, in order to compare the performance of methods that are not in our database. Both the web application and the data are hosted in a single GitHub repository (https://github.com/LCPQ/QUESTDB_website) and available at the following address: https://lcpq.github.io/QUESTDB_website. In this way, extending the database is as simple as adding new data files to the repository, together with the corresponding bibliographic references, and we strongly encourage users to contribute to enlarge this database via GitHub pull requests.

7 | CONCLUDING REMARKS

In the present review article, we have presented and extended the QUEST database of highly accurate excitation energies for molecular systems[15, 93–96] that we started building in 2018 and that is now composed by more than 500 vertical excitations, many of which can be reasonably considered as within 1 kcal/mol (or less) of the FCI limit for the considered CC3/aug-cc-pVTZ geometry and basis set (aug-cc-pVTZ). In particular, we have detailed the specificities of our protocol by providing computational details regarding geometries, basis sets, as well as reference and benchmarked computational methods. The content of our five QUEST subsets has been presented in detail, and for each of them, we have provided the number of reference excitation energies, the nature and size of the molecules, the list of benchmarked methods, as well as other useful specificities. Importantly, we have proposed a new statistical method that produces much safer estimates of the extrapolation error in SCI calculations. This new method based on Gaussian random variables has been tested by computing additional FCI values for five- and six-membered rings. After having discussed the generation of our TBEs, we have reported a comprehensive benchmark for a significant number of methods on the entire QUEST set with, in addition, a specific analysis for each type of excited states. Finally, the main features of the website specifically designed to gather the entire data generated during these past few years have been presented and discussed.

Paraphrasing Thiel's conclusions,[60] we hope that not only the QUEST database will be used for further benchmarking and testing, but that other research groups will also improve it, providing not only corrections (inevitable in such a large dataset), but more importantly extensions with both improved estimates for some compounds and states, or new molecules. In this framework, we provide in the Supporting information a file with all our benchmark data.

Regarding future improvements and extensions, we would like to mention that although our present goal is to produce chemically accurate vertical excitation energies, we are currently devoting great efforts to obtain highly accurate excited-state properties[225, 226] such as dipoles and oscillator strengths for molecules of small and medium sizes,[227, 228] so as to complete previous efforts aiming at determining accurate excited-state geometries.[172, 229] In this context, methods for which one has access to analytic nuclear gradients (e.g., ADC(2), CC2, and EOM-CCSD) and frequencies (e.g., TD-DFT) have an indisputable edge. Reference ground-state properties (such as correlation energies and atomization energies) are also being currently produced.[127, 170] Additional reference energies for charge-transfer excited states[78, 91] and transition metal compounds[52, 54] would be a valuable addition to the present database. Besides this, because computing

500 (or so) excitation energies can be a costly exercise even with cheap computational methods, we are planning on developing a "diet set" (i.e., a much smaller set of excitation energies which can reproduce key results of the full QUEST database, including ranking of approximations) following the philosophy of the "diet GMTKN55" set proposed recently by Gould.[230] We hope to report on this in the near future.

CONFLICT OF INTEREST
The authors have declared no conflicts of interest for this article.

AUTHOR CONTRIBUTIONS
Mickael Veril: Data curation; formal analysis; software; writing-original draft. **Anthony Scemama:** Data curation; formal analysis; software; supervision; writing-review and editing. **Michel Caffarel:** Formal analysis; methodology; writing-review and editing. **Filippo Lipparini:** Data curation; writing-review and editing. **Martial Boggio-Pasqua:** Data curation; writing-review and editing. **Denis Jacquemin:** Conceptualization; methodology; writing-review and editing.

ORCID
Anthony Scemama https://orcid.org/0000-0003-4955-7136
Pierre-François Loos https://orcid.org/0000-0003-0598-7425

RELATED WIRES ARTICLE
Density functional theory with London dispersion corrections

REFERENCES
1. Szabo A, Ostlund NS. *Modern quantum chemistry*. New York: McGraw-Hill; 1989.
2. Jensen F. *Introduction to computational chemistry*. 3rd ed. New York: Wiley; 2017.
3. Cramer CJ. *Essentials of computational chemistry: theories and models*. New York: Wiley; 2004.
4. Helgaker T, Jørgensen P, Olsen J. *Molecular electronic-structure theory*. New York: John Wiley & Sons, Inc.; 2013.
5. Roos BO, Andersson K, Fulscher MP, Malmqvist PA, Serrano-Andrés L. Multiconfigurational perturbation theory: applications in electronic spectroscopy. In: Prigogine I, Rice SA, editors. *Adv. Chem. Phys.* Volume XCIII. New York: Wiley; 1996. p. 219–331.
6. Piecuch P, Kowalski K, Pimienta ISO, Mcguire MJ. Recent advances in electronic structure theory: method of moments of coupled-cluster equations and renormalized coupled-cluster approaches. *Int Rev Phys Chem*. 2002;21:527–655.
7. Dreuw A, Head-Gordon M. Single-reference ab initio methods for the calculation of excited states of large molecules. *Chem Rev*. 2005; 105:4009–37.
8. Krylov AI. Spin-flip equation-of-motion coupled-cluster electronic structure method for a description of excited states, bond breaking, diradicals, and triradicals. *Acc Chem Res*. 2006;39:83–91.PMID: 16489727.
9. Sneskov K, Christiansen O. Excited state coupled cluster methods. *WIREs Comput Mol Sci*. 2012;2:566–84.
10. González L, Escudero D, Serrano-Andrés L. Progress and challenges in the calculation of electronic excited states. *Chem Phys Chem*. 2012;13:28–51.
11. Laurent AD, Jacquemin D. TD-DFT benchmarks: a review. *Int J Quantum Chem*. 2013;113:2019–39.
12. Adamo C, Jacquemin D. The calculations of excited-state properties with time-dependent density functional theory. *Chem Soc Rev*. 2013;42:845–56.
13. Ghosh S, Verma P, Cramer CJ, Gagliardi L, Truhlar DG. Combining wave function methods with density functional theory for excited states. *Chem Rev*. 2018;118:7249–92.
14. Blase X, Duchemin I, Jacquemin D, Loos PF. The Bethe-Salpeter formalism: from physics to chemistry. *J Phys Chem Lett*. 2020;11: 7371–82.
15. Loos PF, Scemama A, Jacquemin D. The quest for highly-accurate excitation energies: a computational perspective. *J Phys Chem Lett*. 2020;11:2374–83.
16. Bernardi F, Olivucci M, Robb MA. Potential energy surface crossings in organic photochemistry. *Chem Soc Rev*. 1996;25:321.
17. Olivucci M. *Computational photochemistry*. Amsterdam/Boston, MA/Paris: Elsevier Science; 2010 OCLC: 800555856.
18. Robb MA, Garavelli M, Olivucci M, Bernardi F. In: Lipkowitz KB, Boyd DB, editors. *A computational strategy for organic photochemistry*. Hoboken, NJ: John Wiley & Sons, Inc.; 2007. p. 87–146.

19. Navizet I, Liu YJ, Ferre N, Roca-Sanjun D, Lindh R. The chemistry of bioluminescence: an analysis of chemical functionalities. *ChemPhysChem*. 2011;*12*:3064–76.

20. Crespo-Otero R, Barbatti M. Recent advances and perspectives on nonadiabatic mixed quantum–classical dynamics. *Chem Rev*. 2018; *118*:7026–68.

21. Robb MA. *Theoretical chemistry for electronic excited states*. Theoretical and computational chemistry series. The Royal Society of Chemistry; 2018.

22. Mai S, González L. Molecular photochemistry: recent developments in theory. *Angew Chem Int Ed*. 2020;*59*:16832–46.

23. Monkhorst HJ. Calculation of properties with the coupled-cluster method. *Int J Quantum Chem*. 1977;*12*:421–32.

24. Helgaker T, Jørgensen P, Handy NC. A numerically stable procedure for calculating Møller-Plesset energy derivatives, derived using the theory of Lagrangians. *Theoret Chim Acta*. 1989;*76*:227–45.

25. Koch H, Jensen HJA, Jo/rgensen P, Helgaker T. Excitation energies from the coupled cluster singles and doubles linear response function (CCSDLR). Applications to Be, CH$^+$, CO, and H$_2$O. *J Chem Phys*. 1990;*93*:3345–50.

26. Christiansen O, Koch H, Jørgensen P. Response functions in the CC3 iterative triple excitation model. *J Chem Phys*. 1995;*103*:7429–41.

27. Christiansen O, Jørgensen P, Hättig C. Response functions from Fourier component variational perturbation theory applied to a time-averaged quasienergy. *Int J Quantum Chem*. 1998;*68*:1–52.

28. Hättig C. Geometry optimizations with the coupled-cluster model CC2 using the resolution-of-the-identity approximation. *J Chem Phys*. 2003;*118*:7751–61.

29. Kállay M, Gauss J. Calculation of excited-state properties using general coupled-cluster and configuration-interaction models. *J Chem Phys*. 2004;*121*:9257–69.

30. Hättig C. Structure optimizations for excited states with correlated second-order methods: CC2 and ADC(2). In: Jensen HJA, editor. *Response theory and molecular properties (a tribute to Jan Linderberg and Poul Jørgensen)*. Advances in Quantum Chemistry. Volume 50. Academic Press; 2005. p. 37–60.

31. Dreuw A, Wormit M. The algebraic diagrammatic construction scheme for the polarization propagator for the calculation of excited states. *WIREs Comput Mol Sci*. 2015;*5*:82–95.

32. Pople JA, Head-Gordon M, Fox DJ, Raghavachari K, Curtiss LA. Gaussian-1 theory: a general procedure for prediction of molecular energies. *J Chem Phys*. 1989;*90*:5622–9.

33. Curtiss LA, Raghavachari K, Trucks GW, Pople JA. Gaussian-2 theory for molecular energies of first- and second-row compounds. *J Chem Phys*. 1991;*94*:7221–30.

34. Curtiss LA, Raghavachari K, Redfern PC, Pople JA. Assessment of Gaussian-2 and density functional theories for the computation of enthalpies of formation. *J Chem Phys*. 1997;*106*:1063–79.

35. Curtiss LA, Raghavachari K, Redfern PC, Rassolov V, Pople JA. Gaussian-3 (G3) theory for molecules containing first and second-row atoms. *J Chem Phys*. 1998;*109*:7764–76.

36. Curtiss LA, Redfern PC, Raghavachari K. Gaussian-4 theory. *J Chem Phys*. 2007;*126*:084108.

37. Ángyán J, Dobson J, Jansen G, Gould T. *London dispersion forces in molecules, solids and nano-structures*. Theoretical and Computational Chemistry Series. The Royal Society of Chemistry; 2020.

38. Jurecka P, Šponer J, Cerný J, Hobza P. Benchmark database of accurate (MP2 and CCSD(T) complete basis set limit) interaction energies of small model complexes, DNA base pairs, and amino acid pairs. *Phys Chem Chem Phys*. 2006;*8*:1985–93.

39. Rezác J, Riley KE, Hobza P. S66: a well-balanced database of benchmark interaction energies relevant to biomolecular structures. *J Chem Theory Comput*. 2011;*7*:2427–38.PMID: 21836824.

40. van Setten MJ, Caruso F, Sharifzadeh S, Ren X, Scheffler M, Liu F, et al. *GW* 100: benchmarking *G*0*W*0 for molecular systems. *J Chem Theory Comput*. 2015;*11*:5665–87.

41. Krause K, Harding ME, Klopper W. Coupled-cluster reference values for the Gw27 and Gw100 test sets for the assessment of Gw methods. *Mol Phys*. 2015;*113*:1952–60.

42. Maggio E, Kresse G. Correlation energy for the homogeneous electron gas: exact Bethe-Salpeter solution and an approximate evaluation. *Phys Rev B*. 2016;*93*:235113.

43. Stuke A, Kunkel C, Golze D, Todorović M, Margraf JT, Reuter K, et al. Atomic structures and orbital energies of 61,489 crystal-forming organic molecules. *Sci Data*. 2020;*7*:58.

44. van Setten MJ, Weigend F, Evers F. The *GW*-method for quantum chemistry applications: theory and implementation. *J Chem Theory Comput*. 2013;*9*:232–46.

45. Bruneval F, Rangel T, Hamed SM, Shao M, Yang C, Neaton JB. Molgw 1: many-body perturbation theory software for atoms, molecules, and clusters. *Comput Phys Commun*. 2016;*208*:149–61.

46. Caruso F, Dauth M, van Setten MJ, Rinke P. Benchmark of GW approaches for the GW100 test set. *J Chem Theory Comput*. 2016;*12*: 5076–87.

47. Govoni M, Galli G. GW100: comparison of methods and accuracy of results obtained with the WEST code. *J Chem Theory Comput*. 2018;*14*:1895–909.

48. Tajti A, Szalay PG, Császár AG, Kállay M, Gauss J, Valeev EF, et al. HEAT: high accuracy extrapolated ab initio thermochemistry. *J Chem Phys*. 2004;*121*:11599–613.

49. Bomble YJ, Vázquez J, Kállay M, Michauk C, Szalay PG, Császár AG, et al. High-accuracy extrapolated ab initio thermochemistry. II. Minor improvements to the protocol and a vital simplification. *J Chem Phys*. 2006;*125*:064108.

50. Harding ME, Vazquez J, Ruscic B, Wilson AK, Gauss J, Stanton JF. High-accuracy extrapolated ab initio thermochemistry. III. Additional improvements and overview. *J Chem Phys*. 2008;*128*:114111.

51. Motta M, Ceperley DM, Chan GKL, Gomez JA, Gull E, Guo S, et al. Towards the solution of the many-electron problem in real materials: equation of state of the hydrogen chain with state-of-the-art many-body methods. *Phys Rev X*. 2017;*7*:031059.

52. Williams KT, Yao Y, Li J, Chen L, Shi H, Motta M, et al. Direct comparison of many-body methods for realistic electronic Hamiltonians. *Phys Rev X*. 2020;*10*:011041.

53. Parr RG, Yang W. *Density-functional theory of atoms and molecules*. Oxford: Clarendon Press; 1989.

54. Zhao Y, Truhlar DG. Comparative assessment of density functional methods for 3d transition-metal chemistry. *J Chem Phys*. 2006;*124*: 224105.

55. Mardirossian N, Head-Gordon M. Thirty years of density functional theory in computational chemistry: an overview and extensive assessment of 200 density functionals. *Mol Phys*. 2017;*115*(19):2315–72.

56. Goerigk L, Grimme S. A general database for main group thermochemistry, kinetics, and noncovalent interactions – assessment of common and reparameterized (meta-)GGA density functionals. *J Chem Theory Comput*. 2010;*6*:107–26.PMID: 26614324.

57. Goerigk L, Grimme S. A thorough benchmark of density functional methods for general main group thermochemistry, kinetics, and noncovalent interactions. *Phys Chem Chem Phys*. 2011;*13*:6670–88.

58. Goerigk L, Grimme S. Efficient and accurate double-hybrid-meta-GGA density functionals—evaluation with the extended GMTKN30 database for general main group thermochemistry, kinetics, and noncovalent interactions. *J Chem Theory Comput*. 2011;*7*:291–309. PMID: 26596152.

59. Goerigk L, Hansen A, Bauer C, Ehrlich S, Najibi A, Grimme S. A look at the density functional theory zoo with the advanced GMTKN55 database for general main group thermochemistry, kinetics and noncovalent interactions. *Phys Chem Chem Phys*. 2017;*19*: 32184–215.

60. Schreiber M, Silva-Junior MR, Sauer SPA, Thiel W. Benchmarks for electronically excited states: CASPT2, CC2, CCSD and CC3. *J Chem Phys*. 2008;*128*:134110.

61. Silva-Junior MR, Schreiber M, Sauer SPA, Thiel W. Benchmarks for electronically excited states: time-dependent density functional theory and density functional theory based multireference configuration interaction. *J Chem Phys*. 2008;*129*:104103.

62. Silva-Junior MR, Schreiber M, Sauer SPA, Thiel W. Benchmarks of electronically excited states: basis set effects on CASPT2 results. *J Chem Phys*. 2010;*133*:174318.

63. Silva-Junior MR, Sauer SPA, Schreiber M, Thiel W. Basis set effects on coupled cluster benchmarks of electronically excited states: CC3, CCSDR(3) and CC2. *Mol Phys*. 2010;*108*:453–65.

64. Christiansen O, Koch H, Jørgensen P. The second-order approximate coupled cluster singles and doubles model CC2. *Chem Phys Lett*. 1995;*243*:409–18.

65. Hättig C, Weigend F. CC2 excitation energy calculations on large molecules using the resolution of the identity approximation. *J Chem Phys*. 2000;*113*:5154–61.

66. Rowe DJ. Equations-of-motion method and the extended shell model. *Rev Mod Phys*. 1968;*40*:153–66.

67. Stanton JF, Bartlett RJ. The equation of motion coupled-cluster method. A systematic biorthogonal approach to molecular excitation energies, transition probabilities, and excited state properties. *J Chem Phys*. 1993;*98*:7029–39.

68. Koch H, Kobayashi R, Sanchez de Merás A, Jo/rgensen P. Calculation of size-intensive transition moments from the coupled cluster singles and doubles linear response function. *J Chem Phys*. 1994;*100*:4393–400.

69. Koch H, Christiansen O, Jorgensen P, Sanchez de Merás AM, Helgaker T. The CC3 model: an iterative coupled cluster approach including connected triples. *J Chem Phys*. 1997;*106*:1808–18.

70. Andersson K, Malmqvist PA, Roos BO, Sadlej AJ, Wolinski K. Second-order perturbation theory with a CASSCF reference function. *J Phys Chem*. 1990;*94*:5483–8.

71. Andersson K, Malmqvist PA, Roos BO. Second-order perturbation theory with a complete active space self-consistent field reference function. *J Chem Phys*. 1992;*96*:1218–26.

72. B O Roos KA, Fulscher MP, Malmqvist PA, Serrano-Andres L. In: Prigogine I, Rice SA, editors. *Adv. Chem. Phys.* Volume XCIII. New York: Wiley; 1996. p. 219–331.

73. Leang SS, Zahariev F, Gordon MS. Benchmarking the performance of time-dependent density functional methods. *J Chem Phys*. 2012; *136*:104101.

74. Runge E, Gross EKU. Density-functional theory for time-dependent systems. *Phys Rev Lett*. 1984;*52*:997–1000.

75. Casida ME. In: Chong DP, editor. *Time-dependent density functional response theory for molecules recent advances in density functional methods*. Singapore: World Scientific; 1995. p. 155–92.

76. Casida ME, Huix-Rotllant M. Progress in time-dependent density-functional theory. *Annu Rev Phys Chem*. 2012;*63*:287–323.

77. Ullrich C. *Time-dependent density-functional theory: concepts and applications. Oxford graduate texts*. New York: Oxford University Press; 2012.

78. Schwabe T, Goerigk L. Time-dependent double-hybrid density functionals with spin-component and spin-opposite scaling. *J Chem Theory Comput*. 2017;*13*:4307–23.

79. Casanova-Paez M, Dardis MB, Goerigk L. ωB2PLYP and ωB2GPPLYP: the first two double-hybrid density functionals with long-range correction optimized for excitation energies. *J Chem Theory Comput*. 2019;*15*:4735.

80. Casanova-Paez M, Goerigk L. Assessing the Tamm–Dancoff approximation, singlet–singlet, and singlet–triplet excitations with the latest long-range corrected double-hybrid density functionals. *J Chem Phys*. 2020;*153*:064106.

81. Furche F, Ahlrichs R. Adiabatic time-dependent density functional methods for excited state properties. *J Chem Phys*. 2002;*117*: 7433–47.

82. Send R, Kühn M, Furche F. Assessing excited state methods by adiabatic excitation energies. *J Chem Theory Comput*. 2011;*7*:2376–86.

83. Winter NOC, Graf NK, Leutwyler S, Hättig C. Benchmarks for 0–0 transitions of aromatic organic molecules: DFT/B3LYP, ADC(2), CC2, SOS-CC2 and SCS-CC2 compared to high-resolution gas-phase data. *Phys Chem Chem Phys*. 2013;*15*:6623–30.

84. Loos PF, Galland N, Jacquemin D. Theoretical 0–0 energies with chemical accuracy. *J Phys Chem Lett*. 2018;*9*:4646–51.

85. Loos PF, Jacquemin D. Chemically accurate 0–0 energies with not-so-accurate excited state geometries. *J Chem Theory Comput*. 2019; *15*:2481–91.

86. Loos PF, Jacquemin D. Evaluating 0–0 energies with theoretical tools: a short review. *ChemPhotoChem*. 2019;*3*:684–96.

87. Dierksen M, Grimme S. A density functional calculation of the vibronic structure of electronic absorption spectra. *J Chem Phys*. 2004; *120*:3544–54.

88. Goerigk L, Grimme S. Assessment of TD-DFT methods and of various spin scaled CIS_nD and CC2 versions for the treatment of low-lying valence excitations of large organic dyes. *J Chem Phys*. 2010;*132*:184103.

89. Jacquemin D, Planchat A, Adamo C, Mennucci B. A TD-DFT assessment of functionals for optical 0–0 transitions in solvated dyes. *J Chem Theory Comput*. 2012;*8*:2359–72.

90. Jacquemin D, Duchemin I, Blase X. 0–0 energies using hybrid schemes: benchmarks of TD-DFT, CIS(D), ADC(2), CC2, and BSE/GW formalisms for 80 real-life compounds. *J Chem Theory Comput*. 2015;*11*:5340–59.

91. Kozma B, Tajti A, Demoulin B, Izsak R, Nooijen M, Szalay PG. A new benchmark set for excitation energy of charge transfer states: systematic investigation of coupled cluster type methods. *J Chem Theory Comput*. 2020;*16*:4213–25.

92. Hoyer CE, Ghosh S, Truhlar DG, Gagliardi L. Multiconfiguration pair-density functional theory is as accurate as CASPT2 for electronic excitation. *J Phys Chem Lett*. 2016;*7*:586–91.

93. Loos PF, Scemama A, Blondel A, Garniron Y, Caffarel M, Jacquemin D. A mountaineering strategy to excited states: highly-accurate reference energies and benchmarks. *J Chem Theory Comput*. 2018;*14*:4360–79.

94. Loos PF, Boggio-Pasqua M, Scemama A, Caffarel M, Jacquemin D. Reference energies for double excitations. *J Chem Theory Comput*. 2019;*15*:1939–56.

95. Loos PF, Lipparini F, Boggio-Pasqua M, Scemama A, Jacquemin D. A mountaineering strategy to excited states: highly-accurate energies and benchmarks for medium size molecules. *J Chem Theory Comput*. 2020;*16*:1711–41.

96. Loos PF, Scemama A, Boggio-Pasqua M, Jacquemin D. A mountaineering strategy to excited states: highly-accurate energies and benchmarks for exotic molecules and radicals. *J Chem Theory Comput*. 2020;*16*:3720–36.

97. Köhn A, Hättig C. Analytic gradients for excited states in the coupled-cluster model CC2 employing the resolution-of-the-identity approximation. *J Chem Phys*. 2003;*119*:5021–36.

98. Fang C, Oruganti B, Durbeej B. How method-dependent are calculated differences between vertical, adiabatic and 0–0 excitation energies? *J Phys Chem A*. 2014;*118*:4157–71.

99. Oruganti B, Fang C, Durbeej B. Assessment of a composite CC2/DFT procedure for calculating 0–0 excitation energies of organic molecules. *Mol Phys*. 2016;*114*:3448–63.

100. Noga J, Bartlett RJ. The full CCSDT model for molecular electronic structure. *J Chem Phys*. 1987;*86*:7041–50.

101. Kucharski SA, Bartlett RJ. Recursive intermediate factorization and complete computational linearization of the coupled-cluster single, double, triple, and quadruple excitation equations. *Theoret Chim Acta*. 1991;*80*:387–405.

102. Kucharski SA, Włoch M, Musiał M, Bartlett RJ. Coupled-cluster theory for excited electronic states: the full equation-of-motion coupled-cluster single, double, and triple excitation method. *J Chem Phys*. 2001;*115*:8263–6.

103. Kowalski K, Piecuch P. The active-space equation-of-motion coupled-cluster methods for excited electronic states: full EOMCCSDt. *J Chem Phys*. 2001;*115*:643–51.

104. Kállay M, Gauss J, Szalay PG. Analytic first derivatives for general coupled-cluster and configuration interaction models. *J Chem Phys*. 2003;*119*:2991–3004.

105. Hirata S, Nooijen M, Bartlett RJ. High-order determinantal equation-of-motion coupled-cluster calculations for electronic excited states. *Chem Phys Lett*. 2000;*326*:255–62.

106. Hirata S. Higher-order equation-of-motion coupled-cluster methods. *J Chem Phys*. 2004;*121*:51–9.

107. Booth GH, Thom AJW, Alavi A. Fermion Monte Carlo without fixed nodes: a game of life, death, and annihilation in Slater determinant space. *J Chem Phys*. 2009;*131*:054106.

108. Booth GH, Alavi A. Approaching chemical accuracy using full configuration-interaction quantum Monte Carlo: a study of ionization potentials. *J Chem Phys*. 2010;*132*:174104.

109. Cleland D, Booth GH, Alavi A. Communications: survival of the fittest: accelerating convergence in full configuration-interaction quantum Monte Carlo. *J Chem Phys*. 2010;*132*:041103.

110. Booth GH, Cleland D, Thom AJW, Alavi A. Breaking the carbon dimer: the challenges of multiple bond dissociation with full configuration interaction quantum Monte Carlo methods. *J Chem Phys*. 2011;*135*:084104.

111. Daday C, Smart S, Booth GH, Alavi A, Filippi C. Full configuration interaction excitations of ethene and butadiene: resolution of an ancient question. *J Chem Theory Comput*. 2012;*8*:4441–51.

112. Blunt NS, Smart SD, Booth GH, Alavi A. An excited-state approach within full configuration interaction quantum Monte Carlo. *J Chem Phys*. 2015;*143*:134117.

113. Ghanem K, Lozovoi AY, Alavi A. Unbiasing the initiator approximation in full configuration interaction quantum Monte Carlo. *J Chem Phys*. 2019;*151*:224108.

114. Deustua JE, Shen J, Piecuch P. Converging high-level coupled-cluster energetics by Monte Carlo sampling and moment expansions. *Phys Rev Lett*. 2017;*119*:223003.

115. Deustua JE, Magoulas I, Shen J, Piecuch P. Communication: approaching exact quantum chemistry by cluster analysis of full configuration interaction quantum Monte Carlo wave functions. *J Chem Phys*. 2018;*149*:151101.

116. Holmes AA, Umrigar CJ, Sharma S. Excited states using semistochastic heat-bath configuration interaction. *J Chem Phys*. 2017;*147*: 164111.

117. Chien AD, Holmes AA, Otten M, Umrigar CJ, Sharma S, Zimmerman PM. Excited states of methylene, polyenes, and ozone from heat-bath configuration interaction. *J Phys Chem A*. 2018;*122*:2714–22.

118. Li J, Otten M, Holmes AA, Sharma S, Umrigar CJ. Fast semistochastic heat-bath configuration interaction. *J Chem Phys*. 2018;*149*: 214110.

119. Yao Y, Giner E, Li J, Toulouse J, Umrigar CJ. Almost exact energies for the Gaussian-2 set with the semistochastic heat-bath configuration interaction method. *The Journal of Chemical Physics*. 2020;*153*(12):124117. http://dx.doi.org/10.1063/5.0018577.

120. Li J, Yao Y, Holmes AA, Otten M, Sun Q, Sharma S, et al. Accurate many-body electronic structure near the basis set limit: application to the chromium dimer. *Phys Rev Research*. 2020;*2*:012015.

121. Eriksen JJ, Lipparini F, Gauss J. Virtual orbital many-body expansions: a possible route towards the full configuration interaction limit. *J Phys Chem Lett*. 2017;*8*:4633–9.

122. Eriksen JJ, Gauss J. Many-body expanded full configuration interaction. I. Weakly correlated regime. *J Chem Theory Comput*. 2018;*14*: 5180–91.

123. Eriksen JJ, Gauss J. Many-body expanded full configuration interaction. II. Strongly correlated regime. *J Chem Theory Comput*. 2019; *15*:4873–84.

124. Eriksen JJ, Gauss J. Generalized many-body expanded full configuration interaction theory. *J Phys Chem Lett*. 2019;*27*:7910–5.

125. Xu E, Uejima M, Ten-no SL. Full coupled-cluster reduction for accurate description of strong electron correlation. *Phys Rev Lett*. 2018; *121*:113001.

126. Xu E, Uejima M, Ten-no SL. Towards Near-Exact Solutions of Molecular Electronic Structure: Full Coupled-Cluster Reduction with a Second-Order Perturbative Correction. *The Journal of Physical Chemistry Letters*. 2020;*11*(22):9775–9780. http://dx.doi.org/10.1021/acs. jpclett.0c03084.

127. Loos PF, Damour Y, Scemama A. The performance of CIPSI on the ground state electronic energy of benzene. *J Chem Phys*. 2020;*153*: 176101.

128. Eriksen JJ. The Shape of Full Configuration Interaction to Come. *The Journal of Physical Chemistry Letters*. 2021;*12*(1):418–432. http:// dx.doi.org/10.1021/acs.jpclett.0c03225.

129. Bender CF, Davidson ER. Studies in configuration interaction: the first-row diatomic hydrides. *Phys Rev*. 1969;*183*:23–30.

130. Whitten JL, Hackmeyer M. Configuration interaction studies of ground and excited states of polyatomic molecules. I. the CI formulation and studies of formaldehyde. *J Chem Phys*. 1969;*51*:5584–96.

131. Huron B, Malrieu JP, Rancurel P. Iterative perturbation calculations of ground and excited state energies from multiconfigurational zeroth-order wavefunctions. *J Chem Phys*. 1973;*58*:5745–59.

132. Abrams ML, Sherrill CD. Important configurations in configuration interaction and coupled-cluster wave functions. *Chem Phys Lett*. 2005;*412*:121–4.

133. Bunge CF, Carbó-Dorca R. Select-divide-and-conquer method for large-scale configuration interaction. *J Chem Phys*. 2006;*125*:014108.

134. Bytautas L, Ruedenberg K. A priori identification of configurational deadwood. *Chem Phys*. 2009;*356*:64–75.

135. Giner E, Scemama A, Caffarel M. Using perturbatively selected configuration interaction in quantum Monte Carlo calculations. *Can J Chem*. 2013;*91*:879–85.

136. Caffarel M, Giner E, Scemama A, Ramrez-Sols A. Spin density distribution in open-shell transition metal systems: a comparative post-Hartree–Fock, density functional theory, and quantum Monte Carlo study of the CuCl Molecule. *J Chem Theory Comput*. 2014;*10*: 5286–96.

137. Giner E, Scemama A, Caffarel M. Fixed-node diffusion Monte Carlo potential energy curve of the fluorine molecule F_2 using selected configuration interaction trial wavefunctions. *J Chem Phys*. 2015;*142*:044115.

138. Garniron Y, Scemama A, Loos PF, Caffarel M. Hybrid stochastic-deterministic calculation of the second-order perturbative contribution of multireference perturbation theory. *J Chem Phys*. 2017;*147*:034101.

139. Caffarel M, Applencourt T, Giner E, Scemama A. Communication: toward an improved control of the fixed-node error in quantum Monte Carlo: the case of the water molecule. *J Chem Phys*. 2016;*144*:151103.

140. Caffarel M, Applencourt T, Giner E, Scemama A. Using CIPSI nodes in diffusion Monte Carlo; 2016. p. 15–46.

141. Holmes AA, Tubman NM, Umrigar CJ. Heat-bath configuration interaction: an efficient selected configuration interaction algorithm inspired by heat-Bath sampling. *J Chem Theory Comput*. 2016;*12*:3674–80.

142. Sharma S, Holmes AA, Jeanmairet G, Alavi A, Umrigar CJ. Semistochastic heat-bath configuration interaction method: selected configuration interaction with semistochastic perturbation theory. *J Chem Theory Comput*. 2017;*13*:1595–604.

143. Scemama A, Garniron Y, Caffarel M, Loos PF. Deterministic construction of nodal surfaces within quantum Monte Carlo: the case of FeS. *J Chem Theory Comput*. 2018;*14*:1395–402.

144. Scemama A, Benali A, Jacquemin D, Caffarel M, Loos PF. Excitation energies from diffusion Monte Carlo using selected configuration interaction nodes. *J Chem Phys*. 2018;*149*:034108.

145. Garniron Y, Scemama A, Giner E, Caffarel M, Loos PF. Selected configuration interaction dressed by perturbation. *J Chem Phys*. 2018;*149*:064103.

146. Evangelista FA. Adaptive multiconfigurational wave functions. *J Chem Phys*. 2014;*140*:124114.

147. Tubman NM, Lee J, Takeshita TY, Head-Gordon M, Whaley KB. A deterministic alternative to the full configuration interaction quantum Monte Carlo method. *J Chem Phys*. 2016;*145*:044112.

148. Tubman NM, Freeman CD, Levine DS, Hait D, Head-Gordon M, Whaley KB. Modern approaches to exact diagonalization and selected configuration interaction with the adaptive sampling CI method. *J Chem Theory Comput*. 2020;*16*:2139–59.

149. Schriber JB, Evangelista FA. Communication: an adaptive configuration interaction approach for strongly correlated electrons with tunable accuracy. *J Chem Phys*. 2016;*144*:161106.

150. Schriber JB, Evangelista FA. Adaptive configuration interaction for computing challenging electronic excited states with tunable accuracy. *J Chem Theory Comput*. 2017;*13*:5354–66.

151. Liu W, Hoffmann MR. iCI: iterative CI toward full CI. *J Chem Theory Comput*. 2016;*12*:1169–78.

152. Per MC, Cleland DM. Energy-based truncation of multi-determinant wavefunctions in quantum Monte Carlo. *J Chem Phys*. 2017;*146*:164101.

153. Ohtsuka Y, Hasegawa J. Selected configuration interaction method using sampled first-order corrections to wave functions. *J Chem Phys*. 2017;*147*:034102.

154. Zimmerman PM. Incremental full configuration interaction. *J Chem Phys*. 2017;*146*:104102.

155. Coe JP. Machine learning configuration interaction. *J Chem Theory Comput*. 2018;*14*:5739–49.

156. Liu W, Hoffmann MR. SDS: the static–dynamic–static framework for strongly correlated electrons. *Theor Chem Acc*. 2014;*133*:1481.

157. Lei Y, Liu W, Hoffmann MR. Further development of SDSPT2 for strongly correlated electrons. *Mol Phys*. 2017;*115*:2696–707.

158. Zhang N, Liu W, Hoffmann MR. Iterative configuration interaction with selection. *J Chem Theory Comput*. 2020;*16*:2296–316.

159. Garniron Y, Gasperich K, Applencourt T, Benali A, Ferté A, Paquier J, et al. Quantum package 2.0: a open-source determinant-driven suite of programs. *J Chem Theory Comput*. 2019;*15*:3591–609.

160. Evangelisti S, Daudey JP, Malrieu JP. Convergence of an improved CIPSI algorithm. *Chem Phys*. 1983;*75*:91–102.

161. Cimiraglia R. Second order perturbation correction to CI energies by use of diagrammatic techniques: an improvement to the CIPSI algorithm. *J Chem Phys*. 1985;*83*:1746–9.

162. Cimiraglia R, Persico M. Recent advances in multireference second order perturbation CI: the CIPSI method revisited. *J Comput Chem*. 1987;*8*:39–47.

163. Illas F, Rubio J, Ricart JM. Approximate natural orbitals and the convergence of a second order multireference many-body perturbation theory (CIPSI) algorithm. *J Chem Phys*. 1988;*89*:6376–84.

164. Povill A, Rubio J, Illas F. Treating large intermediate spaces in the CIPSI method through a direct selected CI algorithm. *Theor Chem Acc*. 1992;*82*:229–38.

165. Scemama A, Giner E, Applencourt T, Caffarel M, QMC using very large configuration interaction-type expansions. Pacifichem, Advances in Quantum Monte Carlo; 2015.

166. Scemama A, Applencourt T, Giner E, Caffarel M. Quantum Monte Carlo with very large multideterminant wavefunctions. *J Comput Chem*. 2016;*37*:1866–75.

167. Scemama A, Caffarel M, Benali A, Jacquemin D, Loos PF. Influence of pseudopotentials on excitation energies from selected configuration interaction and diffusion Monte Carlo. *Res Chem*. 2019;*1*:100002.

168. Dash M, Moroni S, Scemama A, Filippi C. Perturbatively selected configuration-interaction wave functions for efficient geometry optimization in quantum Monte Carlo. arXiv:180409610; 2018.

169. Dash M, Feldt J, Moroni S, Scemama A, Filippi C. Excited states with selected configuration interaction-quantum Monte Carlo: chemically accurate excitation energies and geometries. *J Chem Theory Comput*. 2019;*15*:4896–906.

170. Scemama A, Giner E, Benali A, Loos PF. Taming the fixed-node error in diffusion Monte Carlo via range separation. *J Chem Phys*. 2020;*153*:174107.

171. Benali A, Gasperich K, Jordan KD, Applencourt T, Luo Y, Bennett MC, et al. Towards a systematic improvement of the fixed-node approximation in diffusion Monte Carlo for solids. *J Chem Phys*. 2020;*153*:184111.

172. Budzák Š, Scalmani G, Jacquemin D. Accurate excited-state geometries: a CASPT2 and coupled-cluster reference database for small molecules. *J Chem Theory Comput*. 2017;*13*:6237–52.

173. Aidas K, Angeli C, Bak KL, Bakken V, Bast R, Boman L, et al. The Dalton quantum chemistry program system. *WIREs Comput Mol Sci*. 2014;*4*:269–84.

174. CFOUR, Coupled-Cluster techniques for Computational Chemistry, a quantum-chemical program package by J.F. Stanton, J. Gauss, L. Cheng, M.E. Harding, D.A. Matthews, P.G. Szalay with contributions from A.A. Auer, R.J. Bartlett, U. Benedikt, C. Berger, D.E. Bernholdt, Y.J. Bomble, O. Christiansen, F. Engel, R. Faber, M. Heckert, O. Heun, M. Hilgenberg, C. Huber, T.-C. Jagau, D. Jonsson, J. Jusélius, T. Kirsch, K. Klein, W.J. Lauderdale, F. Lipparini, T. Metzroth, L.A. Mück, D.P. O'Neill, D.R. Price, E. Prochnow, C. Puzzarini, K. Ruud, F. Schiffmann, W. Schwalbach, C. Simmons, S. Stopkowicz, A. Tajti, J. Vázquez, F. Wang, J.D. Watts and the integral packages MOLECULE (J. Almlöf and P.R. Taylor), PROPS (P.R. Taylor), ABACUS (T. Helgaker,

H.J. Aa. Jensen, P. Jørgensen, and J. Olsen), and ECP routines by A. V. Mitin and C. van Wüllen. For the current version, see http://www.cfour.de

175. Frisch MJ, Trucks GW, Schlegel HB, Scuseria GE, Robb MA, Cheeseman JR, et al. *Gaussian 16 Revision A.03*. Wallingford, CT: Gaussian Inc.; 2016.

176. Binkley JS, Pople JA. Self-consistent molecular orbital methods. XIX. Split-valence Gaussian-type basis sets for beryllium. *J Chem Phys*. 1977;*66*:879–80.

177. Clark T, Chandrasekhar J, Spitznagel GW, Schleyer PVR. Efficient diffuse function-augmented basis sets for anion calculations. III. The 3-21+G basis set for first-row elements, Li-F. *J Comput Chem*. 1983;*4*:294–301.

178. Dill JD, Pople JA. Self-consistent molecular orbital methods. XV. Extended Gaussian-type basis sets for lithium, beryllium, and boron. *J Chem Phys*. 1975;*62*:2921–3.

179. Ditchfield R, Hehre WJ, Pople JA. Self-consistent molecular-orbital methods. IX. An extended Gaussian-type basis for molecular-orbital studies of organic molecules. *J Chem Phys*. 1971;*54*:724–8.

180. Francl MM, Pietro WJ, Hehre WJ, Binkley JS, Gordon MS, DeFrees DJ, et al. Self-consistent molecular orbital methods. XXIII. A polarization-type basis set for second-row elements. *J Chem Phys*. 1982;*77*:3654–65.

181. Gordon MS, Binkley JS, Pople JA, Pietro WJ, Hehre WJ. Self-consistent molecular-orbital methods. 22. Small split-valence basis sets for second-row elements. *J Am Chem Soc*. 1982;*104*:2797–803.

182. Hehre WJ, Ditchfield R, Pople JA. Self-consistent molecular orbital methods. XII. Further extensions of Gaussian-type basis sets for use in molecular orbital studies of organic molecules. *J Chem Phys*. 1972;*56*:2257–61.

183. Dunning TH. Gaussian basis sets for use in correlated molecular calculations. I. The atoms boron through neon and hydrogen. *J Chem Phys*. 1989;*90*:1007–23.

184. Kendall RA, Dunning TH, Harrison RJ. Electron affinities of the first-row atoms revisited. Systematic basis sets and wave functions. *J Chem Phys*. 1992;*96*:6796–806.

185. Prascher BP, Woon DE, Peterson KA, Dunning TH, Wilson AK. Gaussian basis sets for use in correlated molecular calculations. VII. Valence, core-valence, and scalar relativistic basis sets for Li, Be, Na, and Mg. *Theor Chem Acc*. 2011;*128*:69–82.

186. Woon DE, Dunning TH. Gaussian basis sets for use in correlated molecular calculations. III. The atoms aluminum through argon. *J Chem Phys*. 1993;*98*:1358–71.

187. Woon DE, Dunning TH. Gaussian basis sets for use in correlated molecular calculations. IV. Calculation of static electrical response properties. *J Chem Phys*. 1994;*100*:2975–88.

188. Feller D. The role of databases in support of computational chemistry calculations. *J Comput Chem*. 1996;*17*:1571–86.

189. Pritchard BP, Altarawy D, Didier B, Gibsom TD, Windus TL. A new basis set exchange: an open, up-to-date resource for the molecular sciences community. *J Chem Inf Model*. 2019;*59*:4814–20.

190. Schuchardt KL, Didier BT, Elsethagen T, Sun L, Gurumoorthi V, Chase J, et al. Basis set exchange: a community database for computational sciences. *J Chem Inf Model*. 2007;*47*:1045–52.

191. Rolik Z, Szegedy L, Ladjánszki I, Ladóczki B, Kállay M. An efficient linear-scaling CCSD(T) method based on local natural orbitals. *J Chem Phys*. 2013;*139*:094105.

192. Kállay M, Rolik Z, Csontos J, Nagy P, Samu G, Mester D, et al. MRCC, quantum chemical program; 2017.

193. Applencourt T, Gasperich K, Scemama A. Spin adaptation with determinant-based selected configuration interaction; 2018.

194. TURBOMOLE V7.3 2018. A development of University of Karlsruhe and Forschungszentrum Karlsruhe GmbH, 1989–2007, TURBOMOLE GmbH, since 2007. http://www.turbomole.com. Accessed 13 Jun 2016.

195. Head-Gordon M, Rico RJ, Oumi M, Lee TJ. A doubles correction to electronic excited states from configuration interaction in the space of single substitutions. *Chem Phys Lett*. 1994;*219*:21–9.

196. Head-Gordon M, Maurice D, Oumi M. A perturbative correction to restricted open-shell configuration-interaction with single substitutions for excited-states of radicals. *Chem Phys Lett*. 1995;*246*:114–21.

197. Krylov AI, Gill PMW. Q-Chem: an engine for innovation. *WIREs Comput Mol Sci*. 2013;*3*:317–26.

198. Stanton JF, Gauss J. Perturbative treatment of the similarity transformed Hamiltonian in equation-of-motion coupled-cluster approximations. *J Chem Phys*. 1995;*103*:1064–76.

199. Trofimov AB, Stelter G, Schirmer J. Electron excitation energies using a consistent third-order propagator approach: comparison with full configuration interaction and coupled cluster results. *J Chem Phys*. 2002;*117*:6402–10.

200. Harbach PHP, Wormit M, Dreuw A. The third-order algebraic diagrammatic construction method (ADC(3)) for the polarization propagator for closed-shell molecules: efficient implementation and benchmarking. *J Chem Phys*. 2014;*141*:064113.

201. Trofimov AB, Schirmer J. Polarization propagator study of electronic excitation in key heterocyclic molecules I. Pyrrole. *Chem Phys*. 1997;*214*:153–70.

202. Christiansen O, Koch H, Jørgensen P. Perturbative triple excitation corrections to coupled cluster singles and doubles excitation energies. *J Chem Phys*. 1996;*105*:1451–9.

203. Watts JD, Bartlett RJ. Iterative and non-iterative triple excitation corrections in coupled-cluster methods for excited electronic states: the EOM-CCSDT-3 and EOM-CCSD($\tilde{T}$) methods. *Chem Phys Lett*. 1996;*258*:581–8.

204. Prochnow E, Harding ME, Gauss J. Parallel calculation of CCSDT and Mk-MRCCSDT energies. *J Chem Theory Comput*. 2010;*6*:2339–47.

205. Neese F. The ORCA program system. *WIREs Comput Mol Sci*. 2012;*2*:73–8.

206. Nooijen M, Bartlett RJ. A new method for excited states: similarity transformed equation-of-motion coupled-cluster theory. *J Chem Phys*. 1997;*106*:6441–8.

207. Dutta AK, Nooijen M, Neese F, Izsák R. Exploring the accuracy of a low scaling similarity transformed equation of motion method for vertical excitation energies. *J Chem Theory Comput*. 2018;*14*:72–91.

208. Krauter CM, Pernpointner M, Dreuw A. Application of the scaled-opposite-spin approximation to algebraic diagrammatic construction schemes of second order. *J Chem Phys*. 2013;*138*:044107.

209. Hellweg A, Grün SA, Hättig C. Benchmarking the performance of spin-component scaled CC2 in ground and electronically excited states. *Phys Chem Chem Phys*. 2008;*10*:4119–27.

210. Parrish RM, Burns LA, Smith DGA, Simmonett AC, DePrince AE, Hohenstein EG, et al. Psi4 1.1: an open-source electronic structure program emphasizing automation, advanced libraries, and interoperability. *J Chem Theory Comput*. 2017;*13*:3185–97.PMID: 28489372.

211. Pitoňák M, Neogrády P, Černý J, Grimme S, Hobza P. Scaled MP3 non-covalent interaction energies agree closely with accurate CCSD(T) benchmark data. *ChemPhysChem*. 2009;*10*:282–9.

212. Loos PF, Jacquemin D. Is ADC(3) as accurate as CC3 for valence and Rydberg transition energies? *J Phys Chem Lett*. 2020;*11*:974–80.

213. Werner HJ, Knowles PJ, Knizia G, Manby FR, Schütz M. Molpro: a general-purpose quantum chemistry program package. *WIREs Comput Mol Sci*. 2011;*2*:242–53.

214. Angeli C, Cimiraglia R, Malrieu JP. N-electron valence state perturbation theory: a fast implementation of the strongly contracted variant. *Chem Phys Lett*. 2001;*350*:297–305.

215. Angeli C, Cimiraglia R, Evangelisti S, Leininger T, Malrieu JP. Introduction of *n*-electron valence states for multireference perturbation theory. *J Chem Phys*. 2001;*114*:10252–64.

216. Angeli C, Cimiraglia R, Malrieu JP. *N*-electron valence state perturbation theory: a spinless formulation and an efficient implementation of the strongly contracted and of the partially contracted variants. *J Chem Phys*. 2002;*117*:9138–53.

217. Finley J, Malmqvist PÅ, Roos BO, Serrano-Andrés L. The multi-state CASPT2 method. *Chem Phys Lett*. 1998;*288*:299–306.

218. Shiozaki T, Győrffy W, Celani P, Werner HJ. Communication: extended multi-state complete active space second-order perturbation theory: energy and nuclear gradients. *J Chem Phys*. 2011;*135*:081106.

219. Svensson M, Humbel S, Froese RDJ, Matsubara T, Sieber S, Morokuma K. ONIOM: a multilayered integrated MO + MM method for geometry optimizations and single point energy predictions. A test for Diels–Alder reactions and Pt(P(t-Bu)$_3$)$_2$ + H$_2$ oxidative addition. *J Phys Chem*. 1996;*100*:19357–63.

220. Svensson M, Humbel S, Morokuma K. Energetics using the single point IMOMO (integrated molecular orbital + molecular orbital) calculations: choices of computational levels and model system. *J Chem Phys*. 1996;*105*:3654–61.

221. Caricato M, Trucks GW, Frisch MJ, Wiberg KB. Electronic transition energies: a study of the performance of a large range of single reference density functional and wave function methods on valence and Rydberg states compared to experiment. *J Chem Theory Comput*. 2010;*6*:370–83.

222. Watson TJ, Lotrich VF, Szalay PG, Perera A, Bartlett RJ. Benchmarking for perturbative triple-excitations in EE-EOM-CC methods. *J Phys Chem A*. 2013;*117*:2569–79.

223. Kánnár D, Szalay PG. Benchmarking coupled cluster methods on valence singlet excited states. *J Chem Theory Comput*. 2014;*10*: 3757–65.

224. Kánnár D, Tajti A, Szalay PG. Accuracy of coupled cluster excitation energies in diffuse basis sets. *J Chem Theory Comput*. 2017;*13*:202–9.

225. Hodecker M, Rehn DR, Dreuw A, Höfener S. Similarities and differences of the Lagrange formalism and the intermediate state representation in the treatment of molecular properties. *J Chem Phys*. 2019;*150*:164125.

226. Eriksen JJ, Gauss J. Ground and excited state first-order properties in many-body expanded full configuration interaction theory. *J Chem Phys*. 2020;*153*:154107.

227. Chrayteh A, Blondel A, Loos PF, Jacquemin D. A mountaineering strategy to excited states: highly-accurate oscillator strengths and dipole moments of small molecules. *J Chem Theory Comput*. 2021;*17*:416–38.

228. Sarkar R, Boggio-Pasqua M, Loos PF, Jacquemin D. Benchmarking TD-DFT and Wave Function Methods for Oscillator Strengths and Excited-State Dipole Moments. *Journal of Chemical Theory and Computation*. 2021. http://dx.doi.org/10.1021/acs.jctc.0c01228.

229. Jacquemin D. What is the key for accurate absorption and emission calculations, energy or geometry ? *J Chem Theory Comput*. 2018; *14*:1534–43.

230. Gould T. 'Diet GMTKN55' offers accelerated benchmarking through a representative subset approach. *Phys Chem Chem Phys*. 2018;*20*: 27735–9.

AUTHOR BIOGRAPHIES

Mickaël Véril was born in Toulouse in 1993. He received his B.Sc. in Molecular Chemistry from the Université Paul Sabatier (Toulouse, France) in 2015 and his M.Sc. in Computational and Theoretical Chemistry and Modeling from the same university in 2018. Since 2018, he is a Ph.D. student in the group of Dr. Pierre-François Loos at the Laboratoire de Chimie et Physique Quantiques in Toulouse. He is currently developing QUANTUM PACKAGE and the web application linked to the QUEST project.

Anthony Scemama received his Ph.D. in Computational and Theoretical Chemistry from the Université Pierre et Marie Curie (Paris, France) in 2004. He then moved to the Netherlands for a one-year postdoctoral stay in the group of Claudia Filippi, and came back in France for another year in the group of Eric Cancès. In 2006, he obtained a Research Engineer position from the "Centre National de la Recherche Scientifique (CNRS) at the Laboratoire de Chimie et Physique Quantiques" in Toulouse (France) to work on computational methods and high-performance computing for quantum chemistry. He was awarded the Crystal medal of the CNRS in 2019.

Michel Caffarel received his Ph.D. in Theoretical Physics and Chemistry from the Université Pierre et Marie Curie (Paris, France) in 1987, before moving to the University of Illinois at Urbana-Champaign for a two-year postdoctoral stay in the group of Prof. David Ceperley. He is currently working as a senior scientist at the "Centre National de la Recherche Scientifique (CNRS)" at the Laboratoire de Chimie et Physique Quantiques in Toulouse (France). His research is mainly focused on the development and application of quantum Monte Carlo methods for theoretical chemistry and condensed-mater physics.

Filippo Lipparini got his Ph.D. in Chemistry from Scuola Normale Superiore, Pisa in 2013. He worked as a Postdoc at the Université Pierre et Marie Curie in Paris and moved to Mainz, Germany, with a fellowship from the Alexander von Humboldt foundation and then as a regular postdoc. Since June 2017 he is assistant professor of Physical Chemistry at the department of Chemistry of the University of Pisa, in Italy. In 2014, he was awarded the "Eolo Scrocco" prize for young researcher in theoretical and computational chemistry by the Italian Chemical Society. His research focuses on mathematical methods and algorithms for computational chemistry, with a particular interest to their application to multiscale methods and electronic structure theory.

Martial Boggio-Pasqua received his Ph.D. in Physical Chemistry from the Université Bordeaux 1 in 1999. He then worked as a post-doctoral research associate at King's College London (2000–2003) and at Imperial College London (2004–2007) with M. Robb and M. Bearpark. He was then appointed as a CNRS researcher at the Laboratoire de Chimie et Physique Quantiques at the Université Paul Sabatier (Toulouse). His main research interests are focused on the theoretical studies of photochemical processes in complex molecular systems including the description of excited-state reaction mechanisms based on static explorations of potential energy surfaces and simulations of nonadiabatic dynamics.

Denis Jacquemin received his Ph.D. in Chemistry from the University of Namur in 1998, before moving to the University of Florida for his postdoctoral stay. He is currently full Professor at the University of Nantes (France). His research is focused on modeling electronically excited-state processes in organic and inorganic dyes as well as photochromes using a large panel of ab initio approaches. His group collaborates with many experimental and theoretical groups. He is the author of more than 500 scientific papers. He has been ERC grantee (2011–2016), member of Institut Universitaire de France (2012–2017) and received the WATOC's Dirac Medal (2014).

Pierre-François Loos received his Ph.D. in Computational and Theoretical Chemistry from the Université Henri Poincaré (Nancy, France) in 2008. From 2009 to 2013, He was undertaking postdoctoral research with Peter M.W. Gill at the Australian National University (ANU). From 2013 to 2017, he was a "Discovery Early Career Researcher Award" recipient and, then, a senior lecturer at the ANU. Since 2017, he holds a researcher position from the "Centre National de la Recherche Scientifique (CNRS) at the Laboratoire de Chimie et Physique Quantiques" in Toulouse (France), and was awarded, in 2019, an ERC consolidator grant for the development of new excited-state methodologies.

SUPPORTING INFORMATION

Additional supporting information may be found online in the Supporting Information section at the end of this article.